

Discrete Time Solution of Plane P-SV Waves
in a Plane Layered Medium

by

CLINT WELLINGTON FRASIER

B.S., California Institute of Technology
(1959)

M.S., California Institute of Technology
(1960)

SUBMITTED IN PARTIAL FULFILLMENT
OF THE REQUIREMENTS FOR THE
DEGREE OF DOCTOR OF
PHILOSOPHY

at the

MASSACHUSETTS INSTITUTE OF TECHNOLOGY
May, 1969

Signature of Author
Department of Earth and Planetary Sciences, May 16, 1969

Certified by
Thesis Supervisor

Accepted by
Chairman, Departmental Committee on Graduate Students

~~WITHDRAWN~~
Lindgren
FROM
JUN 20 1969
MASS. INST. TECH.

ABSTRACT

DISCRETE TIME SOLUTION OF PLANE
P-SV WAVES IN A PLANE LAYERED MEDIUM

by

Clint Wellington Frasier

Submitted to the Department of Earth and Planetary Sciences
in partial fulfillment of the requirement for the
degree of Doctor of Philosophy.

For plane waves at normal incidence to a layered, elastic medium both the forward and inverse discrete time problems have been previously solved. Here, the forward problem of calculating the waves in a medium of plane, homogeneous, isotropic layers is extended to P and SV body waves at non-normal incidence, where the horizontal phase velocity of each wave is greater than the shear and compressional waves of each layer.

Vertical travel times for P and SV waves through each layer are rounded off to unequal integer multiples of a small time increment. This gives a 4 x 4 layer matrix analagous to the 2 x 2 layer matrix for normal incidence obtained by previous authors.

Reflection and transmission responses for layered media are derived as matrix series in integer powers of a Fourier transform variable $z=e^{i\omega t}$. These responses are generated recursively by polynomial division and include all multiply reflected P and SV waves with mode conversions.

For a layered halfspace, the reflection response matrix for a source at the free surface equals the positive time part of the autocorrelation matrix of the transmission response matrix for a deep source. This can be used to convert surface records of teleseismic events to reflection seismograms for mapping the crust. For a known crustal structure, the reverberations contaminating a teleseismic event can be removed in time by a simple convolution, rather than by dividing spectra.

Time domain transmission responses for two crustal models under LASA, and reflection responses for several core-mantle boundary models

are calculated as examples of the method. These responses are useful for studying the first motion and window length of transition layer responses.

Finally, the method is extended to media containing any arrangement of solid and fluid layers.

Thesis Supervisor: Keiiti Aki
Title: Professor of Geophysics

Acknowledgments

The author is extremely grateful for the patient and thorough advice given by Professor Keitti Aki during the writing of this thesis. His excellent technical assistance was complemented by a deep understanding of human nature which made it a pleasure to work with him.

Other persons who constructively criticized parts of this thesis or gave help are Jerry Ware, Stan Laster, Jon Claerbout, Ralph Wiggins, Sven Treitel and Don Helmberger. Professor M. Nafi Toksoz originally recognized the importance of the thesis problem and encouraged the author to look into it.

The assistance of the people mentioned is greatly appreciated.

During his graduate studies at M.I.T., the author received financial support from a Research Assistantship sponsored by Lincoln Laboratory, and from the Advanced Research Projects Agency, monitored by the Air Force Office of Scientific Research under contract AF49(638)-1632.

The author could not have survived graduate school without the good natured encouragement of his wife, Sally, to refresh his mind every day.

Table of Contents

	<u>page</u>
Abstract	2
Acknowledgments	4
Table of Contents	5
Chapter I - INTRODUCTION	7
1.1 Purpose of investigation	7
1.2 Description of chapters	10
Chapter II - MATRIX FORMULATION OF PLANE P AND SV WAVES IN A LAYERED ELASTIC MEDIUM	12
2.1 Introduction	12
2.2 Formulation of the problem	16
2.3 Layer matrices	23
2.4 Conservation of energy across an interface	33
2.5 A simple case	39
2.6 Calculation of particle velocities and stresses for P and SV waves	43
2.7 Figure captions	46
Chapter III - EXTENSION TO MULTILAYER PROBLEMS	49
3.1 Introduction	49
3.2 Layer matrix products for waves at normal incidence	50
3.3 General form of layer matrix products	56
3.4 Transmission and reflection responses of a layered medium	63
3.5 Figure captions	71
Chapter IV - WAVES IN A LAYERED HALFSPACE	73
4.1 Introduction	73
4.2 Transmission and reflection responses of a layered halfspace for a deep source	75
4.3 Transmission and reflection responses for a surface source	80
4.4 Calculation of reflection response $R(z)$ from transmission response $X(z)$.	89
4.5 Estimation of $M(z)$	93
Chapter V - APPLICATION TO TWO TRANSITION ZONES IN THE EARTH	100
5.1 Introduction	100
5.2 Transmission response of two LASA crustal models	102

Table of Contents (cont.)

	<u>page</u>
Chapter V - cont.	
5.3 Reflection response of the core-mantle boundary	107
5.4 Conclusion	112
5.5 Figure captions	113
Chapter VI - PLANE WAVES IN A MEDIUM OF SOLID AND FLUID LAYERS	141
6.1 Introduction	141
6.2 Description of solid and fluid layers	143
6.3 Recursive calculation of reflection response	146
6.4 Reflection and transmission responses for a medium of solid and fluid layers	156
6.5 Figure captions	163
Chapter VII - CONCLUSIONS AND FUTURE WORK	166
References	168
Appendix A	170
Appendix B	205

Chapter I
Introduction

1.1 Purpose of Investigation

Seismic body waves passing through transitional velocity zones of the Earth are often approximated mathematically by plane elastic waves propagating through a stack of homogeneous, isotropic plane layers. For such models, the Haskell-Thomson technique is particularly well suited, because it allows one to impose a sinusoidal elastic wave source at one interface of a layered medium and iterate through the layers to obtain the transmitted waves emerging from the layers. Reflected waves for a layered model are also easily calculated.

Applications of this method to study the filtering effect of the Earth's crust on teleseismic events have been made by Haskell (1960, 1962), Hannon (1964), Phinney (1964), and Fernandez (1965) for long period seismic data, and more recently by Leblanc (1967) for short period data. Teng (1967) computed the spectral response of reflected and transmitted waves from several models of the core-mantle boundary to be used as a guide for examining recorded core phases.

Since seismic body waves are recorded as particle motions in time, it is often desirable to synthesize a time domain response from a spectral response of a transition zone calculated by Haskell's technique. This can be done numerically, but one must always determine experimentally which frequency sampling increment and window

length are to be used for the inversion to time. A basic difficulty is that reflection and transmission responses of layered media are not naturally bandlimited in frequency. As a result, a spurious oscillating precursor occurs in the synthesized time function which can obscure the time and polarity of the theoretical first motion. Other difficulties are discussed with examples by Leblanc (1967).

In the references on crustal studies mentioned above, tele-seismic sources in the mantle are assumed incident to crustal layers of lower velocity. Also, the reflection responses computed by Teng had source waves in the lower mantle incident to a set of layers of lower velocity at the core mantle boundary. Thus, for both of these cases, no critical angles of incidence are reached at layer interfaces for a complete range of incident angles for P sources. Incident angles for S sources in each case can exceed 30° without producing inhomogeneous waves.

The purpose of this thesis is to present a systematic method of calculating the responses of a plane layered medium directly in time for homogeneous plane P and SV waves in order to avoid the problems of spectral inversion described above.

When a plane wave pulse is incident to a set of plane layers, a sequence of multiple reflections inside the layers is generated. The reflection and transmission responses of the layers thus consist of wave trains of reverberations which last indefinitely but decay in time. In this investigation, a technique for generating these wave

trains is developed, such that all P and SV waves with mode conversions are included in each response. High resolution responses with no precursors in time are obtained which can be calculated to any length time window.

The theoretical development of this method is an extension to non-normal incidence of a discrete time problem first solved by Wuenschel (1960) for compressional waves at normal incidence. The basic strategy is to express the vertical travel times of P and SV waves through each layer as unequal integer multiples of a small time increment $\Delta\tau$. The plane P and SV waves are assumed to be arbitrary wave forms which satisfy their respective wave equations and are sampled every $\Delta\tau$ seconds. Taking the Fourier transform of these waves yields series in integer powers of $z=e^{-i\omega\Delta\tau}$. As each wave passes through a layer, it is delayed by an integer multiple of $\Delta\tau$, e.g., $n\Delta\tau$. This causes the Fourier transform of the wave to be multiplied by z^n .

The result is that layer matrices are obtained in which the frequency ω does not occur explicitly but only in powers of $z=e^{-i\omega\Delta\tau}$, which is the delay operator for time $\Delta\tau$. Taking products of such layer matrices for a layered medium, we can calculate reflection and transmission responses which are infinite series in integer powers of z . The coefficients of each series are the time samples of each response occurring at integer multiples of $\Delta\tau$. In this way, numerical inversion over a calculated spectral window is avoided.

1.2 Description of Chapters

This thesis can be divided into three sections. The first section consists of Chapters II to IV which give the theoretical development of the discrete time solution of plane waves in a plane layered elastic medium. Chapter II reviews the discrete time solutions for waves at normal incidence obtained by Wuenschel (1960) and modified by later authors. For non-normal incidence, P and SV waves are defined to be proportional to the total component of instantaneous particle velocity associated with up and down travelling compressional and shear potentials in each layer. The waves are scaled so that the square of each wave equals the instantaneous energy density flux carried by the wave across a unit area of horizontal interface. This choice of waves results in a simple 4×4 layer matrix which is completely analogous in 2×2 partitioned form to the normal incidence case obtained by previous authors. To illustrate the technique, the reflection and transmission responses of a single layer between half-spaces are calculated and expanded into multiply reflected rays inside the layer.

Chapters III and IV contain applications of the layer matrix to multilayer problems. In Chapter III, the reflection and transmission response matrices for a stack of elastic layers between two elastic halfspaces are computed. Responses of a layered halfspace to a deep source below the layering and to a source below the free surface are described in Chapter IV. Principles of reciprocity and

conservation of energy are verified for each response of Chapters III and IV. It is shown that the reflection response matrix of a layered halfspace to a surface source equals the positive time portion of the autocorrelation matrix of the transmission response matrix for a deep source. This suggests that teleseismic events recorded at the free surface of the crust can be converted to reflection seismograms for mapping the crustal layers.

The second section is Chapter V which illustrates the calculation of discrete time responses for two transition zones in the Earth. The first example shows the transmission response of two crustal models under the Large Aperture Seismic Array (LASA). The second example is a set of reflection responses off various models of the core-mantle boundary. These theoretical responses are calculated to demonstrate the high resolution capabilities of the technique for model studies of transition zones.

Chapter VI is the final section of the thesis. In it, the theory of Chapters II to IV is modified so that any arrangement of solid and fluid layers can be treated. Reflection and transmission responses for a medium of interbedded solid and fluid layers between halfspaces are derived.

Matrix Formulation of Plane P and SVWaves in a Layered Elastic Medium2.1 Introduction

The frequency domain solution for plane waves in an elastic medium of homogeneous, isotropic layers was first solved with a matrix iteration by Thomson (1950). Haskell (1953) applied Thomson's matrix formulation to obtain the period equations for Rayleigh and Love waves for a multilayered half space. This technique has been applied very successfully to deduce possible crustal structures of the Earth from the dispersion curves of long period surface waves.

Haskell (1960, 1962) applied his matrix iteration to study the filtering effect of a layered crust on body waves recorded at the surface. Dorman (1962) and Teng (1967) modified Haskell's formulation so that sequences of fluid and solid layers could be treated.

In this chapter, we solve Thomson's problem directly in time for impulsive plane wave sources located at an interface between layers. We consider only P and SV body waves which are homogeneous plane waves, that is, all waves have a phase velocity c which is greater than the compressional and shear velocities of any layer in the medium. A receiver is located at an interface of the layered medium. In our formulation, we calculate all multiply reflected P and SV waves as they are transmitted from source to receiver.

The primary purpose of calculating the impulsive response of a set of elastic layers is to obtain synthetic seismograms for body waves without the intermediate step of numerically inverting a Fourier spectrum calculated by Haskell's method. In short period earthquake phases (~ 1 sec.), crustal layers on the order of five kilometers thick or less can cause rapid oscillations in the amplitude and phase spectra of the frequency responses calculated by Haskell's method. In order to calculate a time record, one must first choose a small frequency sampling increment and tabulate the spectrum over a finite frequency window. If this discrete spectrum is numerically inverted, the time record is contaminated by aliasing. This effect can be eliminated by making the spectrum continuous, i.e., connecting adjacent amplitude and phase points by straight line segments as done by Aki (1960) and Harkrider (1964). Inverting this continuous spectrum yields a bandlimited time record which has an oscillating precursor. Such a precursor is not a problem for long period surface wave synthesis. However, for short period body waves, it obscures the polarity and arrival time of the first motion.

The direct time formulation described in this chapter avoids the inversion problems described above. We obtain a realizable impulsive response for a set of layers with the correct first motion and onset time. Later arrivals, which are multiply reflected P and SV waves, are separated in time with a resolution practically unattainable by spectral inversion.

The problem of plane wave compressional pulses at normal incidence to a layered medium was first solved by Wuenschel (1960). He reduced Haskell's formulation to the normal incidence case and obtained a matrix iteration relating the Laplace transforms of vertical motion and normal stress at the top of a layer to those at the bottom. By ingeniously constraining all layers to have transit times which are integer multiples of a small time increment $\Delta\tau$ Wuenschel showed that for impulsive sources, the vertical motion and stress at each interface could be expressed as a ratio of polynomials in $e^{-2s\Delta\tau}$, which can be expanded into an infinite series in integer powers of $e^{-2s\Delta\tau}$. Such a series is inverted by inspection to yield a series of impulses in time every $2\Delta\tau$ seconds. In this sense, Wuenschel's solution is a time domain solution even though Laplace transforms are used in the formulation.

Later this solution was expressed in terms of up and down travelling waves in each layer by Goupillaud (1961), Sherwood and Trorey (1965), and Robinson and Treitel (1966). This solution is also summarized by Claerbout (1968) in connection with an inverse problem solved by Kunetz (1962), in which the layer impedances are recovered from the upgoing waves recorded at the free surface of a layered halfspace.

In this chapter, we formulate the non-normal incidence problem in terms of up and down travelling impulsive P and SV waves in a layer. This gives a layer iteration which has exactly the same form

as for normal incidence, except that scalar matrix elements in the latter case are replaced by 2×2 matrices in the former. In order to handle the unequal P and SV transit times through a layer we apply Wuenschel's strategy and choose a very small time increment $\Delta\tau$, so that P and SV transit times can be expressed as integer multiples of $\Delta\tau$.

In the following three sections, the basic layer iteration for P and SV waves is derived and compared to the normal incidence case when the two wave types uncouple. Section 2.5 discusses the response of a single layer sandwiched between two halfspaces to impulsive plane wave sources. An expansion of this response into multiply reflected plane waves is demonstrated. The last section of this chapter gives expression for the velocity and stress components in terms of the up and down going P and SV waves in a layer.

2.2 Formulation of the Problem

We consider a horizontally layered elastic medium, each layer being homogeneous and isotropic. In each layer, we have four elastic plane waves to satisfy arbitrary boundary conditions. These waves are the up and down travelling P and SV waves. We restrict ourselves to body waves travelling horizontally in the positive x direction with a phase velocity c which is greater than the compressional and shear velocities of each layer. Thus, inhomogeneous interface waves such as Rayleigh or Stonely waves are not included. All particle motions are in the x - z plane, z being depth. Horizontally polarized shear waves (SH) are uncoupled from the P and SV waves and will not be treated here.

In the n - th layer we define plane wave elastic potentials f (for compressional waves) and F (for shear waves) as shown in Figure 1. The upgoing compressional and shear potentials are given respectively by

$$f_u(\hat{p}_u \cdot \vec{r} - \alpha t) = f_u(x \sin \delta - z \cos \delta - \alpha t)$$

$$F_u(\hat{s}_u \cdot \vec{r} - \beta t) = F_u(x \sin \gamma - z \cos \gamma - \beta t)$$

and the downgoing potentials by

$$f_d(\hat{p}_d \cdot \vec{r} - \alpha t) = f_d(x \sin \delta + z \cos \delta - \alpha t)$$

$$F_d(\hat{s}_d \cdot \vec{r} - \beta t) = F_d(x \sin \gamma + z \cos \gamma - \beta t)$$

(2-1)

Unit vectors \hat{p} and \hat{s} are the directions of P and SV wave propagation in the layer, and subscripts u and d indicate up and down going

waves respectively. Vector \bar{r} is the position vector $\bar{r} = (x, z)$.

Each P and SV potential satisfies its wave equation in two dimensions, i.e.

$$\begin{aligned}\nabla^2 f - \frac{1}{\alpha^2} \frac{\partial^2 f}{\partial t^2} &= 0 \\ \nabla^2 F - \frac{1}{\beta^2} \frac{\partial^2 F}{\partial t^2} &= 0\end{aligned}$$

where α and β are the compressional and shear velocities of the layer. These velocities are related by Snell's Law

$$c = \frac{\alpha}{\sin \delta} = \frac{\beta}{\sin \gamma} \quad (2-2)$$

Associated with each type of potential is a particle velocity vector. For a compressional potential f the velocity vector is

$$\bar{v}_p = \frac{\partial}{\partial t} \bar{\nabla} f = -\alpha f'' \hat{p} \quad (2-3a)$$

and from a shear potential F we obtain a velocity

$$\bar{v}_s = -\frac{\partial}{\partial t} (\nabla \times \hat{y} F) = -\beta F'' \hat{y} \times \hat{s} \quad (2-3b)$$

The double primes in these expressions indicate the second total derivative of each potential with respect to its argument. Unit vector \hat{y} points out of the x-z plane towards the reader as shown in Figure 2.1.

In most multilayer problems, one obtains a matrix iteration relating physical quantities in one layer to the same quantities in an adjacent layer. In elastic wave problems examples of such quantities

are particle displacements, velocities, stresses and potentials.

In this case, we use (2-3a,b) to define the following up and down going P and SV waves in the layer:

$$\begin{aligned}\overline{UP}(\hat{p}_u \cdot \vec{r} - \alpha t) &= \sqrt{\rho \alpha \cos \delta} \overline{V}_{P_u} = -\sqrt{\rho \alpha \cos \delta} \alpha f_u'' \hat{p}_u \\ \overline{US}(\hat{s}_u \cdot \vec{r} - \beta t) &= \sqrt{\rho \beta \cos \gamma} \overline{V}_{S_u} = +\sqrt{\rho \beta \cos \gamma} \beta F_u'' \hat{s}_u \times \hat{y} \\ \overline{DP}(\hat{p}_d \cdot \vec{r} - \alpha t) &= \sqrt{\rho \alpha \cos \delta} \overline{V}_{P_d} = -\sqrt{\rho \alpha \cos \delta} \alpha f_d'' \hat{p}_d \\ \overline{DS}(\hat{s}_d \cdot \vec{r} - \beta t) &= \sqrt{\rho \beta \cos \gamma} \overline{V}_{S_d} = -\sqrt{\rho \beta \cos \gamma} \beta F_d'' \hat{y} \times \hat{s}_d\end{aligned}\tag{2-4}$$

Each wave is expressed as a positive constant times the particle velocity vector for that wave. We define the directions of positive velocity (and positive wave) to be along the unit vectors given in the last column of equations (2-4) above. These directions are shown by large arrows in Figure 2.1.

Although these waves are vectors we can describe them only by their magnitude and sign in the following matrix iteration. At this point, we drop the bars over \overline{UP} , \overline{US} , etc. in (2-4).

In Appendix B, it is shown that UP^2 and US^2 are the energy density flows for the upgoing compressional and shear waves respectively. Similarly DP^2 and DS^2 are down going energy density flows.

Each squared wave has the physical units of power transmitted per unit area of horizontal interface in the x-y plane. Such powers are instantaneous since \mathbf{f} and \mathbf{F} are arbitrary plane waves rather than sinusoidal functions.

Let Z_n be the depth to bottom of the n-th layer. The waves defined by (2-4) are valid throughout the layer. We shall evaluate each wave at the top and bottom of the layer at the horizontal distance $x=0$. At the top of the layer, we define the waves

$$\left. \begin{aligned} UP_n(t) &= UP_n(\hat{p}_u \cdot \bar{r} - \alpha t) \\ US_n(t) &= US_n(\hat{s}_u \cdot \bar{r} - \beta t) \\ DP_n(t) &= DP_n(\hat{p}_d \cdot \bar{r} - \alpha t) \\ DS_n(t) &= DS_n(\hat{s}_d \cdot \bar{r} - \beta t) \end{aligned} \right| \begin{array}{l} x = 0 \\ z = z_{n-1} \end{array} \quad (2-7)$$

Similarly, at the bottom of the n-th layer we define the primed waves at $z = z_n$ to be

$$\left. \begin{aligned} UP'_n(t) &= UP'_n(\hat{p}'_u \cdot \bar{r} - \alpha t) \\ US'_n(t) &= US'_n(\hat{s}'_u \cdot \bar{r} - \beta t) \\ DP'_n(t) &= DP'_n(\hat{p}'_d \cdot \bar{r} - \alpha t) \\ DS'_n(t) &= DS'_n(\hat{s}'_d \cdot \bar{r} - \beta t) \end{aligned} \right| \begin{array}{l} x = 0 \\ z = z_n \end{array} \quad (2-8)$$

The ray directions of the primed and unprimed waves are shown by arrows in Figure 2.2. These waves are functions of time only since their positions are fixed. To keep the figure uncluttered, the velocity vector directions and wave fronts of Figure 2.1 are omitted.

2.3 Layer Matrices

In this section, we derive an iteration which relates waves just above the n -th interface to those just below it. Then an iteration is obtained which connects waves at the top and bottom of the n -th layer. Combining the iterations yields a basic layer iteration which can be applied to multilayer problems.

Figure 2.2 shows four waves arriving at the n -th interface and four leaving it at $x=0$. We can therefore express each wave leaving the interface as a linear combination of those waves arriving, provided we calculate the reflection and transmission coefficients for the interface. From the definitions of the waves in (2-4), (2-7), (2-8), the magnitudes of the reflection and transmission coefficients give ratios of square roots of power reflected by and transmitted through the interface. In addition, the sign of the coefficients must give the correct polarity of particle motion so that waves can be summed properly. These reflection and transmission coefficients are derived in Appendix A.

We denote reflection and transmission coefficients by r and t respectively for incident waves below an interface. For incident waves above the interface, the coefficients are primed, i.e., r' and t' . The type of mode conversion is indicated by subscripts p and s . For example, r_{ps} would equal $DS_{n+1}(+) / UP_{n+1}(+)$ if $UP_{n+1}(+)$ were the only wave arriving at the n -th interface.

From Figure 2.2 we see that the equations for the waves leaving the n -th interface are

$$DP_{n+1} = r_{pp} UP_{n+1} + r_{sp} US_{n+1} + t'_{pp} DP'_n + t'_{sp} DS'_n$$

$$DS_{n+1} = r_{ps} UP_{n+1} + r_{ss} US_{n+1} + t'_{ps} DP'_n + t'_{ss} DS'_n$$

$$UP'_n = r'_{pp} DP'_n + r'_{sp} DS'_n + t_{pp} UP_{n+1} + t_{sp} US_{n+1}$$

$$US'_n = r'_{ps} DP'_n + r'_{ss} DS'_n + t_{ps} UP_{n+1} + t_{ss} US_{n+1}$$

(2-10)

Since these reflection and transmission coefficients apply to the n-th interface, they are understood to be subscripted n.

Let us first separate the primed from the unprimed waves. This will give us an iteration across the n-th interface. Putting only the unprimed functions on the left of (2-10) yields

$$\begin{bmatrix} 1 & 0 & -r_{pp} & -r_{sp} \\ 0 & 1 & -r_{ps} & -r_{ss} \\ \hline 0 & 0 & t_{pp} & t_{sp} \\ 0 & 0 & t_{ps} & t_{ss} \end{bmatrix} \begin{bmatrix} DP \\ DS \\ \hline UP \\ US \end{bmatrix}_{n+1} = \begin{bmatrix} t'_{pp} & t'_{sp} & 0 & 0 \\ t'_{ps} & t'_{ss} & 0 & 0 \\ \hline -r'_{pp} & -r'_{sp} & 1 & 0 \\ -r'_{ps} & -r'_{ss} & 0 & 1 \end{bmatrix} \begin{bmatrix} DP' \\ DS' \\ \hline UP' \\ US' \end{bmatrix}_n$$

(2-11)

Define the following submatrices and vectors:

$$\begin{aligned}
 R_n &= \begin{bmatrix} r_{pp} & r_{sp} \\ r_{ps} & r_{ss} \end{bmatrix}_n & \bar{d}_n &= \begin{bmatrix} DP \\ DS \end{bmatrix}_n \\
 T_n &= \begin{bmatrix} t_{pp} & t_{sp} \\ t_{ps} & t_{ss} \end{bmatrix}_n & \bar{u}_n &= \begin{bmatrix} US \\ US \end{bmatrix}_n \\
 I_2 &= \begin{bmatrix} 1 & 0 \\ 0 & 1 \end{bmatrix}
 \end{aligned}$$

(2-12)

Substituting these into (2-11) gives the partitioned matrix equation

$$\begin{bmatrix} I_2 & -R_n \\ 0 & T_n \end{bmatrix} \begin{bmatrix} \bar{d}_{n+1} \\ \bar{u}_{n+1} \end{bmatrix} = \begin{bmatrix} T_n' & 0 \\ -R_n' & I_2 \end{bmatrix} \begin{bmatrix} \bar{d}_n' \\ \bar{u}_n' \end{bmatrix}$$

(2-13)

where primed matrices and vectors are obtained by priming their elements.

The inverse of the left hand matrix in (2-13) is

$$\begin{bmatrix} I_2 & -R_n \\ 0 & T_n \end{bmatrix}^{-1} = \begin{bmatrix} I_2 & R_n T_n^{-1} \\ 0 & T_n^{-1} \end{bmatrix}$$

Therefore, (2-13) becomes

$$\begin{bmatrix} \bar{d}_{n+1} \\ \bar{u}_{n+1} \end{bmatrix} = \begin{bmatrix} \bar{I}_2 & R_n T_n^{-1} \\ 0 & T_n^{-1} \end{bmatrix} \begin{bmatrix} T_n' & 0 \\ -R_n' & I_2 \end{bmatrix} \begin{bmatrix} d_n' \\ u_n' \end{bmatrix}$$

(2-13a)

We now define A_n , the interface matrix, to be this matrix product,

i.e.

$$\begin{bmatrix} \bar{d}_{n+1} \\ \bar{u}_{n+1} \end{bmatrix} = A_n \begin{bmatrix} d_n' \\ u_n' \end{bmatrix}$$

(2-14)

where the 2×2 partitioned matrices of A_n are $A_{ij}^{(n)}$ given by

$$A_{11}^{(n)} = T_n' - R_n T_n^{-1} R_n' \quad A_{12}^{(n)} = R_n T_n^{-1}$$

$$A_{21}^{(n)} = -T_n^{-1} R_n' \quad A_{22}^{(n)} = T_n^{-1}$$

(2-15)

These submatrices can be reduced to more compact form. In Appendix A it is shown that directly from their solutions that

$$T_n' = T_n^* \quad (2-16a)$$

$$R_n'^* = R_n', \quad R_n^* = R_n \quad (2-16b)$$

and

$$R_n' = -T_n R_n T_n^{-1} \quad (2-16c)$$

The asterisk denotes the transpose of a matrix. Using these three identities we obtain

$$R_n T_n^{-1} = -T_n^{-1} R_n' \quad (2-16d)$$

Hence

$$A_{12}^{(n)} = A_{21}^{(n)} = -T_n^{-1} R_n' \quad (2-17)$$

and

$$A_{11}^{(n)} = T_n' + T_n^{-1} R_n'^* R_n' \quad (2-17a)$$

Matrix $A_{11}^{(n)}$ is further reduced by conserving energy across the n-th interface. Let the downgoing incident wave just above the interface be an arbitrary source vector

$$d_n' = \bar{s}$$

The transmitted wave is therefore $T_n' \bar{s}$ and the reflected wave is $R_n' \bar{s}$. Conservation of instantaneous power through a unit area of interface gives

$$\bar{s}^* \bar{s} = \bar{s}^* (T_n'^* T_n' + R_n'^* R_n') \bar{s}$$

This is possible only if

$$-T_n'^* T_n' + R_n'^* R_n' = I_2 \quad (2-18a)$$

Similarly for an arbitrary incident source from below the interface we obtain

$$T_n^* T_n + R_n^* R_n = I_2 \quad (2-18b)$$

These identities can be verified from their solutions in Appendix A.

Substituting (2-18a) into (2-17a) and using (2-16a) gives

$$\begin{aligned} A_{n''}^{(n)} &= T_n' + T_n^{-1} (I_2 - T_n'^* T_n') \\ &= T_n^{-1} \end{aligned}$$

Therefore, the interface matrix A_n can be written in the simple form

$$A_n = T_n^{-1} \begin{bmatrix} I_2 & -R_n' \\ -R_n' & I_2 \end{bmatrix} \quad (2-19)$$

This interface matrix is interesting because it is completely analogous to the simpler case of compressional waves at normal incidence derived by Goupillaud (1961), Sherwood and Trorey (1966) and others. They obtained interface relations which in our notation can be written as

$$\begin{bmatrix} DP_n \\ UP_n \end{bmatrix} = \frac{1}{t_{PP}} \begin{bmatrix} 1 & -r_{PP}' \\ -r_{PP}' & 1 \end{bmatrix} \begin{bmatrix} DP_n' \\ UP_n' \end{bmatrix}$$

(2-19a)

Hence the 2×2 interface matrix a_n for their case is

$$a_n = \frac{1}{t_{PP}} \begin{bmatrix} 1 & -r_{PP}' \\ -r_{PP}' & 1 \end{bmatrix}$$

The scalar elements of this matrix correspond to the 2×2 submatrices of A_n in (2-19). This similarity is carried over into the derivation of the layer matrix iteration which follows.

The next step in the non-normal incidence case is to relate the waves at the bottom of the n -th layer to those at the top. This is not difficult because only time delays are involved.

The waves $UP_n(t)$ and $UP_n'(t)$ represent the same upgoing plane compressional wave except for a time delay $\tau_p^{(n)}$ it takes the wave front to travel through the n -th layer along the z axis at $x=0$. Similarly $US_n(t)$ equals $US_n'(t)$ after a delay of $\tau_s^{(n)}$ seconds, the shear wave transit time, through the layer. For the down travelling waves $DP_n'(t)$ is delayed by $\tau_p^{(n)}$ relative to $DP_n(t)$. Hence, we can write

$$\begin{aligned}
 DP'_n(t) &= DP_n(t + \tau_p^{(n)}) \\
 DS'_n(t) &= DS_n(t + \tau_s^{(n)}) \\
 UP'_n(t) &= UP_n(t - \tau_p^{(n)}) \\
 US'_n(t) &= US_n(t - \tau_s^{(n)})
 \end{aligned}$$

(2-20)

where from Figure 2 1

$$\tau_p^{(n)} = \frac{h_n \cos \delta_n}{\alpha_n}$$

$$\tau_s^{(n)} = \frac{h_n \cos \gamma_n}{\beta_n}$$

(2-21)

and h_n is the thickness of the n-th layer.

It should be noted that these transit times decrease with increasing angle of incidence rather than increase as one's intuition might guess.

In fact, dividing h_n by $\tau_p^{(n)}$ and $\tau_s^{(n)}$ gives the vertical phase velocities for P and SV wavefronts in the layer. These phase velocities are always greater than α_n for P waves and greater than β_n for SV waves at non-normal incidence.

In our formulation, we shall calculate the response of a layered medium to an impulsive plane wave source incident to an interface.

We know physically that waves recorded at some interface due to such a source is a train of impulses arriving at unequal time intervals due

to varying layer thicknesses and different P and SV transit times through each layer.

In order to simplify our layer iteration we shall choose a small enough time increment $\Delta\tau$ so that to any desired precision we can write

$$\begin{aligned}\tau_p^{(n)} &\doteq l_n \Delta\tau \\ \tau_s^{(n)} &\doteq m_n \Delta\tau\end{aligned}\tag{2-22}$$

where l_n and m_n are integers, m_n is greater than l_n , and $\Delta\tau$ is much smaller than $\tau_p^{(n)}$ or $\tau_s^{(n)}$.

This approximation to the transit terms can be interpreted in two ways. If the layer velocities of a model are exactly specified a priori, then our formulation is approximate, but can be made as accurate as necessary by decreasing $\Delta\tau$ so that the "round off error" introduced by (2-22) becomes small. Such errors show up as a distortion in the high frequencies of the spectrum of the impulse response of the layers. On the other hand, we can make equations (2-22) exact for a suitable $\Delta\tau$ by perturbing the velocities in (2-21) slightly so that $\tau_p^{(n)}$ and $\tau_s^{(n)}$ are exactly divisible by $\Delta\tau$. In this case our formulation is exact, but our layered model has velocities not exactly what we specified beforehand. As $\Delta\tau$ is reduced, the perturbed velocities come as close as desired to the correct velocities.

Assuming that (2-22) is valid and that an impulsive plane wave

source is located somewhere in the layered medium, then the primed and unprimed waves in (2-20) are each a series of pulses occurring at integer multiples of $\Delta\tau$. Taking the Fourier transform of (2-20) and utilizing (2-22) we obtain

$$\begin{aligned} DP'_n(z) &= DP_n(z) z^{l_n} \\ DS'_n(z) &= DS_n(z) z^{m_n} \\ UP'_n(z) &= UP_n(z) z^{-l_n} \\ US'_n(z) &= US_n(z) z^{-m_n} \end{aligned} \tag{2-23}$$

where the transform variable z is defined by

$$z = e^{-i\omega\Delta\tau} \tag{2-24}$$

Each wave in (2-23) is a series in integer powers of z , e.g.

$\sum_k a_k z^k$, because $a_k z^k$ is the transform of an impulse of area a_k at time $k\Delta\tau$. Since $\Delta\tau$ is small compared to the transit times through each layer, many of the coefficients a_k in each series will be zero.

To complete the layer matrix iteration, we define the 2×2 sub-matrix

$$Z_n = \begin{bmatrix} z^{l_n} & 0 \\ 0 & z^{m_n} \end{bmatrix} \tag{2-25}$$

Substituting this matrix and the vectors of (2-12) into (2-23) we get

$$\begin{bmatrix} \bar{d}'_n \\ \bar{u}'_n \end{bmatrix} = \begin{bmatrix} Z_n & 0 \\ 0 & Z_n^{-1} \end{bmatrix} \begin{bmatrix} d_n \\ \bar{u}_n \end{bmatrix} \quad (2-26)$$

Finally, we combine this equation with (2-14) and (2-19) to obtain the basic layer iteration, which is

$$\begin{bmatrix} d_{n+1} \\ \bar{u}_{n+1} \end{bmatrix} = T_n^{-1} \begin{bmatrix} Z_n & -R'_n Z_n^{-1} \\ -R'_n Z_n & Z_n^{-1} \end{bmatrix} \begin{bmatrix} d_n \\ \bar{u}_n \end{bmatrix} \quad (2-27)$$

We shall later refer to the coefficient matrix of this expression as the layer matrix C_n , i.e.

$$C_n = T_n^{-1} \begin{bmatrix} Z_n & -R'_n Z_n^{-1} \\ -R'_n Z_n & Z_n^{-1} \end{bmatrix} \quad (2-27a)$$

Applying this iteration to n adjacent layers of a medium, we obtain

$$\begin{bmatrix} d_{n+1} \\ \bar{u}_{n+1} \end{bmatrix} = Q(z) \begin{bmatrix} d_1 \\ \bar{u}_1 \end{bmatrix} \quad (2-28)$$

where $Q(z)$ is the matrix product

$$Q(z) = C_n C_{n-1} \cdots C_1 \quad (2-28a)$$

At this point, we remark that increasing l_n and m_n by reducing $\Delta\tau$ for a given set of layers does not appreciably increase the computer time required for calculating $Q(z)$ although larger storage is required. This is because the number of multiplications required depends primarily on the number of physical layers in the model. If one considers the multiplication of two polynomials of large degree in z with most of their coefficients equal to zero, this can be arranged by indexing so that all the zero coefficients are ignored.

Our 4×4 layer matrix C_n is analogous to the simpler 2×2 layer matrix derived for normal incidence by Goupillaud, Sherwood and Trorey and other authors. Their matrix relation in our notation is

$$\begin{bmatrix} DP_n \\ UP_n \end{bmatrix} = \frac{1}{t_{pp}} \begin{bmatrix} z^{+l} & -r_{pp}' z^{-l} \\ -r_{pp}' z^{+l} & z^{-l} \end{bmatrix}_n \begin{bmatrix} DP_{n-1} \\ UP_{n-1} \end{bmatrix}$$

2.4 Conservation of Energy Across an Interface

Several useful results for the interface matrix A_n and the layer matrix C_n of the previous section are obtained by conserving the power flowing across a unit area of the n-th interface. The net power flowing downward through the interface must be the same just above and below the interface. Since our up and down travelling waves have amplitudes equal to the square root of the transmitted power for each type of wave this implies the identity

$$\bar{d}_{n+1}^* \bar{d}_{n+1} - \bar{u}_{n+1}^* \bar{u}_{n+1} = \bar{d}_n^* \bar{d}_n - \bar{u}_n^* \bar{u}_n \quad (2-29)$$

which should be true instantaneously in time for any transient waves.

In order to prove (2-29), we first define a tilda operator (\sim) as follows: Let M be a square matrix with $2m$ rows, which is partitioned in 4 $m \times m$ submatrices M_{ij} . Then \tilde{M} equals M except that the off diagonal submatrices M_{12} and M_{21} are multiplied by -1.

Now we can write (2-14) in the form

$$\begin{bmatrix} \bar{d}_{n+1} \\ -\bar{u}_{n+1} \end{bmatrix} = \begin{bmatrix} A_{11} & -A_{12} \\ -A_{21} & A_{22} \end{bmatrix} \begin{bmatrix} \bar{d}_n \\ -\bar{u}_n \end{bmatrix} = \tilde{A}_n \begin{bmatrix} \bar{d}_n \\ -\bar{u}_n \end{bmatrix}$$

Taking the scalar dot product of the transpose of this equation and

(2-14), we obtain

$$\bar{d}_{n+1}^* \bar{d}_{n+1} - \bar{u}_{n+1}^* \bar{u}_{n+1} = \begin{bmatrix} \bar{d}_n^{*'} & , & - & \bar{u}_n^{*'} \end{bmatrix} \tilde{A}_n^* A_n \begin{bmatrix} \bar{d}_n' \\ \bar{u}_n' \end{bmatrix}$$

In order to prove (2-29), we shall show that

$$\tilde{A}_n^* A_n = I_4 \quad (2-30)$$

From (2-19) and (2-16b)

$$\tilde{A}_n^* A_n = \begin{bmatrix} I_2 & R_n' \\ R_n' & I_2 \end{bmatrix} \begin{matrix} T_n^{*-1} \\ T_n^{-1} \end{matrix} \begin{bmatrix} I_2 & -R_n' \\ -R_n' & I_2 \end{bmatrix}$$

Multiplying these matrices gives

$$\tilde{A}_n^* A_n = \begin{bmatrix} (TT^*)^{-1} - R'(TT^*)^{-1}R', & R'(TT^*)^{-1} - (TT^*)^{-1}R' \\ R'(TT^*)^{-1} - (TT^*)^{-1}R', & (TT^*)^{-1} - R'(TT^*)^{-1}R' \end{bmatrix}_n$$

Consider the diagonal matrices of this product. Let

$$D = (TT^*)^{-1} - R'(TT^*)^{-1}R'$$

Using (2-16a), we write this as

$$D = (T'^* T')^{-1} - R' (T'^* T')^{-1} R'$$

Hence

$$(T'^* T') D = I_2 - (T'^* T') R' (T'^* T')^{-1} R'$$

Using (2-16c) twice and (2-16a) we can show that

$$(T'^* T') R' = R' (T'^* T')$$

Therefore,

$$(T'^* T') D = I_2 - R' R = T'^* T'$$

from (2-18a). Thus we finally have

$$D = I_2$$

for the diagonal matrices of $\tilde{A}_n^* A_n$. For the off diagonal matrices, we note that

$$R' (T'^* T')^{-1} = [(I_2 - R' R') R'^{-1}]^{-1} = [R'^{-1} - R']^{-1}$$

$$(T'^* T')^{-1} R' = [R'^{-1} (I - R' R')]^{-1} = [R'^{-1} - R']^{-1}$$

using (2-18a). Since these products are equal, their difference is the null matrix. Therefore, we have shown that

$$\tilde{A}_n^* A_n = I_4$$

(2-30)

and that (2-29) is true. Matrix \tilde{A}_n is obtained from A_n by changing the sign of the elements of the last two columns and then the last two rows. This does not change the determinant, hence \tilde{A}_n and A_n have equal determinants. From equation (2-30), we deduce then that

$$\det|\tilde{A}_n^*| = \det|A_n| = 1$$

(2-31)

Therefore, A_n and its inverse commute, i.e.

$$\tilde{A}_n^* A_n = A_n \tilde{A}_n^* = I_4$$

(2-31a)

These results for A_n can be easily extended to products of layer matrices like C_n in (2-27). Matrix C_n can be written as

$$C_n(z) = A_n \begin{bmatrix} Z_n & 0 \\ 0 & Z_n^{-1} \end{bmatrix}$$

(2-32)

For a matrix product $P = MN$ where M and N are square

with an even number of rows, one can show that $\tilde{P} = \tilde{M} \tilde{N}^*$.^{37.}

Therefore

$$\tilde{C}_n^* \left(\frac{1}{z} \right) C_n(z) = \begin{bmatrix} Z_n^{-1} & 0 \\ 0 & Z_n \end{bmatrix} \tilde{A}_n^* A_n \begin{bmatrix} Z_n & 0 \\ 0 & Z_n^{-1} \end{bmatrix}$$

which reduces to

$$\tilde{C}_n^* \left(\frac{1}{z} \right) C_n(z) = I_4$$

using (2-31). Also

$$\begin{aligned} \det |C_n(z)| &= \det |A_n| \det \begin{bmatrix} Z_n & 0 \\ 0 & Z_n^{-1} \end{bmatrix} \\ &= \det |\tilde{C}_n^* \left(\frac{1}{z} \right)| = 1 \end{aligned}$$

(2-32a)

using (2-30) and (2-24). As with A_n , $C_n(z)$ and its inverse commute, i.e.

$$\tilde{C}_n^* \left(\frac{1}{z} \right) C_n(z) = C_n(z) \tilde{C}_n^* \left(\frac{1}{z} \right) = I_4$$

(2-33)

For a product of layer matrices

$$Q(z) = C_n(z) C_{n-1}(z) \cdots C_1(z)$$

(2-34)

we obtain

$$\tilde{Q}_{(1/z)}^* Q(z) = \tilde{C}_1^* \tilde{C}_2^* \cdots \tilde{C}_n^* C_n(z) \cdots C_1(z) \quad (2-35)$$

which reduces to

$$\tilde{Q}_{(1/z)}^* Q(z) = I_4$$

by repeated application of (2-33). Taking the determinant of (2-34) gives

$$\det |Q(z)| = \prod_{k=1}^n \det |C_k(z)| = 1 \quad (2-36)$$

using (2-32a). Thus $Q(z)$ also commutes with its inverse, i.e.

$$\tilde{Q}_{(1/z)}^* Q(z) = Q(z) \tilde{Q}_{(1/z)}^* = I_4 \quad (2-37)$$

2.5 A Simple Case

In order to clarify this matrix technique, we consider a simple example, that of single layer between two halfspaces. Setting $n = 1$ in (2-27), we have

$$\begin{bmatrix} \underline{d}_2 \\ \bar{u}_2 \end{bmatrix} = T_1^{-1} \begin{bmatrix} Z_1 & -R_1' Z_1^{-1} \\ -R_1' Z_1 & Z_1^{-1} \end{bmatrix} \begin{bmatrix} \underline{d}_1 \\ \bar{u}_1 \end{bmatrix} \quad (2-38)$$

Let us assume that an impulsive source \bar{s}_2 is incident to the layer from below in the halfspace which is layer 2. Also, we suppose that no sources exist in the upper halfspace, layer 0. In this case,

$\underline{d}_1 = R_0 \bar{u}_1$. Equation (2-38) then becomes

$$\begin{bmatrix} \underline{d}_2 \\ \bar{s}_2 \end{bmatrix} = T_1^{-1} \begin{bmatrix} Z_1 & -R_1' Z_1^{-1} \\ -R_1' Z_1 & Z_1^{-1} \end{bmatrix} \begin{bmatrix} R_0 \bar{u}_1 \\ \bar{u}_1 \end{bmatrix}$$

Solving for \bar{u}_1 and \underline{d}_2 in terms of \bar{s}_2 gives

$$\bar{u}_1 = Z_1 (I_2 - R_1' Z_1 R_0 Z_1)^{-1} T_1 \bar{s}_2$$

$$\underline{d}_2 = T_1^{-1} (Z_1 R_0 Z_1 - R_1') (I - R_1' Z_1 R_0 Z_1)^{-1} T_1 \bar{s}_2$$

For an impulsive source \bar{s}_2 at time zero, we know on physical grounds that \bar{u}_1 and \bar{d}_2 must be trains of impulses which exist only for positive time and die out with increasing time. This implies that the inverse matrix in each wave vector must have a converging expansion in a power series in positive powers of Z_1 , i.e.

$$(\mathbb{I}_2 - R_1 Z_1 R_0 Z_1)^{-1} = \sum_{i=0}^{\infty} (R_1' Z_1 R_0 Z_1)^i \quad (2-39)$$

This is proved mathematically in Chapter III for any number of layers.

Our solutions for \bar{u}_1 and \bar{d}_2 become

$$\bar{u}_1 = \sum_{i=0}^{\infty} Z_1 (R_1' Z_1 R_0 Z_1)^i T_1 \bar{s}_2 \quad (2-40)$$

$$\bar{d}_2 = (T_1^{-1} Z_1 R_0 Z_1 + R_1 T_1^{-1}) \sum_{i=0}^{\infty} (R_1' Z_1 R_0 Z_1)^i T_1 \bar{s}_2 \quad (2-41)$$

These expansions are simply the summation of all the multiply reflected rays inside the layer. This is seen by noting the sequence of matrices operating on \bar{s}_2 from right to left in each term of the summation. For \bar{u}_1 , the first term is

$$Z_1 T_1 \bar{s}_2$$

Multiplication of \bar{s}_2 by T_1 gives the first arrivals across the bottom interface with all P and SV conversions included. Then

multiplication by Z_1 delays the P and SV components of this transmitted vector by their different transit times through the layer.

Thus, $Z_1 T_1 \bar{s}_2$ contains the first P and SV arrivals at the top of the layer due to \bar{s}_2 incident on the bottom of the layer.

The second term in \bar{u}_1 is

$$Z_1 R_1' Z_1 R_0 Z_1 T_1 \bar{s}_2$$

This vector represents the first term after two later internal reflections within the layer, one at interface 0 and the other at interface 1. Each multiplication by Z_1 between and after reflections indicates another transit through the layer by the P and SV components of the vector. Later terms in the expansion for \bar{u}_1 represent higher order multiple reflections inside the layer.

The expansion for \bar{d}_2 is similarly interpreted. We see that the first term is

$$R_1 \bar{s}_2$$

which is the source vector reflected off the bottom of the layer with no time delay. The next vector wave is the sum of two terms in (2-41) which are quadratic in Z_1 . Using (2-16d) these terms sum to give

$$T_1' Z_1 R_0 Z_1 T_1 \bar{s}_2$$

This vector contains all waves which have travelling up through layer

1 and back down into the layer halfspace with one internal reflection at the top of layer 1. As in the case for \bar{u}_1 , later terms in the expansion of \bar{d}_2 are waves multiply reflected within layer 1 before being transmitted to the lower halfspace.

This method of expansion into multiply reflected waves is very cumbersome for more than one layer. A systematic way of calculating such inverse matrices recursively is given in Chapter IV for multilayer problems.

2.6 Calculation of Particle Velocities and Stresses from P and SV Waves

It is useful to compute the horizontal and vertical components of particle velocity at an interface due to all four waves UP, US, DP and DS. This is necessary when comparing theoretical results to recorded seismograph data, since velocity components are usually recorded in the field.

Using equations (2-4) and Figure 2, we find the total horizontal and vertical velocity components to be

$$\begin{aligned} \dot{u} &= \frac{\sin \delta}{\sqrt{\rho_{\alpha} \cos \delta}} (UP + DP) + \frac{\cos \gamma}{\sqrt{\rho_{\beta} \cos \gamma}} (US + DS) \\ \dot{w} &= \frac{-\cos \delta}{\sqrt{\rho_{\alpha} \cos \delta}} (UP - DP) + \frac{\sin \gamma}{\sqrt{\rho_{\beta} \cos \gamma}} (US - DS) \end{aligned} \quad (2-42)$$

From Snell's law, we have

$$\cos \delta = p_{\alpha} \sin \delta \quad , \quad \cos \gamma = p_{\beta} \sin \gamma \quad (2-42a)$$

where

$$p_{\alpha} = \sqrt{\left(\frac{c}{\alpha}\right)^2 - 1} \quad , \quad p_{\beta} = \sqrt{\left(\frac{c}{\beta}\right)^2 - 1} \quad (2-42b)$$

Substituting these relations into (2-42), we obtain the velocity vector

$$\sqrt{\rho c} \begin{bmatrix} \dot{u} \\ \dot{w} \end{bmatrix} = \begin{bmatrix} \frac{1}{\sqrt{\rho_\alpha}} & \sqrt{\rho_\beta} \\ \sqrt{\rho_\alpha} & -\frac{1}{\sqrt{\rho_\beta}} \end{bmatrix} \begin{bmatrix} DP \\ DS \end{bmatrix} + \begin{bmatrix} \frac{1}{\sqrt{\rho_\alpha}} & \sqrt{\rho_\beta} \\ -\sqrt{\rho_\alpha} & \frac{1}{\sqrt{\rho_\beta}} \end{bmatrix} \begin{bmatrix} UP \\ US \end{bmatrix}$$

(2-43)

Generally speaking, we cannot recover the four up and down travelling waves in (2-43) from a single two component seismograph record. However, if the receiver is at the free surface of a layered halfspace, then the up and down travelling wave vectors are related by

$$\bar{d} = R_o \bar{u}$$

where R_o is the reflection coefficient matrix for waves incident from below the free surface. If the properties of the surface layer are known, then R_o can be calculated, assuming the phase velocity is determined by other means. Then we can invert (2-43) to obtain

$$\begin{bmatrix} UP \\ US \end{bmatrix} = \sqrt{\rho c} K^{-1} \begin{bmatrix} \dot{u} \\ \dot{w} \end{bmatrix}$$

(2-44)

where K is the 2×2 matrix

$$K = \begin{bmatrix} \frac{1}{\sqrt{\rho\alpha}} & \sqrt{\rho\beta} \\ \sqrt{\rho\alpha} & -\frac{1}{\sqrt{\rho\beta}} \end{bmatrix} R_0 + \begin{bmatrix} \frac{1}{\sqrt{\rho\alpha}} & \sqrt{\rho\beta} \\ -\sqrt{\rho\alpha} & \frac{1}{\sqrt{\rho\beta}} \end{bmatrix} \quad (2-45)$$

It is also desirable to compute records of the normal and tangential stress at an interface due to the four travelling waves. The stress components are given in Appendix A by equation (A-7) in terms of elastic potentials. Replacing the elastic potentials by their corresponding waves as defined by (2-6) gives us the stress components as

$$\tau_{zz} = -\frac{(\lambda + 2\mu \cos^2 \delta)}{\sqrt{\rho\alpha^3 \cos \delta}} (UP + DP) + \frac{2\mu \sin \delta \cos \delta}{\sqrt{\rho\beta^3 \cos \delta}} (US + DS)$$

$$\tau_{zx} = \frac{2\mu \sin \delta \cos \delta}{\sqrt{\rho\alpha^3 \cos \delta}} (UP - DP) + \frac{\mu (\cos^2 \delta - \sin^2 \delta)}{\sqrt{\rho\beta^3 \cos \delta}} (US - DS)$$

These equations reduce further using (2-42a) and (2-42b). Finally,

we obtain

$$\frac{1}{\sqrt{\rho c}} \begin{bmatrix} \tau_{zz} \\ \tau_{zx} \end{bmatrix} = \begin{bmatrix} -\gamma & \sqrt{\rho\beta}(1-\gamma) \\ -\sqrt{\rho\alpha}(1-\gamma) & -\gamma \end{bmatrix} \begin{bmatrix} DP \\ DS \end{bmatrix} + \begin{bmatrix} -\gamma & \sqrt{\rho\beta}(1-\gamma) \\ \sqrt{\rho\alpha}(1-\gamma) & \gamma \end{bmatrix} \begin{bmatrix} UP \\ US \end{bmatrix} \quad (2-46)$$

where $\gamma = 1 - 2(\beta/c)^2$.

2.7 Figure Captions

2.1 Elastic plane waves in an isotropic homogeneous layer.

Shear and compressional waves have phase velocity c in x direction.

Instantaneous particle velocities are measured in direction of large arrows in x - z plane.

2.2 Instantaneous waves measured at $x=0$ on each interface.

Primed waves are evaluated at the bottom of each layer, unprimed waves at the top.

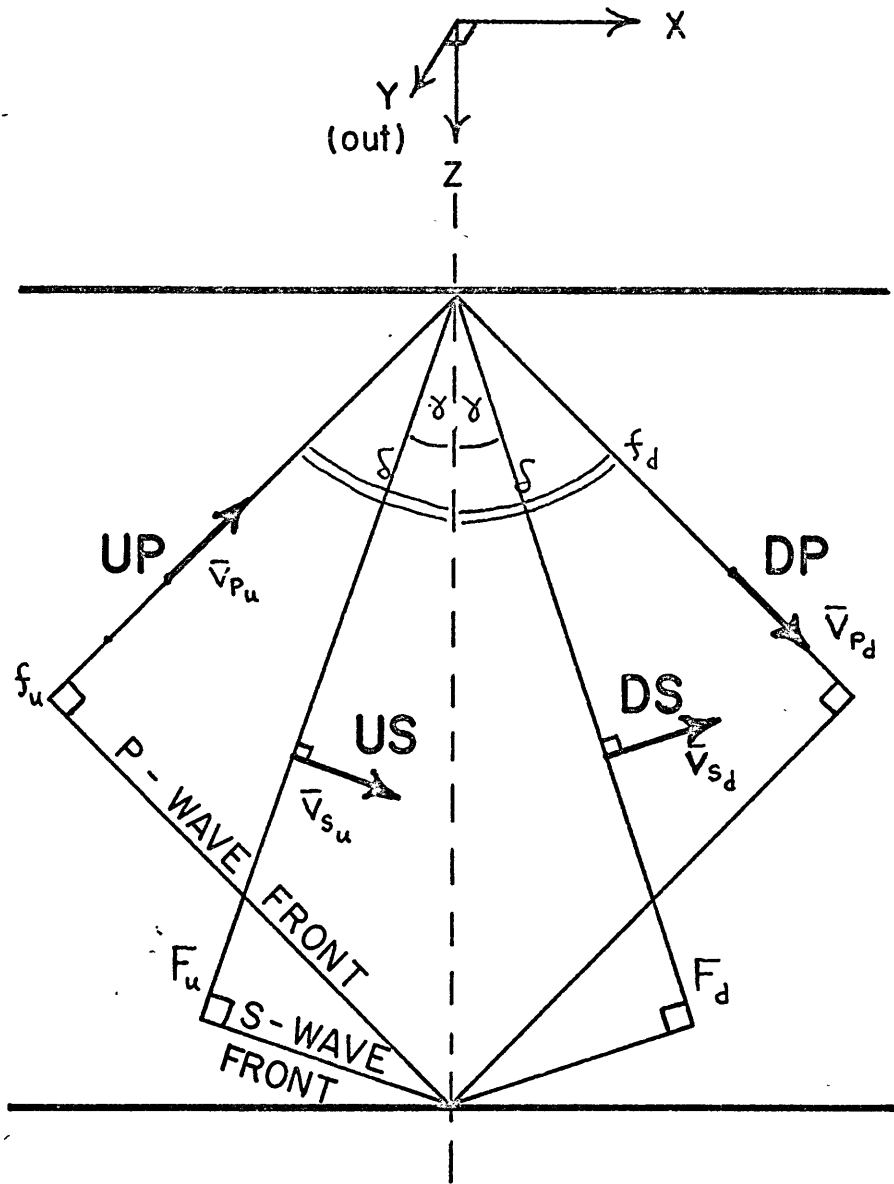


FIGURE 2.1

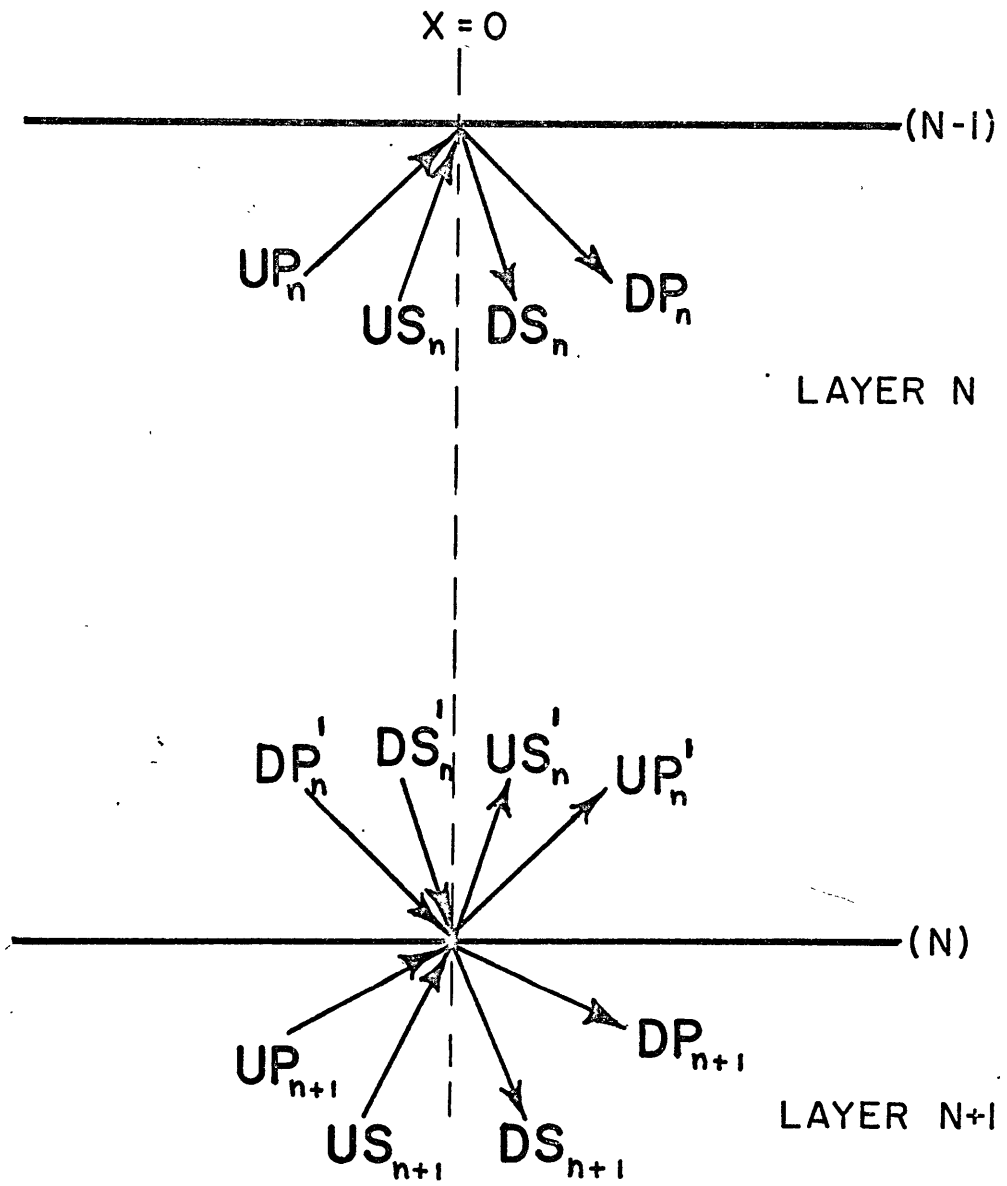


FIGURE 2.2

Chapter III

Extension to Multilayer Problems

3.1 Introduction

In this chapter, we apply the layer matrix iteration of Chapter II to some multilayer problems. Section 3.2 shows how our 4×4 layer matrix reduced at normal incidence to two 2×2 layer matrices, one for P waves and one for SV waves. The general form of products of such layer matrices is discussed both as a review of previous work, e.g. Goupilland (1961), Sherwood and Trorey (1965), and as an introduction to section 3.3 which examines products of layer matrices for non-normal incidence. In section 3.4, the reflection and transmission responses of a stack of layers between two halfspaces are computed. Finally, we use the principle of conservation of energy to obtain a relation between the reflection and transmission responses of section 3.4.

3.2 Layer Matrix Products for Waves at Normal Incidence

In this section, we show how the P and SV waves uncouple in the layer matrix iteration when the waves are at normal incidence to the layers. We then consider products of such layer matrices. The form of such products has been discussed by Goupillaud (1961), Sherwood and Trorey (1965), Robinson and Treitel (1966), and Claerbout (1968).

Our treatment differs from that of the above authors only in the definition of reflection and transmission coefficients. The reflection and transmission coefficients, in our case, are defined in terms of the square root of the instantaneous power carried by each wave, whereas the other authors define their coefficients in terms of particle velocities or pressures caused by the waves in a layer. As a result of this, our reflection and transmission coefficients are related by different identities, although in the end our layer iteration has exactly the same form as that of the other authors.

The uncoupling of P and SV waves as the phase velocity goes to infinity is most easily seen from (2-11). Letting all reflection and transmission coefficients go to zero which convert modes, e.g. r_{ps} , t_{ps} we obtain the interface relation

$$\begin{bmatrix} 1 & 0 & -r_{pp} & 0 \\ 0 & 1 & 0 & -r_{ss} \\ 0 & 0 & t_{pp} & 0 \\ 0 & 0 & 0 & t_{ss} \end{bmatrix} \begin{bmatrix} DP \\ DS \\ UP \\ US \end{bmatrix}_{n+1} = \begin{bmatrix} t'_{pp} & 0 & 0 & 0 \\ 0 & t'_{ss} & 0 & 0 \\ -r'_{pp} & 0 & 1 & 0 \\ 0 & -r'_{ss} & 0 & 1 \end{bmatrix} \begin{bmatrix} DP' \\ DS' \\ UP' \\ US' \end{bmatrix}_n$$

which splits into the following separate relations for P and SV waves:

$$\begin{bmatrix} 1 & -r_{pp} \\ 0 & t_{pp} \end{bmatrix} \begin{bmatrix} DP \\ UP \end{bmatrix}_{n+1} = \begin{bmatrix} t'_{pp} & 0 \\ -r'_{pp} & 1 \end{bmatrix} \begin{bmatrix} DP' \\ UP' \end{bmatrix}_n \quad (3-1)$$

and

$$\begin{bmatrix} 1 & -r_{ss} \\ 0 & t_{ss} \end{bmatrix} \begin{bmatrix} DS \\ US \end{bmatrix}_{n+1} = \begin{bmatrix} t'_{ss} & 0 \\ -r'_{ss} & 1 \end{bmatrix} \begin{bmatrix} DS' \\ US' \end{bmatrix}_n \quad (3-2)$$

From (2-23), we obtain

$$\begin{bmatrix} DP \\ UP \end{bmatrix}_n = \begin{bmatrix} z^{-l} & 0 \\ 0 & z^{+l} \end{bmatrix} \begin{bmatrix} DP' \\ UP' \end{bmatrix}_n$$

$$\begin{bmatrix} DS \\ US \end{bmatrix}_n = \begin{bmatrix} z^{-m} & 0 \\ 0 & z^m \end{bmatrix} \begin{bmatrix} DS' \\ US' \end{bmatrix}_n \quad (3-4)$$

Since the P and SV equations have identical form and are uncoupled, we need only consider one type of wave. Dropping all references to P waves in (3-1) and inverting the matrix on the right-hand side gives

$$\begin{bmatrix} D' \\ U' \end{bmatrix}_n = \frac{1}{t} \begin{bmatrix} 1 & r' \\ r' & 1 \end{bmatrix} \begin{bmatrix} D \\ U \end{bmatrix}_{n+1} \quad (3-5)$$

where we have used the identities

$$\begin{aligned} r'^2 + t^2 &= 1 \\ t &= t', \quad r = -r' \end{aligned} \quad (3-6)$$

These identities come from (2-18a), (2-16a) and (2-16c) when the phase velocity goes to infinity.

Now, we insert (3-3) into (3-5) to get the basic layer matrix relation in the form

$$\begin{bmatrix} D \\ U \end{bmatrix}_n = \frac{z^{-2l_n}}{t_n} \begin{bmatrix} 1 & r' \\ r' z^{2l} & z^{2l} \end{bmatrix} \begin{bmatrix} D \\ U \end{bmatrix}_{n+1} \quad (3-7)$$

which is essentially the same as obtained by Claerbout (1968). We now follow Claerbout and postulate that iterating over n layers gives a product of layer matrices with the following form:

$$\begin{bmatrix} D(z) \\ U(z) \end{bmatrix}_1 = z^{-K_n} \begin{bmatrix} f(z) & q(z) \\ z^{2K} q(1/z) & z^{2K} f(1/z) \end{bmatrix}_n \begin{bmatrix} D(z) \\ U(z) \end{bmatrix}_{n+1} \quad (3-8)$$

where

$$K_n = \sum_{i=1}^n l_i \quad (3-9)$$

and $f(z)$ and $q(z)$ are polynomials in z defined by

$$\begin{aligned} f(z) &= \frac{1}{\prod_{i=1}^n t_i} \left(1 + f_1 z + f_2 z^2 + \dots + f_{2(K_n - l_1)} z^{2(K_n - l_1)} \right) \\ q(z) &= \frac{1}{\prod_{i=1}^n t_i} \left(r_n + q_1 z + q_2 z^2 + \dots + q_{2(K_n - l_1)} z^{2(K_n - l_1)} \right) \end{aligned} \quad (3-10)$$

This also implies that $z^{2K_n} f(1/z)$ and $z^{2K_n} q(1/z)$ are polynomials so that each element within the matrix of (3-8) is a polynomial.

By comparison with (3-7), we see that (3-8) is true for $n = 1$.

Let us assume (3-8) is true for arbitrary n . Then, using (3-7), we obtain

$$\frac{1}{z} \begin{bmatrix} f_n(z) & q_n(z) \\ z^{2k_n} q_n(1/z) & z^{2k_n} f_n(1/z) \end{bmatrix} \cdot \frac{z^{-l_{n+1}}}{t_{n+1}} \begin{bmatrix} 1 & r'_{n+1} \\ r'_{n+1} z^{2l_{n+1}} & z^{2l_{n+1}} \end{bmatrix}$$

$$= \frac{1}{z} \begin{bmatrix} f_{n+1}(z) & q_{n+1}(z) \\ z^{2k_{n+1}} q_{n+1}(1/z) & z^{2k_{n+1}} f_{n+1}(1/z) \end{bmatrix}$$

where

$$\begin{aligned} f_{n+1}(z) &= (f_n(z) + r'_{n+1} z^{2l_{n+1}} q_n(z)) / t_{n+1} \\ q_{n+1}(z) &= (r'_{n+1} f_n(z) + z^{2l_{n+1}} q_n(z)) / t_{n+1} \end{aligned} \tag{3-11}$$

Since

$$\begin{aligned} f_1(z) &= 1/t_1 \\ q_1(z) &= r'_1/t_1 \end{aligned}$$

the iteration in (3-11) indicates that $f_n(z)$ and $q_n(z)$ are polynomials of degree $2(k_n - l_1)$ which have the form shown in (3-10).

This completes the induction proof of (3-8).

The determinant of the matrix in (3-7) is

$$\det = \frac{1 - r_n'^2}{t_n^2} = 1$$

using (3-6). Since the matrix of (3-8) is a product of matrices like that of (3-7), it also has a determinant equal to 1. This gives an important identity relating $f(z)$ and $g(z)$, namely

$$f(z)f(1/z) - g(z)g(1/z) = 1 \tag{3-12}$$

Claerbout obtains a constant different from 1 in this equation due to his definition of reflection and transmission coefficients. This equation states that the autocorrelations of the polynomials $f(z)$ and $g(z)$ differ by only an impulse of amplitude 1 at zero time. For all real ω this equation also indicates that the power spectra of $f(z)$ and $g(z)$ differ by a constant equal to 1.

3.3 General Form of Layer Matrix Products

In this section, we use the strategy of the previous section to show that at non-normal incidence a product of layer matrices

$$Q_n(z) = C_n(z) C_{n-1}(z) \cdots C_1(z) \quad (3-13)$$

has an inverse which can be written in partitioned form as

$$Q_n^{-1}(z) = \tilde{Q}_n^*(1/z) = z^{-S_n} \begin{bmatrix} F(z) & G(z) \\ z^{2S} G(1/z) & z^{2S} F(1/z) \end{bmatrix}_n \quad (3-13a)$$

where

$$S_n = \sum_{i=1}^n m_i \quad (3-14)$$

We shall also show that $F(z)$ and $G(z)$ are matrix polynomials of the form

$$\begin{aligned} F(z) &= F_0 + F_1 z + F_2 z^2 + \cdots + F_{2S_n - l_1 - m_1} z^{2S_n - l_1 - m_1} \\ G(z) &= G_0 + G_1 z + G_2 z^2 + \cdots + G_{2S_n - l_1 - m_1} z^{2S_n - l_1 - m_1} \end{aligned} \quad (3-15)$$

where F_i and G_i are real 2×2 matrix coefficients of z^i .

From this, we see that $z^{2S_n} F(1/z)$ and $z^{2S_n} G(1/z)$ in (3-13a) are matrix polynomials containing only positive powers of z .

From (3-13), we obtain an iteration for $Q_n(z)$, i.e.

$$Q_n(z) = C_n(z) Q_{n-1}(z) \quad (3-16)$$

Using (2-33) and this relation, we obtain

$$Q_n^{-1}(z) = Q_{n-1}^{-1}(z) \tilde{C}_n^*(1/z) \quad (3-17)$$

which is the iteration we shall use to prove (3-13a). For $n=1$, we have using (2-27a)

$$Q_1^{-1}(z) = \tilde{C}_1^*(1/z) = \begin{bmatrix} z_1^{-1} & z_1^{-1} R_1' \\ z_1 R_1' & z_1 \end{bmatrix} T_1^{*-1} \quad (3-18)$$

Since the SV transit time, $m_i \Delta \tau$, is always greater than the P transit time, $l_i \Delta \tau$, through the i -th layer we can factor z^{-m_1} out of the brackets in (3-18) and leave only positive powers of z inside. Thus, we can define matrix polynomials $F_1(z)$ and $G_1(z)$ by

$$\begin{aligned} z^{-m_1} F_1(z) &= z_1^{-1} T_1^{*-1} \\ z^{-m_1} G_1(z) &= z_1^{-1} R_1' T_1^{*-1} \end{aligned} \quad (3-19)$$

Then (3-18) can be written as

$$Q_1^{-1}(z) = z^{-m_1} \begin{bmatrix} F_1(z) & G_1(z) \\ z^{2m_1} G_1(1/z) & z^{2m_1} F_1(1/z) \end{bmatrix} \quad (3-20)$$

where from (3-19)

$$F_1(z) = \begin{bmatrix} z^{m_1 - l_1} & 0 \\ 0 & 1 \end{bmatrix} T_1^{*-1} \quad (3-21)$$

and

$$G_1(z) = \begin{bmatrix} z^{m_1 - l_1} & 0 \\ 0 & 1 \end{bmatrix} R_1 T_1^{*-1}$$

Clearly $F_1(z)$ and $G_1(z)$ can be written in the polynomial matrix form of (3-15), the highest power of z being $m_1 - l_1$.

Therefore, we have verified (3-15) and (3-13a) for $n=1$. To complete the proof, we assume the forms of (3-13a) and (3-15) are true for $(n-1)$ layers and show that this implies they are true for n layers.

From (3-17) we have

$$Q_n^{-1}(z) = z^{-s_{n-1}} \begin{bmatrix} F_{n-1}(z) & G_{n-1}(z) \\ z^{2s_{n-1}} G_{n-1}(1/z) & z^{2s_{n-1}} F_{n-1}(1/z) \end{bmatrix} \begin{bmatrix} z_n^{-1} & z_n^{-1} R_n' \\ z_n R_n' & z_n \end{bmatrix} T_n^{*-1} \quad (3-22)$$

Now we factor z^{-m_n} out of the right-hand brackets in this equation.

This leaves only positive powers of z within these brackets to be multiplied by polynomial matrices of the left-hand brackets. Thus, we have

$$Q_n^{-1}(z) = z^{-s_n} \begin{bmatrix} F_n(z) & G_n(z) \\ z^{2s_n} G_n(1/z) & z^{2s_n} F_n(1/z) \end{bmatrix} \quad (3-23)$$

where

$$F_n(z) = z^{m_n} (F_{n-1}(z) z_n^{-1} + G_{n-1}(z) z_n R_n') T_n^{*-1}$$

and

$$G_n(z) = z^{m_n} (F_{n-1}(z) z_n^{-1} R_n' + G_{n-1}(z) z_n) T_n^{*-1}$$

(3-24)

This verifies (3-13a) for all n . From this iteration, we see that

$F_n(z)$ and $G_n(z)$ each have degree $2m_n$ higher than $F_{n-1}(z)$ and $G_{n-1}(z)$ due to the term

$$z^{m_n} Z_n$$

which occurs in each iteration. Thus, if $F_{n-1}(z)$ has degree

$$2S_{n-1} - l_1 - m_1, \text{ then } F_n(z) \text{ has degree } 2S_n - l_1 - m_1.$$

This completes the proof of (3-15) by induction.

A useful result of (3-13a) and (3-15) is that only two submatrices of $Q_n^{-1}(z)$ need to be determined by iteration since the remaining two submatrices are obtained by replacing z by $1/z$ in the first two. This is the same as reversing each sequence of pulses in time, i.e. replacing t by $-t$ in the pulse sequence represented by each polynomial in z .

So far in this section, we have essentially duplicated the proofs of section 3.2. Equations (3-13a), (3-15) and (3-24) in this section are matrix extensions to non-normal incidence of equations (3-8), (3-10) and (3-11) of the previous section. The only complication which prevents both sets of equations from being completely analogous is that Z_i^{-1} does not commute with other matrices in the non-normal incidence case and cannot be factored out in as simple fashion as z^{-l_i} was in the normal incidence case.

Finally, we derive several identities for the non-normal incidence case which are analogous to (3-12) in the normal incidence case. From (2-37), we see that $Q_n(z)$ and its inverse commute since they have non-zero determinants. $Q_n(z)$ is obtained from $Q_n^{-1}(z)$ in (3-13a), i.e.

$$Q_n(z) = \tilde{Q}_n^{*-1}(1/z) = z^{-s_n} \begin{bmatrix} z^{2s_n} F_n^*(1/z) & -G_n^*(z) \\ -z^{2s_n} G_n^*(1/z) & F_n^*(z) \end{bmatrix} \quad (3-25)$$

Thus, $Q_n(z)$ can also be expressed as z^{-s_n} times 2×2 polynomial matrices. Taking the product

$$Q_n^{*-1}(z) Q_n(z) = I_4$$

we obtain the identities

$$F_n(z) F_n^*(1/z) - G_n(z) G_n^*(1/z) = I_2 \quad (3-26)$$

$$F_n(z) G_n^*(z) - G_n(z) F_n^*(z) = 0 \quad (3-27)$$

I_2 and I_4 are respectively 2×2 and 4×4 identity matrices.

From

$$Q_n(z) Q_n^{*-1}(z) = I_4$$

we derive

$$F_n^*(1/z) F_n(z) - G_n^*(z) G_n(1/z) = I_2 \quad (3-28)$$

$$G_n^*(1/z) F_n(z) - F_n^*(z) G_n(1/z) = 0 \quad (3-29)$$

These identities are used in the next section and in Chapter IV which describes plane waves in a layered halfspace.

3.4 Transmission and Reflection Responses of a Layered Medium

We now consider the solution of P and SV plane waves in multilayer media. In this section, we treat the case of n elastic layers between two elastic halfspaces as shown in Figure 3.1. We shall assume that a known upgoing plane wave source \bar{S}_{n+1} is incident to the n -th interface from the lower halfspace. With no other sources in the medium, we shall calculate the reflected vector \bar{d}_1 and the transmitted vector \bar{u}_1 in terms of \bar{S}_{n+1} .

Substituting (3-13a) into (2-28) yields

$$\begin{bmatrix} \bar{d}_1 \\ \bar{u}_1 \end{bmatrix} = \frac{1}{z} \begin{bmatrix} F(z) & G(z) \\ z^{2s} G(1/z) & z^{2s} F(1/z) \end{bmatrix} \begin{bmatrix} \bar{d}_{n+1} \\ \bar{u}_{n+1} \end{bmatrix} \quad (3-30)$$

Letting

$$\begin{aligned} \bar{d}_1 &= R_0 \bar{u}_1 \\ \bar{u}_{n+1} &= \bar{S}_{n+1} \end{aligned}$$

we find

$$\begin{bmatrix} R_0 \bar{u}_1 \\ \bar{u}_1 \end{bmatrix} = \frac{1}{z} \begin{bmatrix} F(z) & G(z) \\ z^{2s} G(1/z) & z^{2s} F(1/z) \end{bmatrix} \begin{bmatrix} \bar{d}_{n+1} \\ \bar{S}_{n+1} \end{bmatrix} \quad (3-31)$$

Multiplying the second row of this equation by R_0 and subtracting it from the first row gives

$$\begin{bmatrix} 0 \\ \bar{u}_1 \end{bmatrix} = \frac{z^{-s}}{z} \begin{bmatrix} F(z) - z^{2s} R_0 G(1/z) & G(z) - z^{2s} R_0 F(1/z) \\ z^{2s} G(1/z) & z^{2s} F(1/z) \end{bmatrix} \begin{bmatrix} \bar{d}_{n+1} \\ \bar{s}_{n+1} \end{bmatrix} \quad (3-32)$$

From the first row, we obtain

$$\bar{d}_{n+1} = R^{(n)}(z) \bar{s}_{n+1} \quad (3-33)$$

where we define $R^{(n)}(z)$ to be the reflection response of the n layers given by

$$R^{(n)}(z) = - \left[F(z) - z^{2s} R_0 G(1/z) \right]^{-1} \left[G(z) - z^{2s} R_0 F(1/z) \right] \quad (3-34)$$

We also define a transmission response $T^{(0)}(z)$ for the layers such that

$$\bar{u}'_0 = T^{(0)}(z) \bar{s}_{n+1} = T_0 \bar{u}_1 \quad (3-35)$$

To calculate \bar{u}_1 , most easily, we invert (3-31) using (3-25) yielding

$$\begin{bmatrix} \bar{d}_{n+1} \\ \bar{s}_{n+1} \end{bmatrix} = \frac{z^{-s}}{z} \begin{bmatrix} z^{2s} F^*(1/z) & -G^*(z) \\ -z^{2s} G^*(1/z) & F^*(z) \end{bmatrix} \begin{bmatrix} R_0 \bar{u}_1 \\ \bar{u}_1 \end{bmatrix} \quad (3-36)$$

From the second row, we obtain

$$\bar{u}_1 = z^s \left[F^*(z) - z^{2s} G^*(1/z) R_o \right]^{-1} \bar{s}_{n+1} \quad (3-37)$$

Comparing this equation to (3-35), we see that the transmission response is

$$T_{(z)}^{(o)} = z^s T_o \left[F^*(z) - z^{2s} G^*(1/z) R_o \right]^{-1} \quad (3-38)$$

Substituting (3-37) into the first row of (3-36) gives another expression for the reflection response, i.e.

$$R_{(z)}^{(n)} = - \left[G^*(z) - z^{2s} F^*(1/z) R_o \right] \left[F^*(z) - z^{2s} G^*(1/z) R_o \right]^{-1} \quad (3-39)$$

If we transpose this solution for $R_{(z)}^{(n)}$ we obtain the solution given in (3-34). Therefore, the reflection response is symmetric, namely

$$R_{(z)}^{*(n)} = R_{(z)}^{(n)} \quad (3-40)$$

This is a proof of the reciprocity relation between source and receiver when both are located just below the n-th interface. That is, the reflection coefficient for P to SV conversion equals the coefficient for SV to P conversion, all waves having the same phase velocity c .

Setting the right-hand sides of (3-39) and (3-34) equal to each other yields another relation

$$\begin{aligned}
& [F(z) - z^{2s} R_o G(1/z)] [G^*(z) - z^{2s} F^*(1/z) R_o] \\
& = [G(z) - z^{2s} R_o F(1/z)] [F^*(z) - z^{2s} G^*(1/z) R_o]
\end{aligned}
\tag{3-41}$$

which can be verified by applying identities (3-26) through (3-29) to each product of this equation. One can show that the reflection and transmission responses are simply related to each other by conserving energy through the stack of layers. When $\bar{u}_{n+1} = \bar{s}_{n+1}$ is the only wave vector incident to the n layers, we have

$$\bar{s}_{n+1}^*(1/z) \cdot \bar{s}_{n+1}(z) = \bar{d}_{n+1}^*(1/z) \cdot \bar{d}_{n+1}(z) + \bar{u}_o^*(1/z) \cdot \bar{u}_o(z)
\tag{3-42}$$

For real ω , i.e. $|z| = 1$, each scalar product on the right-hand side of this equation represents the energy density flow of the P and SV components leaving the n layers through an interface. The left-hand side contains the energy density flow of the incident source waves. Putting in the reflection and transmission responses, this equation becomes

$$\bar{s}_{n+1}^*(1/z) \cdot \bar{s}_{n+1}(z) = \bar{s}_{n+1}^*(1/z) \left\{ R_{(n)}^*(1/z) R_{(n)}(z) + T_{(n)}^*(1/z) T_{(n)}(z) \right\} \cdot \bar{s}_{n+1}(z)$$

for arbitrary sources. This is only possible if

$$R_{(n)}^*(1/z) R_{(n)}(z) + T_{(n)}^*(1/z) T_{(n)}(z) = I_2
\tag{3-43}$$

We shall prove this equation using the solutions for $R_{(z)}^{(n)}$ and $T_{(z)}^{(n)}$ given by (3-38) and (3-39). They give

$$\begin{aligned}
 R_{(1/2)}^{*(n)} R_{(z)}^{(n)} + T_{(1/2)}^{*(0)} T_{(z)}^{(0)} &= [F(1/2) - z^{-2s} R_0 G(z)]^{-1} \\
 \cdot \left\{ [z^{-2s} R_0 F(z) - G(1/2)] [z^{2s} F^*(1/2) R_0 - G^*(z)] + T_0^* T_0 \right\} \\
 \cdot [F^*(z) - z^{2s} G^*(1/2) R_0]^{-1}
 \end{aligned} \tag{3-44}$$

We now evaluate the terms within braces $\{ \}$ of this equation using (3-41). Multiplying (3-41) by $z^{-2s} R_0$ from the left, we get

$$\begin{aligned}
 [z^{-2s} R_0 F(z) - R_0^2 G(1/2)] [z^{2s} F^*(1/2) R_0 - G^*(z)] \\
 = [R_0^2 F(1/2) - z^{-2s} R_0 G(z)] [F^*(z) - z^{2s} G^*(1/2) R_0]
 \end{aligned} \tag{3-45}$$

Now, since

$$R_0^2 + T_0^* T_0 = I_2$$

we can write (3-45) as

$$\begin{aligned}
 [z^{-2s} R_0 F(z) - G(1/2)] [z^{2s} F^*(1/2) R_0 - G^*(z)] \\
 = -T_0^* T_0 \left\{ G(1/2) [z^{2s} F^*(1/2) R_0 - G^*(z)] + F(1/2) [F^*(z) - z^{2s} G^*(1/2) R_0] \right\} \\
 + [F(1/2) - z^{-2s} R_0 G(z)] [F^*(z) - z^{2s} G^*(1/2) R_0]
 \end{aligned} \tag{3-46}$$

Rearranging the terms inside braces in this expression gives

$$\left\{ \right\} = z^{2s} \left[G(1/z) F^*(1/z) - F(1/z) G^*(1/z) \right] R_0 + \left[F(1/z) F^*(z) - G(1/z) G^*(z) \right]$$

But from (3-26) and (3-27), we see that the terms of the first bracket vanish, and the second bracket reduces to I_2 . Therefore,

$$\left\{ \right\} = I_2$$

and (3-46) reduces to

$$\begin{aligned} & \left[z^{-2s} R_0 F(z) - G(1/z) \right] \left[z^{2s} F^*(1/z) - G^*(z) \right] = \\ & T_0^* T_0 + \left[F(1/z) - z^{-2s} R_0 G(z) \right] \left[F^*(z) - z^{2s} G^*(1/z) R_0 \right] \end{aligned} \quad (3-47)$$

The left-hand side of this equation is the same as the product of the bracketed terms inside the braces of (3-44). Substituting (3-47) into (3-44) gives

$$\begin{aligned} & \left[F(1/z) - z^{-2s} R_0 G(z) \right]^{-1} \left\{ \left[F(1/z) - z^{-2s} R_0 G(z) \right] \left[F^*(z) - z^{2s} G^*(1/z) R_0 \right] \right\} \cdot \\ & \left[F^*(z) - z^{2s} G^*(1/z) R_0 \right]^{-1} \end{aligned}$$

which equals I_2 . This completes the proof of (3-43).

Finally, we shall calculate the transmission response for a source just above the 0 interface and verify the principle of reciprocity for transmitted waves through the layers.

Let a source $\vec{d}_0^i = \vec{S}_0^i$ be incident from above the layers

at interface 0. Then setting

$$\bar{u}_{n+1} = 0$$

and

$$\bar{d}_1 = R_0 \bar{u}_1 + T_0' \bar{s}_0'$$

in (3-30) gives the equation

$$\begin{bmatrix} R_0 \bar{u}_1 + T_0' \bar{s}_0' \\ \bar{u}_1 \end{bmatrix} = \frac{1}{z^{-s}} \begin{bmatrix} F(z) & G(z) \\ z^{2s} G(1/z) & z^{2s} F(1/z) \end{bmatrix} \begin{bmatrix} \bar{d}_{n+1} \\ 0 \end{bmatrix} \quad (3-48)$$

Multiplying the second row of this equation by R_0 and subtracting the result from the first row gives

$$T_0' \bar{s}_0' = \frac{1}{z^{-s}} (F(z) - z^{2s} R_0 G(1/z)) \bar{d}_{n+1}$$

Solving for \bar{d}_{n+1} we obtain

$$\bar{d}_{n+1} = T^{(n)}(z) \bar{s}_0' \quad (3-49)$$

where $T^{(n)}(z)$ is the transmission response given by

$$T^{(n)}(z) = z^s [F(z) - z^{2s} R_0 G(1/z)]^{-1} T_0' \quad (3-50)$$

This transmission response is related to $T^{(0)}(z)$ by the reciprocity principle. For example, a unit impulsive SV source just below the n -th interface generates a transmitted P wave just above the 0 interface which equals the SV wave recorded below the n -th interface generated by a unit impulsive P source above the 0 interface; all waves and sources having a common phase velocity C .

This reciprocity relation can be expressed in terms of the transmission responses, i.e.

$$T^{(n)*}(z) = T^{(0)}(z) \quad (3-51)$$

This is easily verified from the solutions given by (3-50) and (3-38). Taking the transpose of (3-50) gives

$$T^{(n)*}(z) = z^s T_0 \left[F^x(z) - z^{2s} G^{(1/2)*} R_0 \right]^{-1} \quad (3-52)$$

where we have used the identity

$$T_0^* = T_0$$

Comparing (3-52) to (3-38) we see that

$$T^{(n)*}(z) = T^{(0)}(z)$$

as conjectured.

3.5 Figure Captions

3.1 Stack of n elastic homogeneous layers between two elastic halfspaces. An upgoing source \bar{S}_{n+1} is incident to the layers from the lower halfspace.

UPPER HALF SPACE

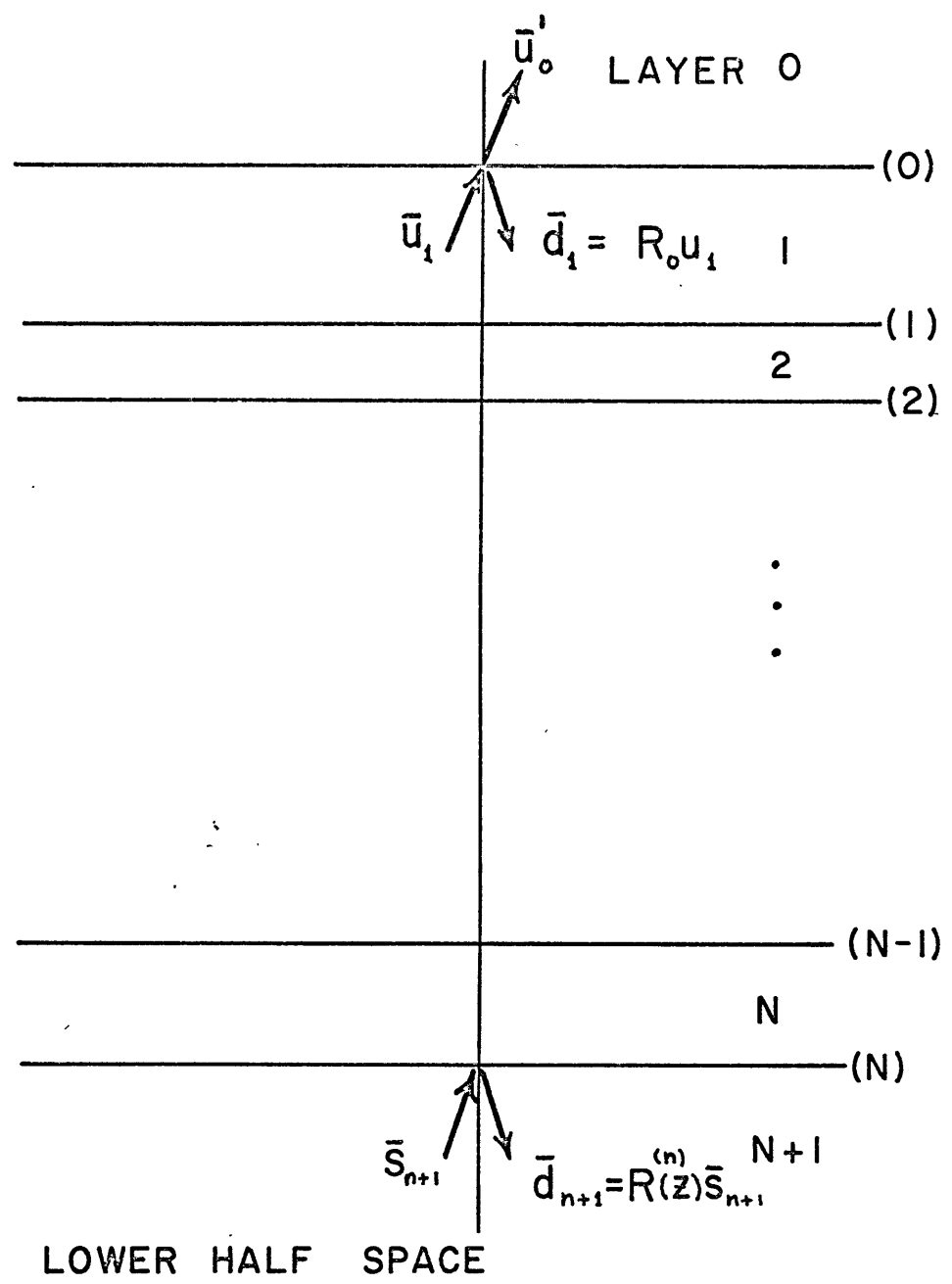


FIGURE 3.1

Chapter IV

Waves in a Layered Halfspace

4.1 Introduction

This chapter describes the propagation of homogeneous plane waves in a layered halfspace, the uppermost interface being free. As in Chapter III, we can define reflection and transmission responses of a layered halfspace for a deep upgoing plane wave source. Since no energy is transmitted across the free surface, the transmission response is defined in terms of upgoing waves arriving at the free surface from below. Such a response is useful, for example, in computing the distortion produced by a layered crust on teleseismic events recorded at the Earth's surface.

The reflection response contains all the energy of the incident source since no waves pass through the free surface. As shown in Section 4.2, this implies that

$$R_{(z)}^{(n)*} R_{(z)}^{(n)} = I_2$$

which is a special case of the conservation of energy theorem given in Chapter III.

Section 4.3 describes the reflection and transmission response when a downgoing source is located just below the free surface. This transmission response equals the transpose of the transmission response

for a deep source.

In Section 4.4, it is shown that the reflection response for a surface source equals the positive time part of the autocorrelation matrix of the transmission response due to a deep source. This is an extension to non-normal incidence of a theorem proved by Claerbout for compressional waves at normal incidence. A possible use for this theorem is to obtain reflection seismograms for the Earth's crust from teleseismic events recorded at the free surface. At normal incidence, it is possible in principle to use the surface source reflection response to calculate the impedances of the crustal layers as described by Kunetz (1962) and Claerbout (1968). Unfortunately, this inversion scheme is not easily extended to non-normal incidence for reasons given in Section 4.3.

The estimation of the matrix polynomial

$$M(z) = F(z) - z^{2S} R_0 G(1/z)$$

for observed transmitted waves at the free surface is discussed in Section 4.4. The calculation of $M(z)$ is useful because each reflection and transmission response discussed above can be obtained from $M(z)$ and R_0 the reflection coefficient matrix for the free surface. One may also remove the crustal reverberations contaminating teleseismic waves by premultiplying the upgoing waves \bar{u} by $M^*(z)$.

4.2 Transmission and Reflection Responses of a Layered Halfspace for a Deep Source

We now adapt the results of the previous chapter to solve for the P and SV plane waves in a layered halfspace. Let the upper halfspace in Figure 3.1 be a vacuum so that interface 0 is free. This change affects only the reflection and transmission coefficients at interface 0. No transmitted waves are possible across interface 0 so that

$T_0 = 0$. Also by conservation of energy

$$R_0^* R_0 = R_0^2 = I_2 \quad (4-1)$$

For a deep plane wave source $\bar{u}_{n+1} = \bar{s}_{n+1}$, the waves transmitted through the layers to the free surface are given by (3-37), i.e.

$$\bar{u}_1 = z^s M^{*-1}(z) \bar{s}_{n+1} \quad (4-2)$$

where we define the matrix

$$M(z) = [F(z) - z^{2s} R_0 G(1/z)] \quad (4-3)$$

We shall call the matrix coefficient of \bar{s}_{n+1} in (4-2) the transmission response $X(z)$ of a layered halfspace generated by

a deep source. Thus,

$$X(z) = z^s M^{*-1}(z) = z^s [F^*(z) - z^{2s} G^*(1/z) R_0]^{-1} \quad (4-5)$$

The reflection response generated by \bar{S}_{n+1} and recorded just below the n-th interface is given by (3-39). Using (4-1) and (4-3) this reflection response can be written as

$$\begin{aligned} R^{(n)}(z) &= z^{2s} [F^*(1/z) - z^{-2s} G^*(z) R_0] R_0 [F^*(z) - z^{2s} G^*(1/z) R_0]^{-1} \\ &= z^{2s} M^*(1/z) R_0 M^{*-1}(z) \end{aligned} \quad (4-6)$$

Similarly, from (3-34), we obtain an alternate expression

$$R^{(n)}(z) = z^{2s} M^{-1}(z) R_0 M(1/z) \quad (4-7)$$

Comparing these last two equations, we see that $R^{(n)}(z)$ is symmetric as in the previous chapter in which interface 0 was not free. Taking the transpose conjugate of (4-6) and multiplying it by (4-7), we have

$$R^{*(n)}(1/z) R^{(n)}(z) = z^{-2s} M^{-1}(1/z) R_0 M(z) z^{2s} M^{-1}(z) R_0 M(1/z)$$

which reduces to

$$R^{*(n)}(z) R^{(n)}(z) = I_2 \quad (4-8)$$

using (4-1). This is a special case of the conservation of energy theorem, equation (3-43), in which no waves are transmitted across the free interface, interface 0.

We define the elements of the reflection response by

$$R^{(n)}(z) = \begin{bmatrix} r_{pp}(z) & r_{sp}(z) \\ r_{ps}(z) & r_{ss}(z) \end{bmatrix}_n \quad (4-8a)$$

This notation is similar to that used in (2-12) to define the reflection matrix for a single interface. In this case, the elements of are frequency dependent rather than constant as in (2-12).

Putting these elements into (4-8) yields three scalar identities, which are

$$r_{pp}(1/z) r_{pp}(z) + r_{ps}(1/z) r_{ps}(z) = 1 \quad (4-9)$$

$$r_{pp}(1/z) r_{sp}(z) + r_{ps}(1/z) r_{ss}(z) = 0 \quad (4-10)$$

$$r_{sp}(1/z) r_{sp}(z) + r_{ss}(1/z) r_{ss}(z) = 1 \quad (4-11)$$

Equations (4-9) and (4-11) state that energy is conserved when the incident source at the bottom of the layers is either an impulsive P or SV wave of unit power. In the frequency domain, these two equations

show that the sum of the power spectra of reflected P and SV waves equals 1 for either type of incident impulsive source. Moreover, since $R^{(n)}(z)$ is symmetric, we also have

$$r_{ps}(z) = r_{sp}(z) \quad (4-12)$$

Using this relation and subtracting (4-11) from (4-9) gives

$$r_{pp}(1/z)r_{pp}(z) = r_{ss}(1/z)r_{ss}(z) \quad (4-13)$$

which shows that impulsive responses $r_{pp}(z)$ and $r_{ss}(z)$ have equal power spectra. Thus, their Fourier spectra differ only by a phase shift.

Let us define the Fourier spectra

$$\begin{aligned} r_{pp}(z) &= A_{pp}(\omega) e^{-i\phi_{pp}(\omega)} \\ r_{ps}(z) &= A_{ps}(\omega) e^{-i\phi_{ps}(\omega)} \\ r_{ss}(z) &= A_{ss}(\omega) e^{-i\phi_{ss}(\omega)} \end{aligned} \quad (4-14)$$

where

$$z = e^{-i\omega\Delta t}$$

Each $A(\omega)$ in (4-14) is a non-negative amplitude spectrum and each $\phi(\omega)$ is the phase lag spectrum associated with $A(\omega)$. For real ω replacing z by $1/z$ on the left-hand side of (4-14) is equivalent to reversing the sign of ω on the right-hand side. Since each element of $R^{(n)}(z)$ represents a real time function, changing the sign of ω only changes the sign of the phase lag $\phi(\omega)$ of each term in (4-14).

Substituting the above spectra into (4-13) and (4-9) yields two relations for the amplitude spectra of (4-14):

$$A_{ss}(\omega) = A_{pp}(\omega) \quad (4-15)$$

$$A_{ps}(\omega) = \sqrt{1 - A_{pp}^2(\omega)} \quad (4-16)$$

We now utilize (4-10) to obtain an interesting equation relating the phase lags. Combining (4-10) with (4-12) and substituting (4-14) and (4-15) into the result, we derive

$$e^{-i(-\phi_{pp}(\omega) + \phi_{ps}(\omega))} = -e^{-i(-\phi_{ps}(\omega) + \phi_{ss}(\omega))}$$

Thus

$$\phi_{ps}(\omega) = \frac{(\phi_{pp}(\omega) + \phi_{ss}(\omega))}{2} \pm \frac{\pi}{2} \quad (4-17)$$

Let us consider the low frequency limit of (4-17). For very long wavelengths, the effect of the stack of layers above interface n disappears and the reflection coefficients of $R^{(n)}(z)$ become those of a homogeneous halfspace. For large phase velocity, i.e.

$$c \gg \alpha > \beta$$

the elements of $R^{(n)}(z)$ are obtained from equations (A-61) in Appendix

A:

$$r_{pp} \approx \frac{-1 + 4\left(\frac{\beta}{c}\right)^2 [1 + \beta/\alpha]}{+1 - 4\left(\frac{\beta}{c}\right)^2 [1 - \beta/\alpha]} < 0$$

$$r_{ss} = -r_{pp} > 0$$

$$r_{ps} \approx \frac{4\frac{\beta^2}{c\sqrt{\alpha\beta}}}{1 - 4\left(\frac{\beta}{c}\right)^2 [1 - \beta/\alpha]} > 0$$

Therefore, $\phi_{ps}(0) = 0$, $\phi_{ss}(0) = 0$, and $\phi_{pp}(0) = \pm \pi$

for large phase velocities. Equation (4-17) can thus be written with no sign ambiguity as

$$\phi_{ps} = \frac{(\phi_{pp}(\omega) - \phi_{pp}(0) + \phi_{ss}(\omega))}{2} \quad (4-18)$$

Equations (4-15), (4-16), and (4-18) show that given the Fourier amplitude and phase spectra of any two of the four elements of $R^{(n)}(z)$ we can easily calculate the spectra of the other two elements.

4.3 Transmission and Reflection Responses of a Layered Halfspace for a Surface Source

In this section, we place a downgoing source vector \bar{s}_1 just below the free surface of the halfspace and solve for the upgoing vector \bar{u}_1 and the downgoing vector \bar{d}_{n+1} . These solutions will give us respectively the reflection and transmission responses of the medium for a surface source.

The downgoing wave \bar{d}_1 equals the source vector \bar{s}_1 plus the upgoing vector \bar{u}_1 as it is reflected at the free surfaces. This reflected vector is $R_0 \bar{u}_1$, where R_0 is the reflection matrix for the free surface. Assuming that no deep sources exist in the lower halfspace, we set $\bar{u}_{n+1} = 0$. Putting these quantities into (3-30), we obtain

$$\begin{bmatrix} R_0 \bar{u}_1 + \bar{s}_1 \\ \bar{u}_1 \end{bmatrix} = \frac{1}{z^{-s}} \begin{bmatrix} F(z) & G(z) \\ z^{2s} G(1/z) & z^{2s} F(1/z) \end{bmatrix} \begin{bmatrix} \bar{d}_{n+1} \\ 0 \end{bmatrix}$$

(4-26)

We now premultiply the second row of this equation by R_0 and subtract the result from the first row, giving

$$\begin{bmatrix} \bar{s}_1 \\ \bar{u}_1 \end{bmatrix} = z^{-s} \begin{bmatrix} F(z) - z^{2s} R_0 G(1/z), G(z) - z^{2s} R_0 F(1/z) \\ z^{2s} G(1/z) & z^{2s} F(1/z) \end{bmatrix} \begin{bmatrix} d_{n+1} \\ 0 \end{bmatrix}$$

(4-27)

From the first row of this equation, we find

$$\begin{aligned} d_{n+1} &= z^s [F(z) - z^{2s} R_0 G(1/z)]^{-1} \bar{s}_1 \\ &= z^s M^{-1}(z) \bar{s}_1 \end{aligned}$$

(4-28)

and from the second row

$$\bar{u}_1 = z^{2s} G(1/z) M^{-1}(z) \bar{s}_1$$

(4-29)

Taking the matrix coefficient of \bar{s}_1 in each of the last two equations, we define the reflection response $R(z)$ and transmission response $T^{(n)}(z)$ as follows:

$$R(z) = z^{2s} G(1/z) M^{-1}(z) \quad (4-30)$$

$$T(z) = z^s M^{-1}(z) \quad (4-31)$$

where

$$\bar{u}_1 = R(z) \bar{s}_1 \quad (4-32)$$

$$\bar{d}_{r+1} = T(z) \bar{s}_1 \quad (4-33)$$

There are two additional reciprocity relations we can obtain by interchanging source and receiver positions, i.e.,

$$T^*(z) = X(z) \quad (4-34)$$

and

$$R^*(z) = R(z) \quad (4-34a)$$

The first relation is obvious from (4-3) and (4-5). The second relation is easily shown if we write $R(z)$ in the form

$$R(z) = [F(z) G(1/z) z^{-2s} - R_0]^{-1}$$

using (4-30) and (4-3). To show that $R(z)$ is symmetric, it is only required to show that

$$F(z) G(1/z)^{-1} = G(1/z)^{-1*} F^*(z) \quad ,$$

which follows from (3-29).

In both this and the previous sections, it is necessary to calculate $M(z)$ for each transmission and reflection response. We now derive a useful recursion relation for obtaining $M(z)$ for n layers. Equations (3-24) which give recursion formulas for $F(z)$ and $G(z)$ can be written as

$$F_n(z) = z^{m_n} (F_{n-1}(z) + G_{n-1}(z) Z_n R'_n Z_n) Z_n^{-1} T_n^{*-1}$$

$$-z^{2s_n} R_o G_n(1/z) = -z^{m_n} (z^{2s_{n-1}} R_o G_{n-1}(1/z) + z^{2s_{n-1}} R_o F_{n-1}(1/z) Z_n R'_n Z_n) Z_n^{-1} T_n^{*-1}$$

where S_n is given by (3-14). Summing these equations using (4-3) yields

$$M_n(z) = z^{m_n} \left[M_{n-1}(z) - z^{2s_{n-1}} R_o M_{n-1}(1/z) Z_n R'_n Z_n \right] Z_n^{-1} T_n^{*-1}$$

(4-35)

This relation is a matrix extension of a scalar relation derived by Claerbout (1968) for compressional waves at normal incidence. To start the recursion, we let

$$M_1(z) = z^{m_1} \left[I_2 - R_o Z_1 R'_1 Z_1 \right] Z_1^{-1} T_1^{*-1}$$

(4-36)

from (3-19).

These two equations can be used to calculate $M_n(z)$ much more rapidly than calculating $F_n(z)$ and $G_n(z)$ separately using equations (3-24). We can also use (4-35) to show conceptually how the rays are summed in a multilayer transmission problem. Let us write this equation as

$$M_n(z) = z^{m_n} M_{n-1}(z) \left[I_2 - z^{2s_{n-1}} M_{n-1}^{-1}(z) R_{n-1} M_{n-1}(1/z) Z_n R_n' Z_n \right] Z_n^{-1} T_n^{*-1}$$

or using (4-7)

$$M_n(z) = z^{m_n} M_{n-1}(z) \left[I_2 - R^{(n-1)}(z) Z_n R_n' Z_n \right] Z_n^{-1} T_n^{*-1} \quad (4-37)$$

where $R^{(n-1)}(z)$ is the reflection response of the $n-1$ layers above the $(n-1)$ -th interface for a source located just below that interface. Iterating upward through the layers using this equation and (4-36) we obtain

$$M_n(z) = z^{s_n} \left[I_2 - R^{(0)} Z_1 R_1' Z_1 \right] Z_1^{-1} T_1^{*-1} \left[I_2 - R^{(1)} Z_2 R_2' Z_2 \right] Z_2^{-1} T_2^{*-1} \cdots \left[I_2 - R^{(n-1)} Z_n R_n' Z_n \right] Z_n^{-1} T_n^{*-1} \quad (4-37)$$

For a deep source just below the n -th interface the transmission response recorded just below the free surface is given by (4-5).

Using (4-37) this transmission response becomes

$$\begin{aligned}
 X(z) = & \left[I_2 - Z_1 R_1' Z_1 R^{(0)} \right]^{-1} Z_1 T_1 \left[I_2 - Z_2 R_2' Z_2 R^{(1)} \right]^{-1} Z_2 T_2 \\
 & \cdots \left[I_2 - Z_n R_n' Z_n R^{(n-1)} \right]^{-1} Z_n T_n
 \end{aligned} \tag{4-38}$$

On physical grounds, each reflection function $R^{(k)}(z)$ is an infinite series in positive powers of z , the first term being R_k the reflection coefficient matrix for the k -th interface. Since $X(z)$ is realizable each inverse in (4-38) must have a converging series expansion in positive powers of z . Thus we can write

$$\begin{aligned}
 & \left[I_2 - Z_k R_k' Z_k R^{(k-1)} \right]^{-1} Z_k T_k = \\
 & Z_k T_k + (Z_k R_k' Z_k R^{(k-1)}) Z_k T_k + (Z_k R_k' Z_k R_k' Z_k R^{(k-1)}) Z_k T_k + \cdots
 \end{aligned} \tag{4-39}$$

Let us consider the transmitted wave

$$\bar{u}_1 = X(z) \bar{S}_{n+1} \tag{4-39a}$$

The accumulation of multiple reflected waves inside the n -th layer is given by

$$\left[\mathbf{I}_2 - \mathbf{Z}_n \mathbf{R}'_n \mathbf{Z}_n \mathbf{R}^{(n-1)}(\mathbf{z}) \right]^{-1} \mathbf{Z}_n \mathbf{T}_n \bar{\mathbf{s}}_{n+1}$$

(4-40)

from (4-38). Assuming an expansion like (4-39) for this expression, we see that the first three terms of (4-40) are

$$\mathbf{Z}_n \mathbf{T}_n \bar{\mathbf{s}}_{n+1} + (\mathbf{Z}_n \mathbf{R}'_n \mathbf{Z}_n \mathbf{R}^{(n-1)}(\mathbf{z})) \mathbf{Z}_n \mathbf{T}_n \bar{\mathbf{s}}_{n+1} + (\quad)^2 \mathbf{Z}_n \mathbf{T}_n \bar{\mathbf{s}}_{n+1}$$

(4-41)

Each of these terms adds a contribution to $\bar{\mathbf{u}}_n$, the upgoing wave just below the (n-1)-th interface. The first term contains the direct P and SV arrivals, due to $\bar{\mathbf{s}}_{n+1}$ being transmitted through the n-th layer. The second and third terms represent the first term after multiple internal reflections inside the n-th layer. Each reflection off the (n-1)th interface, indicated by $\mathbf{R}^{(n-1)}(\mathbf{z})$, increases the complexity of the waves because $\mathbf{R}^{(n-1)}(\mathbf{z})$ is the reflection response of all the n-1 layers above the n-th layer. Thus, we have

$$\bar{\mathbf{u}}_n = \left[\mathbf{I}_2 - \mathbf{Z}_n \mathbf{R}'_n \mathbf{Z}_n \mathbf{R}^{(n-1)}(\mathbf{z}) \right]^{-1} \mathbf{Z}_n \mathbf{T}_n \bar{\mathbf{s}}_{n+1}$$

Each term of $\bar{\mathbf{u}}_n$ which is already very complex, is now operated on in a similar fashion by the next matrix operator in (4-38) which results in

$$\bar{\mathbf{u}}_{n-1} = \left[\mathbf{I}_2 - \mathbf{Z}_{n-1} \mathbf{R}'_{n-1} \mathbf{Z}_{n-1} \mathbf{R}^{(n-2)}(\mathbf{z}) \right]^{-1} \mathbf{Z}_{n-1} \mathbf{T}_{n-1} \bar{\mathbf{u}}_n$$

This matrix multiplication generates multiple reflections inside the (n-1)-th layer, each reflection being "filtered" by the reflection response of the (n-2) layers above the (n-1)-th layer.

Continuing this process through the layers gives the transmitted wave \bar{u}_1 , evaluated just below the free surface. If we take the first term of the expansion of each inverse of (4-38), we see that the direct P and SV waves transmitted through the layers are given by

$$\bar{u}_{1,(\text{direct})} = Z_1 T_1 Z_2 T_2 \cdots Z_n T_n \bar{s}_{n+1}$$

(4-42)

This term contains all possible combinations of P and SV waves transmitted through each of the n layers, with no reflections.

4.4 Calculation of Reflection Response $R(z)$ from the Transmission Response $X(z)$

In this section, we prove a useful relation which enables us to calculate the reflection response $R(z)$ due to a surface plane wave source, from the transmission response $X(z)$ generated by a deep source. A possible application of this relation is to convert horizontal and vertical component seismograms for teleseismic events to reflection-type seismograms caused by surface plane wave sources. Such reflection seismograms are usually easier to interpret than transmission seismograms in mapping layers of the Earth's crust.

The relation we shall prove is

$$\bar{I}_2 + R_0 R(z) + R(1/z) R_0 = X(1/z) X^*(z) \quad (4-43)$$

Responses $R(z)$ and $X(z)$ are used to calculate the up-going waves \bar{r}_1 and \bar{x}_1 recorded below the free surface, i.e.,

$$\bar{r}_1 = R(z) \bar{s}_1 \quad (4-44)$$

and

$$\bar{x}_1 = X(z) \bar{s}_{n+1} \quad (4-45)$$

where \bar{s}_1 is a downgoing source located just below the free surface, and \bar{s}_{n+1} is an upgoing source just below the n-th interface.

$R(z)$ represents a realizable time function. Therefore, it must contain only positive powers of z . Similarly, $R(1/z)$ must contain only negative powers of z . To obtain $R(z)$ using (4-43), we calculate the autocorrelation matrix $X(1/z)X^*(z)$ which contains positive and negative powers of z , and set those terms containing positive powers of z equal to $R_0 R(z)$.

This remarkable theorem was formulated in the normal incidence case by Claerbout (1968). He derived a scalar relation similar to (4-43) for compressional waves.

At normal incidence, each matrix in (4-43) becomes diagonal so that two uncoupled scalar theorems are obtained, one for P waves and one for SV waves.

The proof of (4-43) we now give is a little more complex than Claerbout's proof, but follows his steps almost exactly. We first substitute the expression for $X(z)$ given by (4-5) into (4-43). This gives the equation we shall prove, i.e.

$$M^*(1/z) \left[I_2 + R_0 R(z) + R(1/z) R_0 \right] = M^{-1}(z) \quad (4-46)$$

From the first row of (4-26) and equation (4-28) we obtain

$$\bar{s}_1 + R_0 \bar{r}_1 = F(z) M^{-1}(z)$$

Using (4-44) this yields

$$I_2 + R_0 R(z) = F(z) M^{-1}(z) \quad (4-47)$$

Transposing (4-30) we obtain

$$R(1/z) R_0 = z^{-2S} M_{-1}^*(1/z) G^*(z) R_0 \quad (4-48)$$

Summing these two equations, we find that

$$\begin{aligned} & M_{-1}^*(1/z) [I_2 + R_0 R(z) + R(1/z) R_0] = \\ & M_{-1}^*(1/z) \left\{ F(z) M^{-1}(z) + z^{-2S} M_{-1}^*(1/z) G^*(z) R_0 \right\} = \\ & \left\{ M_{-1}^*(1/z) F(z) + z^{-2S} G^*(z) R_0 M^{-1}(z) \right\} M^{-1}(z) \end{aligned} \quad (4-49)$$

We replace $M_{-1}^*(1/z)$ and $M^{-1}(z)$ inside the braces $\{ \}$ on the right-hand side of this equation by expressions in $F(z)$ and $G(z)$ from (4-3). The result is

$$\left\{ [F_{-1}^*(1/z) - z^{-2S} G^*(z) R_0] F(z) + z^{-2S} G^*(z) R_0 [F(z) - z^{2S} R_0 G(1/z)] \right\}$$

Since the two middle terms cancel and $R_0^2 = I_2$, this reduces to

$$\left\{ F^{*}({}^{1/2}) F(z) - G^{*}(z) G({}^{1/2}) \right\}$$

But this expression equals I_2 from (3-28). Equation (4-49)

therefore reduces to

$$M^{*}({}^{1/2}) [I_2 + R_0 R(z) + R({}^{1/2}) R_0] = M^{-1}(z)$$

proving (4-46) and (4-43).

4.5 Estimation of $M(z)$

A useful inverse problem is to estimate the matrix polynomial $M(z)$ from recorded data at the free surface. Given $M(z)$ and the reflection coefficient matrix R_0 for the free surface, equations (4-5), (4-7), (4-31), and (4-43) show how to calculate transmission and reflection responses for a layered halfspace for a plane wave source located either at the free surface or just below the deepest interface. An important application would be to remove the effects of crustal reverberation on teleseismic events recorded at the free surface of the Earth's crust. To see this, we rewrite (4-2) as

$$M^*(z) \bar{u}(z) = z^S \bar{S}(z) \quad (4-50)$$

where $\bar{u}(z)$ is a vector of the upgoing P and SV waves arriving at the free surface, and $\bar{S}(z)$ is an upgoing plane wave teleseismic event incident to the base of the crust. $M(z)$, $\bar{u}(z)$ and $\bar{S}(z)$ each represent time functions sampled every $\Delta\tau$ sec. The term z^S in (4-51) has the effect of delaying the source in time by $S\Delta\tau$ which is the one-way transit time for SV waves through the crustal layers.

If we have calculated $M(z)$ for the crustal structure below the receiver, we can perform the multiplication of $M^*(z)$ by $\bar{u}(z)$ indicated by (4-50) to obtain the upgoing wave $\bar{S}(z)$ which is uncontaminated by crustal reverberations. This multiplication corresponds

to a straight forward convolution in time.

The first step is to convert recorded horizontal and vertical velocity components at the free surface to P and SV components of $\bar{u}(z)$. To do this, we need to know the phase velocity c of the teleseismic event and the physical quantities α_1 , β_1 , and ρ_1 for the uppermost crustal layer. From this information, we can calculate

$$\bar{u}(z) = \begin{bmatrix} UP(z) \\ US(z) \end{bmatrix} = \sqrt{\rho_1 c} K_1^{-1} \begin{bmatrix} \dot{u}(z) \\ \dot{w}(z) \end{bmatrix} \quad (4-51)$$

where matrix K_1 is given by (2-45).

We now assume that our particle velocity data has been transformed to upgoing waves \bar{u} . Let us define the following series in z .

$$\begin{aligned} \bar{s}(z) &= \sum_{t=0}^K \bar{s}_t z^t \\ \bar{u}(z) &= \sum_{t=0}^{\infty} \bar{u}_t z^{t+p} \\ M(z) &= \sum_{t=0}^{2S} M_t z^t \end{aligned}$$

(4-52)

The source is assumed to have a finite time duration $K\Delta\tau$, and time

is defined to be zero when the first source vector \bar{S}_0 arrives at the base of the crust. The recorded waves $\bar{u}(z)$ at the surface have an infinite number of terms, the first sample \bar{u}_0 arriving at time $\rho\Delta\tau$ which is the one-way transit time through the crust for P waves. $M(z)$ is a matrix polynomial of degree $2S$ with real matrix coefficients M_t .

Inserting equations (4-52) into (4-50) yields an equation in which an infinite series of z on the left equals a polynomial in z on the right-hand side. Equating coefficients of powers on each side of the equation, we obtain an infinite set of linear equations in the matrix coefficients of M_t , i.e.

$$\begin{bmatrix} \bar{u}_0^* \\ \bar{u}_1^* & \bar{u}_0^* \\ \bar{u}_2^* & \bar{u}_1^* & \bar{u}_0^* \\ \vdots & \vdots & \ddots \\ \bar{u}_{2S}^* & \bar{u}_{2S-1}^* \\ \bar{u}_{2S+1}^* & \bar{u}_{2S}^* \\ \vdots & \vdots \\ \bar{u}_{\infty+2S}^* \end{bmatrix} \begin{bmatrix} 0 \\ \vdots \\ \vdots \\ \vdots \\ \vdots \\ \vdots \\ \vdots \\ \vdots \end{bmatrix} = \begin{bmatrix} M_0 \\ M_1 \\ M_2 \\ \vdots \\ M_{2S} \end{bmatrix} \begin{bmatrix} \bar{u}_0^* \\ \bar{u}_1^* \\ \vdots \\ \bar{u}_\infty^* \end{bmatrix} = \begin{bmatrix} 0 \\ 0 \\ \vdots \\ 0 \\ \bar{u}_0^* \\ \bar{u}_1^* \\ \vdots \\ \bar{u}_\infty^* \\ 0 \\ \vdots \end{bmatrix} \left. \vphantom{\begin{bmatrix} 0 \\ 0 \\ \vdots \\ 0 \\ \bar{u}_0^* \\ \bar{u}_1^* \\ \vdots \\ \bar{u}_\infty^* \\ 0 \\ \vdots \end{bmatrix}} \right\} \begin{array}{l} \text{S-P} \\ \text{zeros} \end{array}$$

These equations illustrate the recursive nature of the observed data $\bar{u}(z)$. For n greater than $s-p+k$ we have

$$\bar{u}_n^* M_0 = - \left\{ \bar{u}_{n-1}^* M_1 + \bar{u}_{n-2}^* M_2 + \dots + \bar{u}_{n-2s}^* M_{2s} \right\} \quad (4-54)$$

independent of the source $\bar{S}(z)$. This equation seems to give a rapid matrix recursion for calculating $\bar{u}(z)$ if $M(z)$ were known. To do this both sides of (4-54) would have to be multiplied by M_0^{-1} to give \bar{u}_n^* in terms of earlier values of $\bar{u}(z)$. Unfortunately, this is not possible because M_0 is always singular. It can be shown from (4-37) that for any number of layers the first term of $M(z)$ has the form

$$M_0 = \begin{bmatrix} 0 & 0 \\ m_{21} & m_{22} \end{bmatrix}$$

which cannot be inverted. The basic reason for this is that P and SV transit times through a layer are always unequal integer multiples of $\Delta\tau$.

Another reason M_0 must be singular is seen directly from the first $s-p$ equations of (4-53). If M_0 were non-singular, these equations would force the first $s-p$ data samples to vanish, i.e.

$$\bar{u}_0^* = \bar{u}_1^* = \dots = \bar{u}_{s-p-1}^* = 0.$$

This is impossible on physical grounds, because the first arrival of $\bar{u}(z)$ should be \bar{u}_0 , the direct P wave through the crustal layers.

In the case of normal incidence, we can treat P and SV components separately and derive a set of equations like (4-53) and a recursion relation like (4-54) for each component. All terms will be scalar terms rather than vectors or matrices and the s-p leading zeros in (4-54) will not occur. As a result, the scalar recursion equations can be used to compute $UP(z)$ (or $US(z)$). Such computations are described by Claerbout (1968).

Returning to the non-normal incidence case, we consider the inverse problem of calculating $M(z)$ from $\bar{U}(z)$ and $\bar{S}(z)$. The infinite number of rows in (4-53) do not overdetermine the system of equations if the solution for $M(z)$ is exact. In any practical computations, however, there are errors in $\bar{U}(z)$ due to inexact transformation of particle velocity components to upgoing P and SV components of $\bar{U}(z)$. Also, estimates of $\bar{S}(z)$ will certainly have errors. Therefore, instead of choosing $4s+2$ rows of data to compute M_0, M_1, \dots, M_{2s} , it is more practical to compute the least squares solution of $M(z)$ utilizing all the rows of data. In the absence of errors in $\bar{U}(z)$ or $\bar{S}(z)$ the least squares solution is, of course, also the exact solution.

To do this, we multiply both sides of (4-53) from the left by the transpose of the coefficient matrix. This gives the normal equations for a two channel filter problem. These equations are well known (Backus, et.al., 1964, Schneider, et. al., 1964) and can be rapidly solved by an adaptation of a recursion algorithm by Levinson

to multichannel problems (Wiggins and Robinson, 1965). The normal equations we obtain are

$$\begin{bmatrix} R_0 & R_{-1} & \cdots & R_{-2s} \\ R_1 & R_0 & \cdots & R_{-2s+1} \\ \vdots & \vdots & \ddots & \vdots \\ R_{2s} & R_{2s-1} & \cdots & R_0 \end{bmatrix} \begin{bmatrix} M_0 \\ M_1 \\ \vdots \\ M_{2s} \end{bmatrix} = \begin{bmatrix} Y_0 \\ Y_1 \\ \vdots \\ Y_{k+1-p} \\ \vdots \\ 0 \end{bmatrix} \quad (4-55)$$

where R_τ and Y_τ are 2×2 correlation matrices defined by

$$R_\tau = \sum_{t=0}^{\infty} \bar{u}_{t-\tau} \bar{u}_t^*$$

$$Y_\tau = \sum_{t=0}^k \bar{u}_{t-\tau+s-p} \bar{s}_t^* \quad (4-56)$$



The Libraries
Massachusetts Institute of Technology
Cambridge, Massachusetts 02139

Institute Archives and Special Collections
Room 14N-118
(617) 253-6888

This is the most complete text of the thesis available. The following page(s) were not included in the copy of the thesis deposited in the Institute Archives by the author:

Chapter V

Application to Two Transition Zones in the Earth

5.1 Introduction

The discrete time calculation of P-SV body waves described in the previous chapters can be readily applied to many transition zones within the Earth. The only serious restriction for the method is that critical angles of reflection must not be exceeded at any interface between layers of an assumed model, since this introduces inhomogeneous waves into the model response.

In this chapter, the time domain responses of two transition zones are illustrated by computed examples. The first zone is the crust of the Earth. In section 5.2, the transmission responses of two plane layer crustal models under the Large Aperature Seismic Array (LASA) in Montana are calculated for normal and non-normal incidence of impulsive teleseismic sources. The second transition zone considered is the core-mantle boundary. Reflection responses in time for five models of this zone are calculated for a wide range of incident angles for P and SV sources in the mantles. These responses are described in section 5.3.

A computer program was written in Fortran IV for the IBM 360, Model 65, to solve for the reflection and transmission responses of a stack of elastic layers between two halfspaces to an upgoing source in the lower elastic halfspace as shown in Figure 3.1. The program

allows the upper halfspace to be solid, fluid, or vacuum. If the upper halfspace is a vacuum (i.e., interface 0 is free), then the matrix polynomial $M(z)$ for all the layers is calculated using the iteration given by (4-35). The transmission response $X(z)$ for the layered halfspace is then given by (4-5), i.e.,

$$X(z) = z^s M^{*-1}(z) = z^s \frac{\text{Adj}(M^*(z))}{\det |M(z)|} \quad (5-1)$$

where $\det |M(z)|$ is a polynomial in integer powers of z . On the other hand, if the upper halfspace is solid or fluid then the iterations in (3-24) are utilized to calculate matrix polynomials $F(z)$ and $G(z)$ separately for the stack of layers. From (3-34), the reflection response $R^{(n)}(z)$ for the layers is given by

$$R^{(n)}(z) = - [F(z) - z^{2s} R_0 G(1/z)]^{-1} [G(z) - z^{2s} R_0 F(1/z)] \quad (5-2)$$

This expression is used to calculate the core-mantle reflection response where the upper halfspace is taken to be the fluid core and the lower halfspace the solid mantle.

5.2 Transmission Response of Two LASA Crustal Models

In their study of crustal variations under LASA, Glover and Alexander (1969) computed long period spectral responses of plane layered crustal models which were approximations to models obtained by seismic refraction studies in Montana.

Two of their models, USGS3 and T11 are used in this section to illustrate the horizontal and vertical components generated at the surface by impulsive teleseismic sources. These two crustal models have the layer parameters listed in Table 5.1.

With a time increment of $\Delta\tau = .05$ sec., which is the sample interval of the LASA digital recording equipment, matrix polynomials $M(z)$ were calculated for each model for horizontal phase velocities corresponding to incident P wave angles of 0° and 30° in the mantle. The four elements of each $M(z)$ are displayed as sampled functions of time in Figures 5.1 to 5.4. For display purposes, each time function has been convolved with a gaussian pulse having a width of $3\Delta\tau$ sec. The actual time resolution of the computed response is $\Delta\tau = .05$ sec., which is 1/20 the interval between vertical timing lines.

At normal incidence, the matrix $M(z)$ for each model is diagonal, so that the transmission response $X(z)$ is also diagonal containing only the uncoupled P and SV responses, i.e., upgoing P and SV waves generated respectively by impulsive P and SV sources incident to the crust from the mantle.

As shown in Figures 5.2 and 5.4, at non-normal incidence, the

Layer Parameters

Model	Layer No.	α km/sec	β km/sec	ρ g/cm ³	d km
USGS3	1	3.00	1.77	2.40	2.5
	2	6.15	3.61	2.90	19.5
	3	6.70	3.96	3.02	27.0
	4	8.30	4.60	3.65	∞
TII	1	2.60	1.50	2.31	.3
	2	3.70	1.85	2.54	2.0
	3	6.08	3.51	2.85	15.0
	4	6.97	4.11	3.10	17.0
	5	7.58	4.47	3.22	23.0
	6	8.07	4.67	3.55	∞

TABLE 5.1 Parameters of LASA Crustal Models Based on Seismic Refraction Studies (after Glover and Alexander (1969)).

off-diagonal elements of $M(z)$ are no longer zero, indicating that coupling between P and SV waves in the transmission response $X(z)$ is significant.

The vertical and horizontal components of motion generated at the free surface of each model by impulsive P and SV sources can be obtained from $X(z)$ by taking the matrix product

$$V(z) = \frac{1}{\sqrt{\rho_1 c}} K X(z) \quad (5-3)$$

where K is a scalar matrix given by (2-45). The first column of $V(z)$ contains horizontal and vertical velocity components caused by an impulsive P source, whereas the second column of $V(z)$ contains velocity components generated by an SV source in the mantle.

Plots of the four velocity components of $V(z)$ for each model are shown in Figures 5.5 to 5.8. The upper two records in each figure are generated by an impulsive P wave and the lower two records are due to an impulsive SV source, all waves having the phase velocity indicated in each figure.

The time functions are generated recursively in the computer program by dividing $\text{Adj}(M(z))$ by the polynomial $\det |M(z)|$. The infinite series obtained in integer powers of z can be terminated after some arbitrary power z^n has been reached. This corresponds to calculating a time window of length $n\Delta\tau$ for each response.

In each particle velocity figure, zero time is defined to be the

arrival time of the first direct P wave through each model. At normal incidence the SV wave in each model lags about six seconds behind the first P motion. At non-normal incidence, some direct P wave energy arrives at zero time even for those traces generated by impulsive SV sources in the mantle.

Once $M(z)$ has been calculated for a layered halfspace, the frequency response of the medium for any ω is obtained by setting $z = e^{-i\omega\Delta\tau}$. This has a computational advantage over Haskell's method if a large window of spectral points are to be computed, because in Haskell's technique, a new iteration through the layers has to be computed for each frequency.

Since vertical transit times for P and SV plane waves in each layer are rounded off to integer multiples of the sampling increment $\Delta\tau$, there is some time distortion introduced in the transmission response of the crustal models. This distortion is too small to be seen in Figures 5.5 to 5.8, and can only be detected in the frequency domain. Figure 5.8a shows the frequency response of the velocity components plotted in Figure 5.6 for model USGS3. The four spectra are obtained from (5-3) and (5-1), i.e.

$$V(\omega) = \frac{e^{-i\omega\Delta\tau}}{\sqrt{\rho_1 c}} K M^{-1}(\omega) \quad (5-4)$$

Thus, it is only necessary to invert the spectral matrix of $M(z)$ to obtain $V(\omega)$ rather than Fourier analyze the particle velocity data

directly.

Figure 5.8b shows the same spectral responses calculated exactly using Haskell's matrix formation. Comparing this figure to Figure 5.8a, we see that responses calculated from $M(z)$ have some slight distortion in amplitude and phase which increases with frequency. This distortion can be neglected over the frequency range shown in any practical computations.

5.3 Reflection Response of the Core-Mantle Boundary

Recently, Teng (1967) computed the reflection and transmission responses of five plane layered models of the core-mantle boundary of the Earth. Using Haskell's technique, he computed the amplitude response of each model for incident plane P and SV waves over a period range of 2 to 100 seconds. From these responses, Teng qualitatively discussed several questions:

(1) For an assumed structure of the core-mantle boundary, what effects on core phases can be expected and which core phases are more sensitive to the layered structure?

(2) At which epicentral distances do these effects become more pronounced?

(3) What frequency bands (or records from what instruments) are most suitable to detect these effects?

(4) What window length is best suitable for a study of the core-mantle boundary?

Most of these questions can be directly answered by examining the impulsive responses in time of the various models. In this section, the reflection responses of each model considered by Teng are calculated. These can be used as guides for estimating the variation of amplitude and wave shape of reflected core phases at different angles of incidence in the mantle.

A listing of layer parameters for each model is given in Table 5.2. These models are arranged in increasing complexity of their

Layer Parameters

Model No.	Layer No.	α km/sec	β km/sec	ρ gr/cm ³	Thickness km
1	0	8.040	0.000	10.060	∞
	1	13.680	7.200	5.355	20.00
	2	13.700	7.225	5.325	80.00
	3	13.700	7.250	5.300	∞
2	0	8.150	0.000	9.400	∞
	1	13.720	7.195	5.675	18.00
	2	13.710	7.200	5.665	20.00
	3	13.700	7.205	5.655	20.00
	4	13.690	7.215	5.645	20.00
	5	13.680	7.220	5.640	∞
3	0	8.150	0.000	9.400	∞
	1	10.200	5.200	6.200	11.00
	2	11.600	6.100	5.670	13.00
	3	13.000	6.840	5.660	12.00
	4	13.690	7.210	5.650	∞
4	0	8.300	0.000	9.500	∞
	1	10.000	2.800	6.700	30.00
	2	13.600	7.500	5.500	∞
5	0	8.300	0.000	9.500	∞
	1	13.300	4.800	6.700	100.00
	2	13.600	7.500	5.500	∞

The interface between the zeroth and the first layers corresponds to a depth of 2898 km. The model number refers to:

- (1) Gutenberg - Bullard I (Landisman et al, 1965)
- (2) Standard model (Dorman et al, 1966)
- (3) Model R 1 (Dorman et al, 1966)
- (4) Model 94 (Phinney and Alexander, 1966)
- (5) Model 81 (Phinney and Alexander, 1966)

TABLE 5.2 Models of Core Mantle Boundary (after Teng(1967)).

spectral reflection response. Models 1 to 3 represent a transitional lower mantle meeting a fluid core at a sharp interface. These models were obtained from free oscillation studies (Landisman, et al, 1965, and Dorman, et al, 1966). Models 4 and 5 were suggested by Phinney and Alexander (1966) to fit observed P waves diffracted along the core mantle boundary. Models 1 and 2 have more than one layer but the impedance contrast between layers is negligible except for the interface 0 which is between the fluid core and first solid mantle layer. On the other hand, models 4 and 5 each have one layer between mantle and core, but the contrasts in shear velocity and density across each interface are large enough to cause strong oscillations in the amplitude spectra of the reflection response. Figure 5.9 is a duplication of Teng's Figure 2, showing the amplitude spectra of SV to SV and P to P reflection coefficients for the 5 models each calculated for an incident angle of 60° in the mantle. For the more complex models, it is clearly difficult to interpret these spectral responses in terms of reflected core phases in time, especially for short period phases. One can synthesize a time domain response by inverting a band limited spectrum, but strong oscillating precursors will result.

The impulsive reflection response in time for each model was calculated for incident angles of 0° to 75° for P waves and 0° to $\sim 32^\circ$ for incident SV waves. These responses are plotted in Figures 5.10 to 5.24. These figures are arranged in three groups of five. The first group contains the P to P reflection response $r_{pp}(t)$ for

models 1 to 5. The second group is a set of P to SV reflection responses $r_{ps}(t)$ and the third group are the SV to SV reflection responses $r_{ss}(t)$ for the five models. On all figures the vertical scale equals 1. between adjacent traces. No reflection response can exceed 1. at any time although the SV to SV responses are often nearly 1. because the fluid core is a ^{near} perfect reflector for shear waves. Source and receiver are located just below the lowest interface in each model of Table 5.2., and time equals zero when each impulsive source is excited.

Let us examine first the r_{pp} responses in Figures 5.10 to 5.14. As Teng pointed out from the frequency responses, Models 1 and 2 are indistinguishable, and in fact the effect of the layering is nil since only the reflection off the fluid core shows up. Model 3 has an interesting response for two reasons. At normal incidence, two short period phases of opposite polarity might be detected since they are separated by 5 sec. However, long period data would be destructively interfered because of the opposite polarity of the two pulses. At large angles of incidence, it is seen that one could easily mistime the first arrivals of this response by 5 seconds and also obtain the incorrect polarity. It appears that a time window of 5 to 10 seconds is needed to adequately detect such a feature in the response. Models 4 and 5 offer even more chance of mistaking the arrival time and polarity of the first motion of the r_{pp} response. Also, much larger time windows of 30 to 60 seconds would be needed to discriminate these last two

models from numbers 1 to 3.

Kanamori (1967) showed that transition zones with linear velocity and density gradients must be sharp ($\leq .25$ km) to produce PcP phases so similar in shape to P events for $\Delta \approx 47^\circ$ to 75° . Thus, to explain observed core phases a sharp discontinuity must exist at the core-mantle boundary.

In view of the model responses discussed above, however, it is possible that more than one discontinuity could exist and not be easily detected since most studies utilize only the first few seconds of short period PcP phases for calculations of first motion and amplitude.

Buchbinder (1968), for example, documents evidence from earthquakes and explosions showing that PcP first motions go through a sign reversal at $\Delta = 32^\circ$, corresponding to an incident angle of about 36° at the core-mantle boundary. Assuming a single plane interface between mantle and core, Buchbinder found that with acceptable velocities for the mantle and core, an abnormal density ratio of 1. was needed to produce a first motion sign reversal at 36° incidence angle.

One possible way to avoid this density problem is to insert a layer of intermediate velocities and density between core and mantle. The reflection response, $r_{pp}(t)$ for Model 4, shown in Figure 5.13, has a weak first impulse which changes polarity between 15° and 30° incident angle. To strengthen this first impulse and move the sign change to the interval between 30° and 40° , it is only necessary to lower the compressional velocity of layer 1 in Model 4.

The reflection responses r_{ps} and r_{ss} for Models 4 and 5 show even more pronounced multiple reflections due to the strong reflection coefficients for P to SV and SV to SV waves at the fluid core boundary. Of particular interest is r_{ss} for Model 4. At normal incidence, it predicts three strong arrivals separated by about 20 sec. time. As the angle of incidence increases, the first and third arrivals die out and a new first arrival of opposite polarity emerges. If such layering exists, this variation with incidence angle could be verified with good quality long period ScS data.

5.4 Conclusion

The present time domain approach to layered media problems can give high resolution reflection and transmission responses with no precursors in time. These responses can be directly compared with observed records of particle velocity. The roundoff error introduced by the discrete time formulation is negligible provided $\Delta\tau$ is chosen small enough. For thin crustal layers (~ 2 km. thick) $\Delta\tau = .05$ was found to be fine enough for frequencies up to 2 cps.

In calculating each time domain response, polynomial matrices are obtained which can be Fourier analyzed to obtain the spectral response of the layers, without repeating the layer iteration for each frequency value.

Simple reflection responses in time for core-mantle boundary models are much easier to interpret than spectral responses in terms of recorded data.

5.5 Figure Captions

- 5.1 Elements of 2×2 matrix polynomial $M(z)$ for crustal model USGS3. Normal incidence case.
- 5.2 Elements of 2×2 matrix polynomial $M(z)$ for crustal model USGS3. Phase velocity of 16.60 km/sec corresponds to P waves incident at 30° and SV waves incident at 16.1° to base of crust.
- 5.3 Elements of 2×2 matrix polynomial $M(z)$ for crustal model T11. Normal incidence case.
- 5.4 Elements of 2×2 matrix polynomial $M(z)$ for crustal model T11. Phase velocity of 16.14 km/sec corresponds to P waves incident at 30° and SV waves incident at 16.8° to base of crust.
- 5.5 Particle velocity components at free surface of crust model USGS3. Top trace is generated by impulsive P-source at normal incidence. Bottom trace is generated by impulsive SV-source at normal incidence.
- 5.6 Particle velocity components at free surface of crust model USGS3. Traces 1 and 2 are generated by P source at 30° incidence and traces 3 and 4 are generated SV source at 16.1° incidence.
- 5.7 Particle velocity components at free surface of crust model T11. Top trace is generated by impulsive P-source at normal incidence. Bottom trace is generated by impulsive SV-source at normal incidence.
- 5.8 Particle velocity components at free surface of crust model T11. Traces 1 and 2 are generated by P-source at 30° incidence, and traces 3 and 4 are generated by SV-source at 16.8° incidence.

5.8a Spectral response of horizontal and vertical velocity components shown in Figure 5.6 for model USGS3 at non-normal incidence. Solid lines are responses for impulsive P-source and dashed lines are for impulsive S-sources. Responses are calculated by inverting the spectral matrix of $M(z)$.

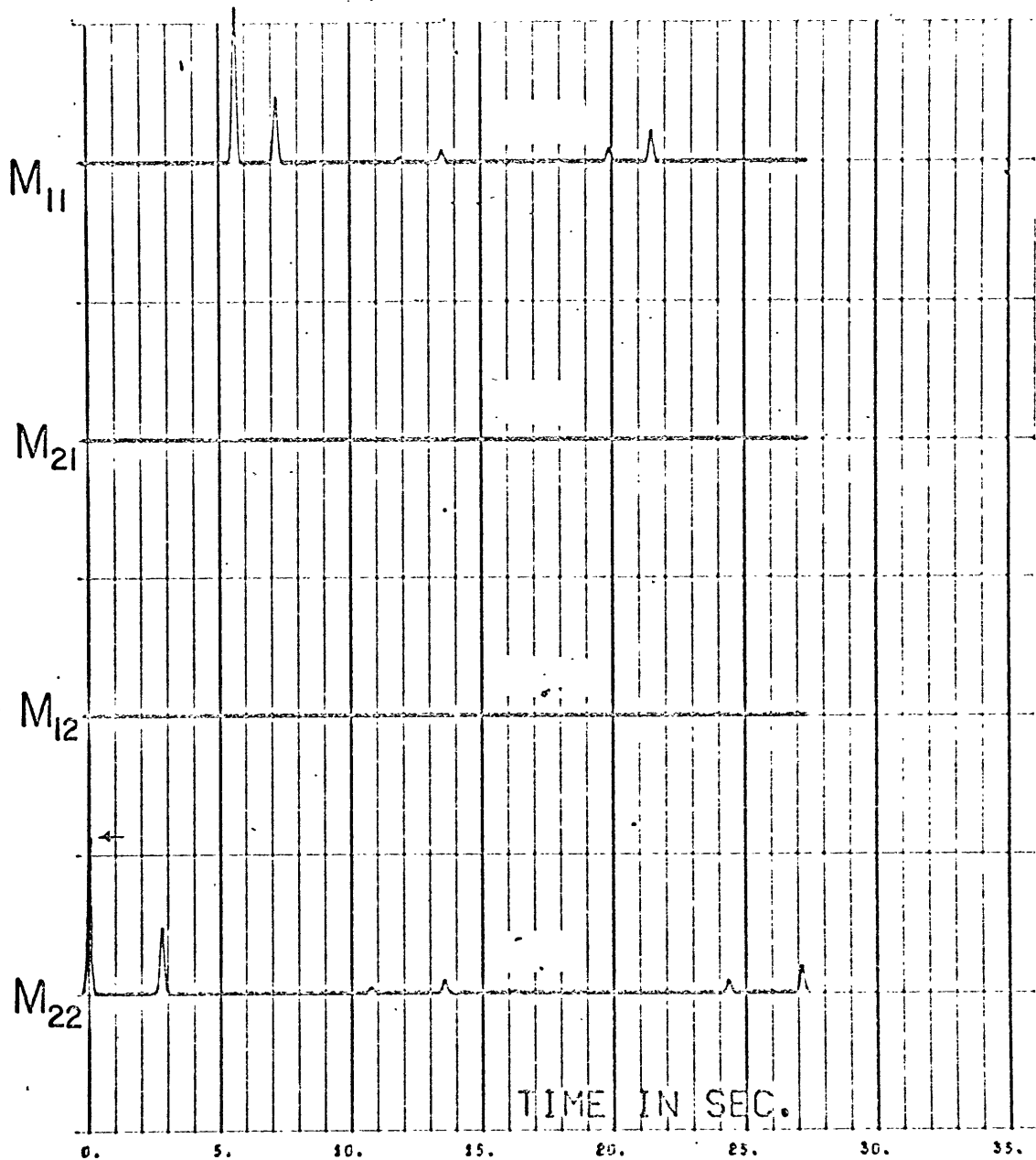
5.8b Spectral response of the velocity components in Figure 5.6 for model USGS3 at non-normal incidence. Responses are calculated by Haskell's method as a check on the accuracy of the response in Figure 5.8a.

5.9 Reflection responses $r_{pp}(\omega)$ and $r_{ss}(\omega)$ for 5 models of the core-mantle boundary over the period range 2 to 100 sec. (after Teng, 1967).

5.10 - 5.14 Reflection responses r_{pp} in time at different angles of incidence to the core mantle boundary. Figures are for models 1 to 5 given in Table 5.1. Vertical scale equals 1. between traces.

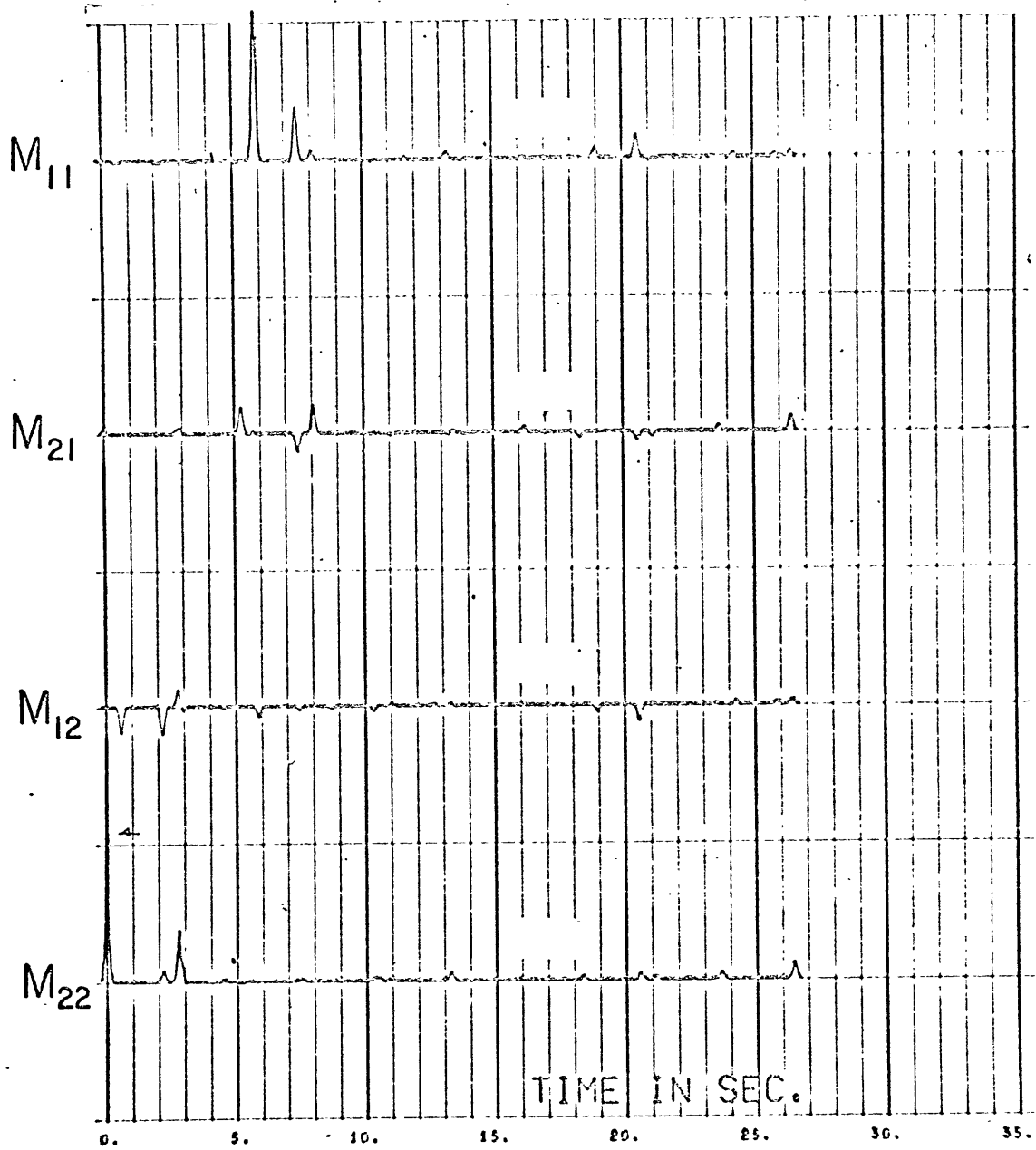
5.15 - 5.19 Reflection responses r_{ps} in time at different angles of incidence to the core mantle boundary. Figures are for models 1 to 5 given in Table 5.1. Vertical scale equals 1. between traces.

5.20 - 5.24 Reflection responses r_{ss} in time at different angles of incidence to the core mantle boundary. Figures are for models 1 to 5 given in Table 5.1. Vertical scale equals 1. between traces.



POLYNOMIAL MATRIX $M(Z)$, CRUST MODEL USGS3
PHASE VELOCITY = INFINITY.

FIGURE 5.1



POLYNOMIAL MATRIX $M(z)$, CRUST MODEL USGS3
PHASE VELOCITY = 16.60 KM/SEC.

FIGURE 5.2

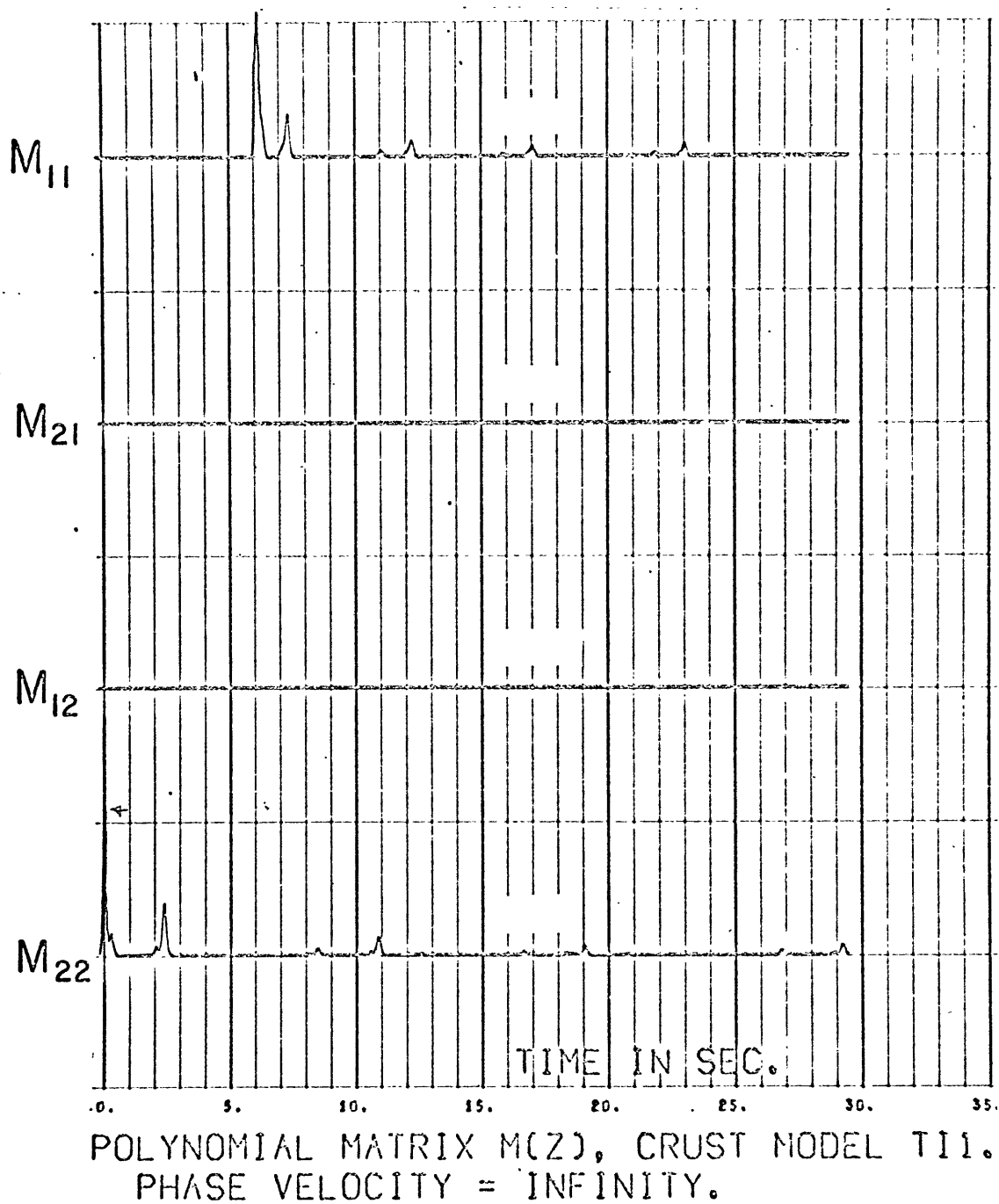


FIGURE 5.3

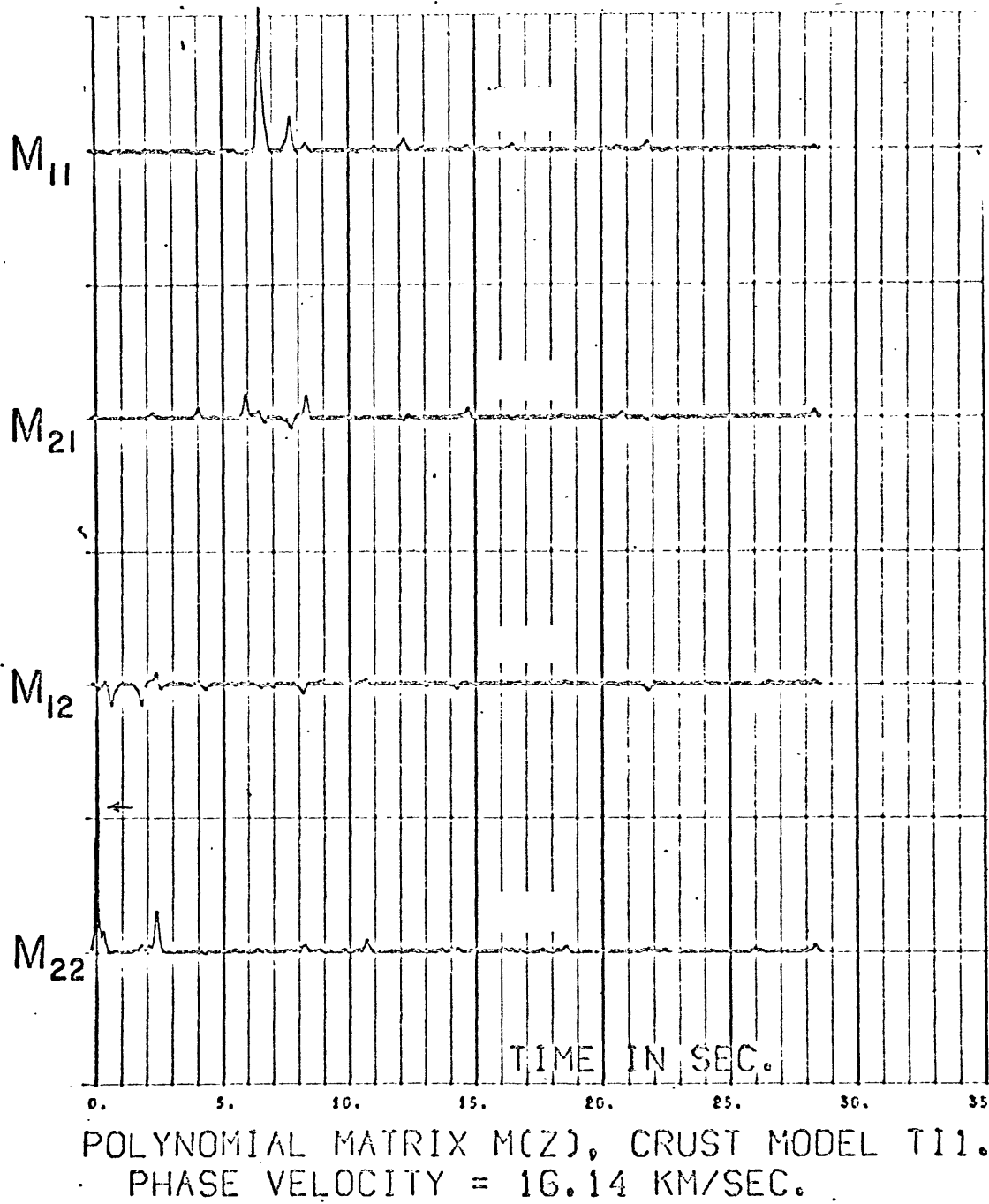
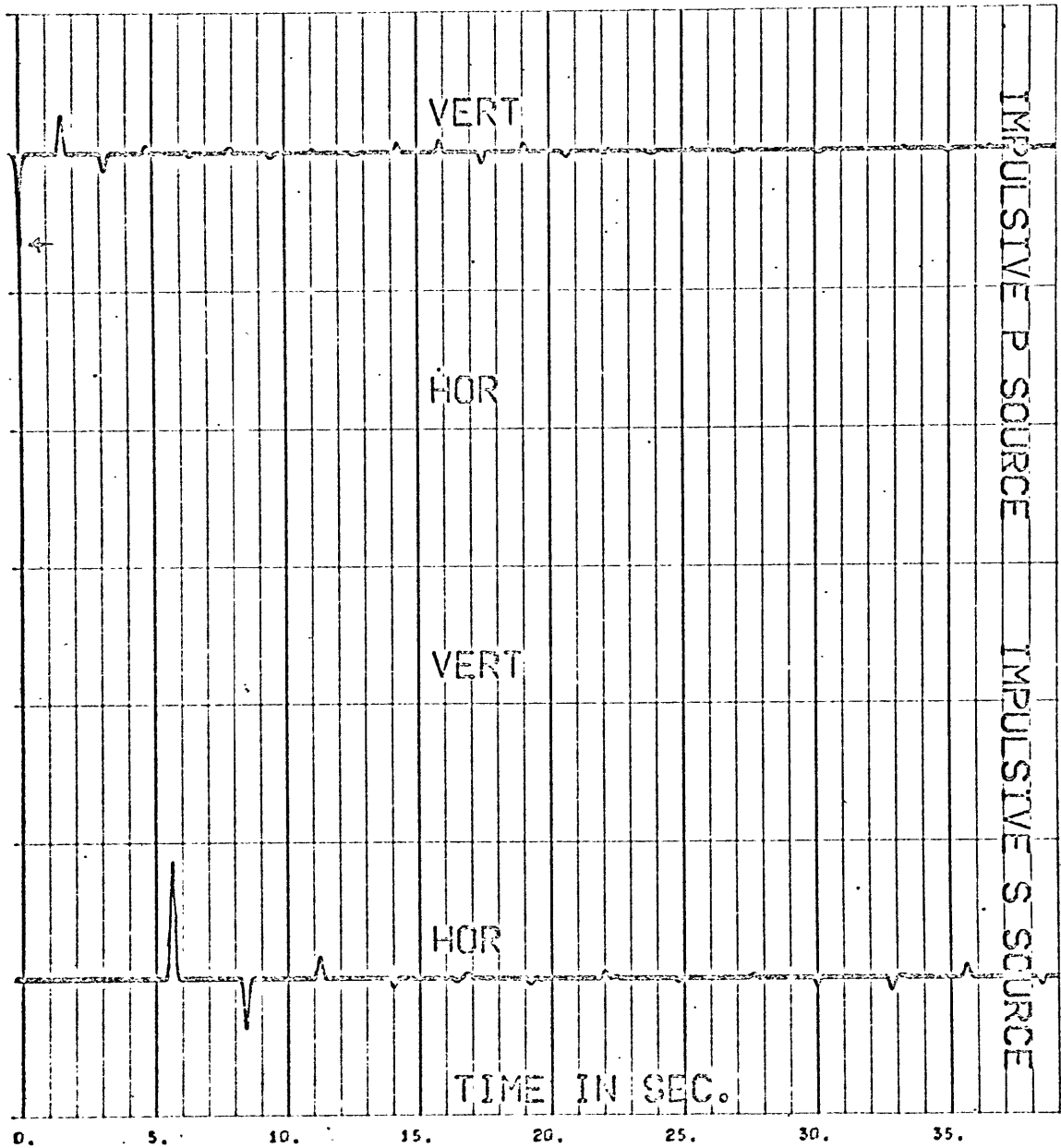


FIGURE 5.4

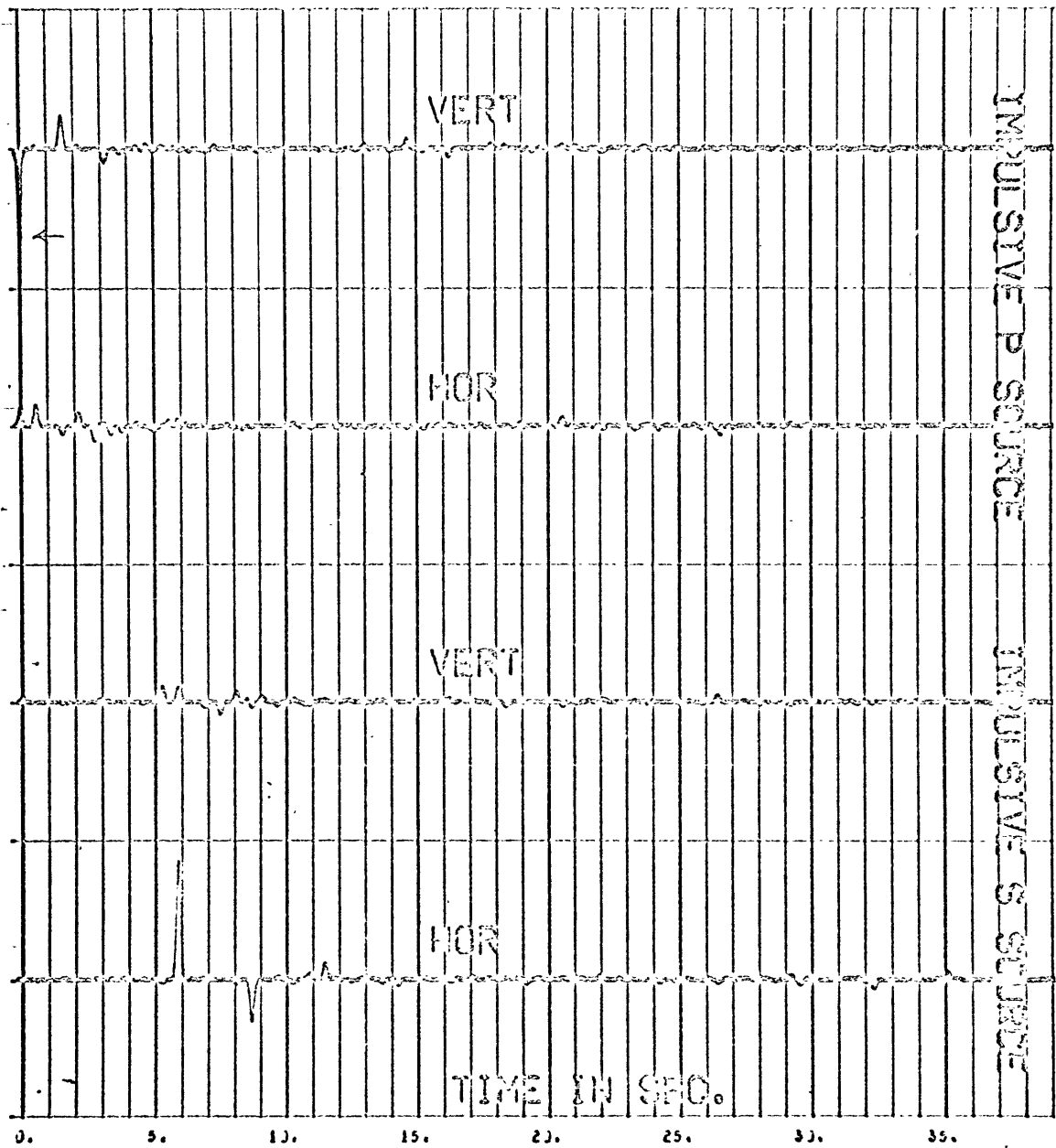
PARTICLE VELOCITY AT SURFACE



TRANSMISSION RESPONSE-CRUST MODEL USGS3.
PHASE VELOCITY = INFINITY.

FIGURE 5.5

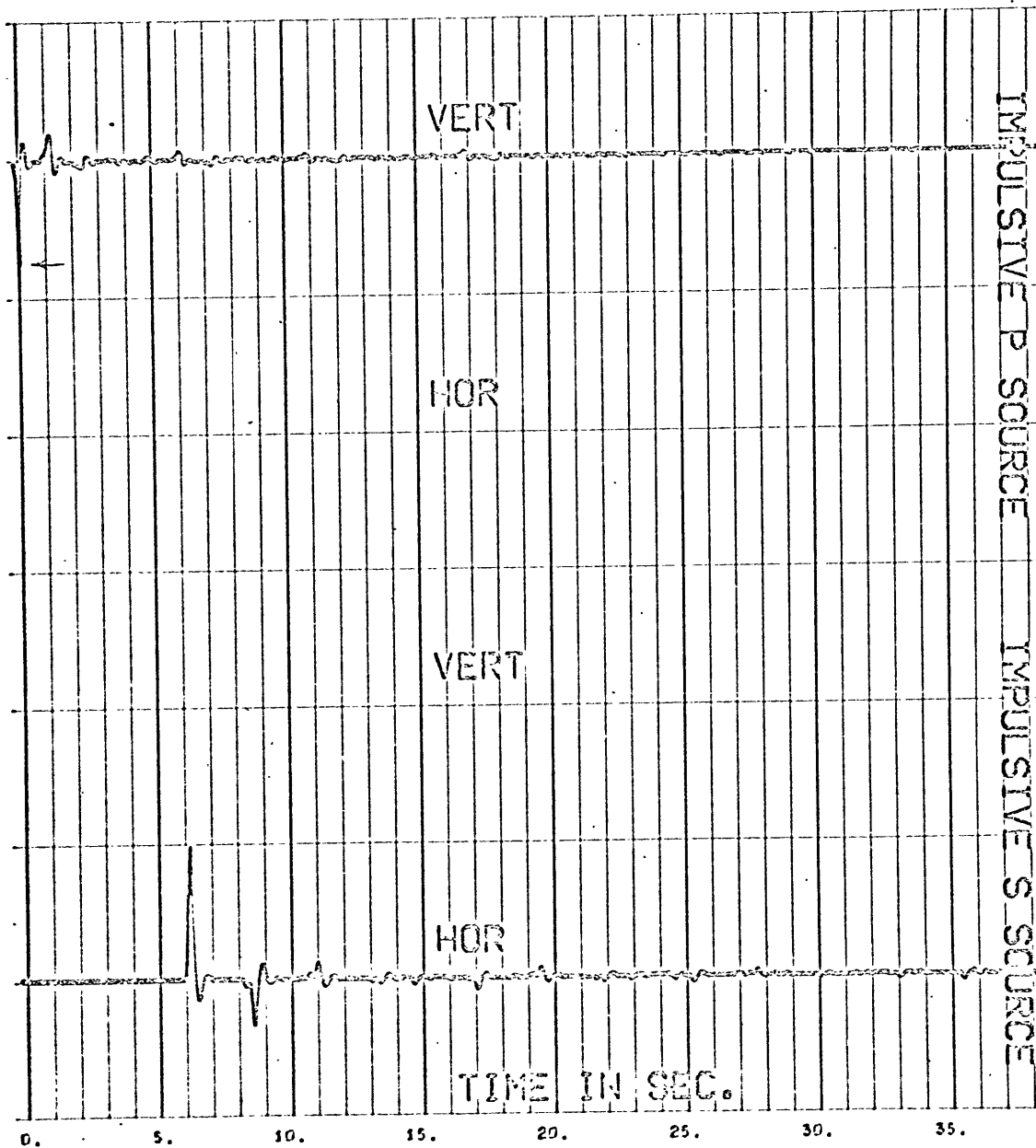
PARTICLE VELOCITY AT SURFACE



TRANSMISSION RESPONSE-CRUST MODEL USGS3.
 PHASE VELOCITY = 16.60 KM/SEC.

FIGURE 5.6

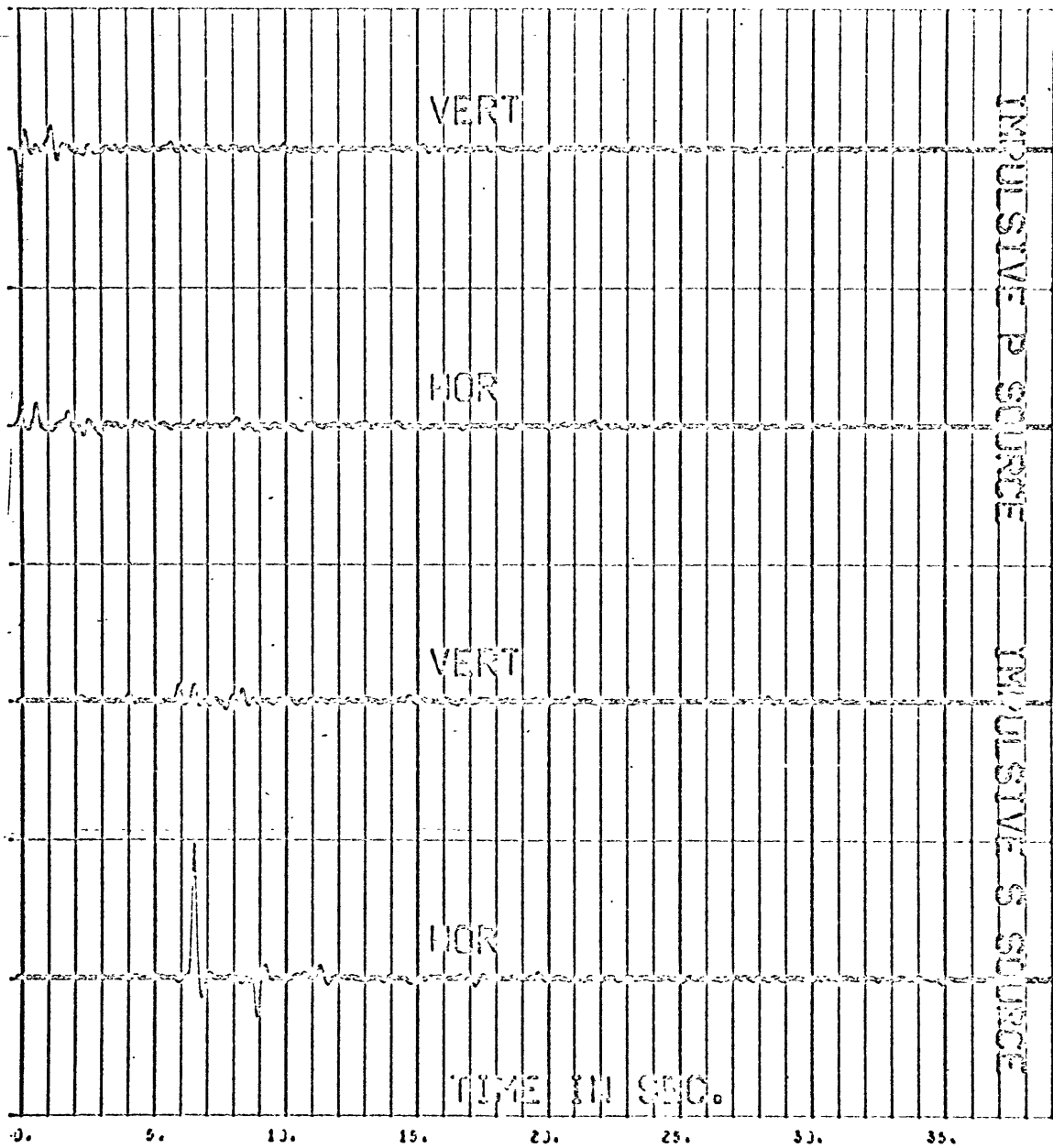
PARTICLE VELOCITY AT SURFACE



TRANSMISSION RESPONSE-CRUST MODEL T11.
PHASE VELOCITY = INFINITY.

FIGURE 5.7

PARTICLE VELOCITY AT SURFACE



TRANSMISSION RESPONSE-CRUST MODEL T11 .
PHASE VELOCITY = 16.14 KM/SEC

FIGURE 5.8

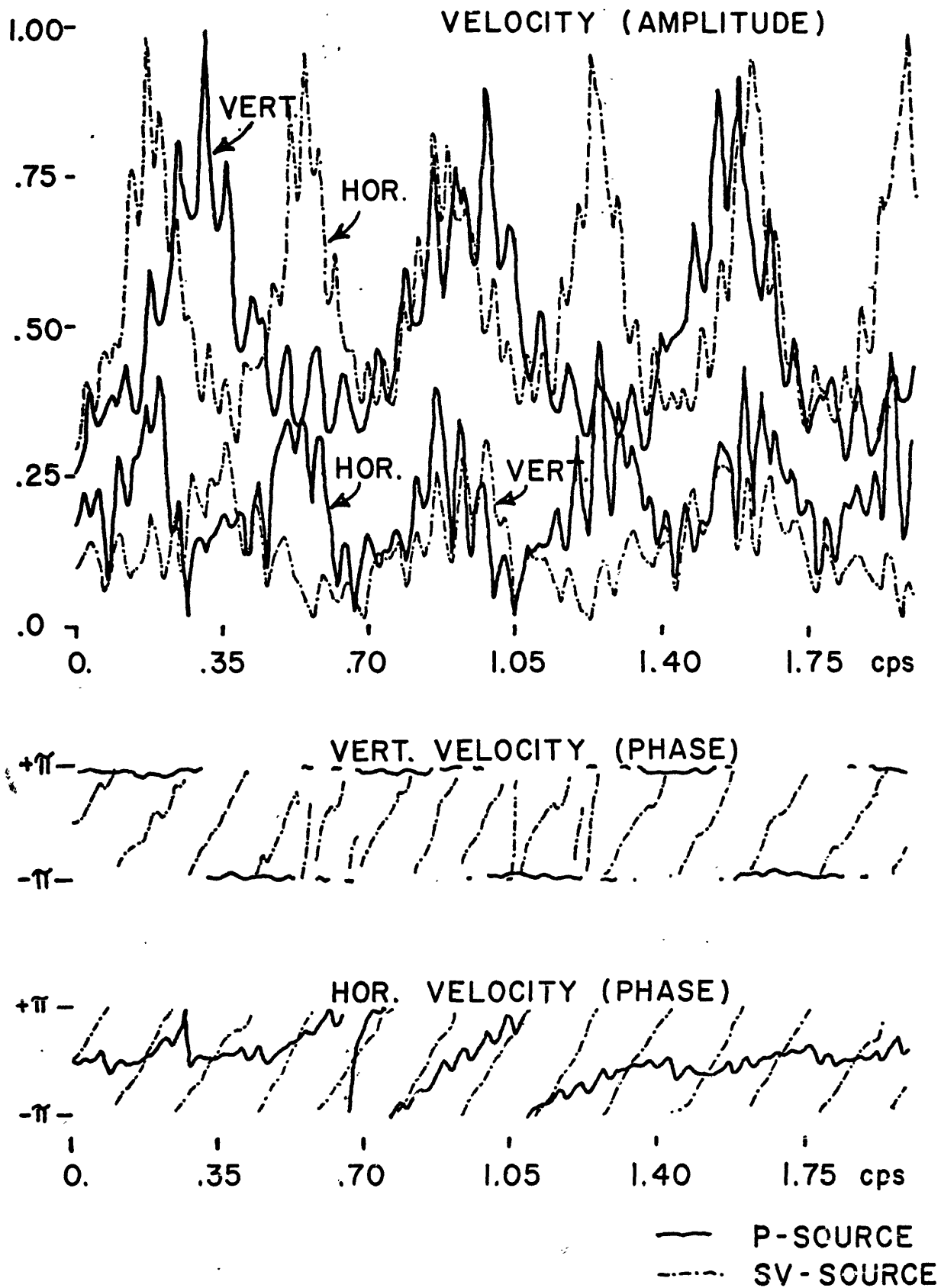


FIGURE 5.8a

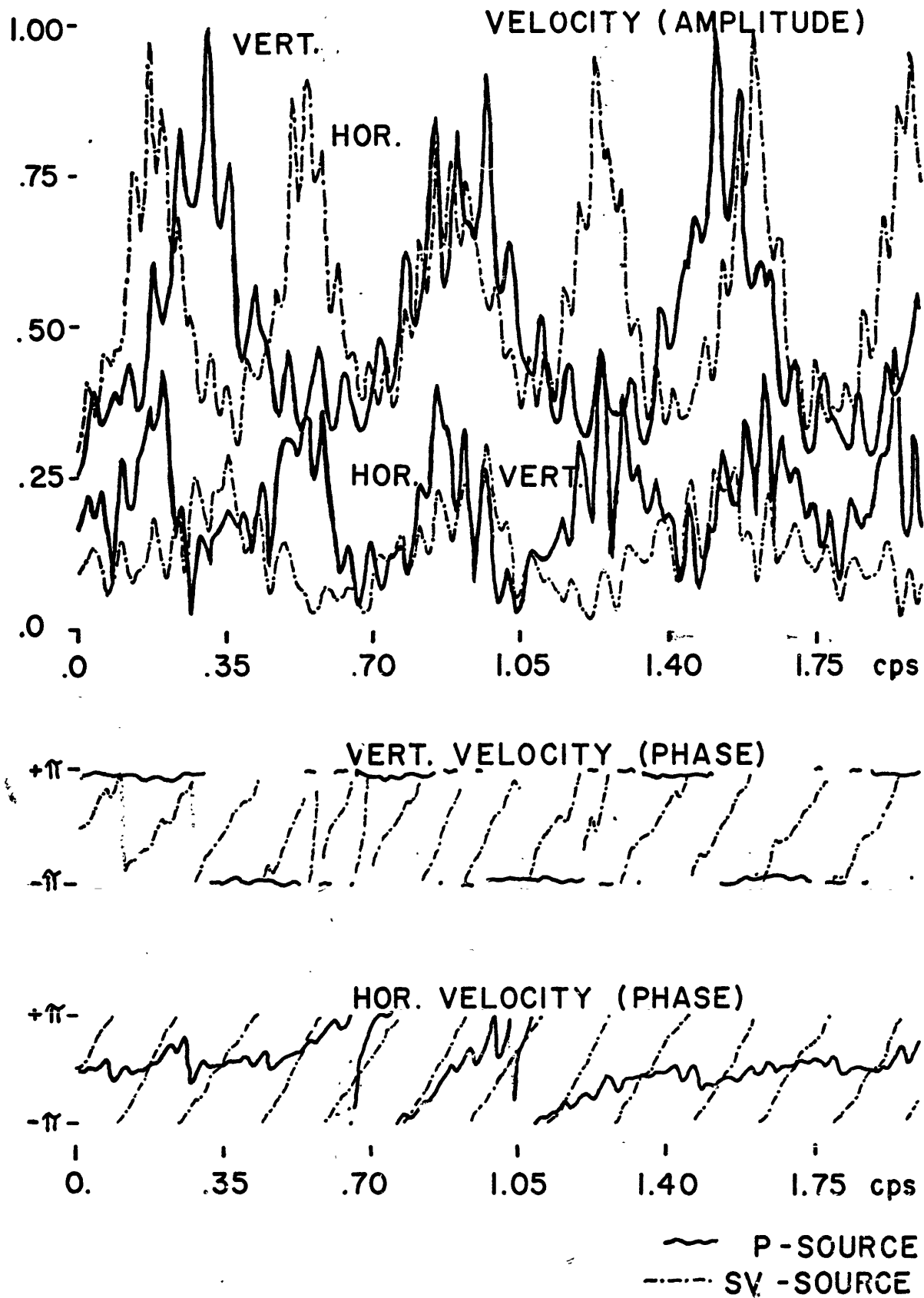


FIGURE 5.8b

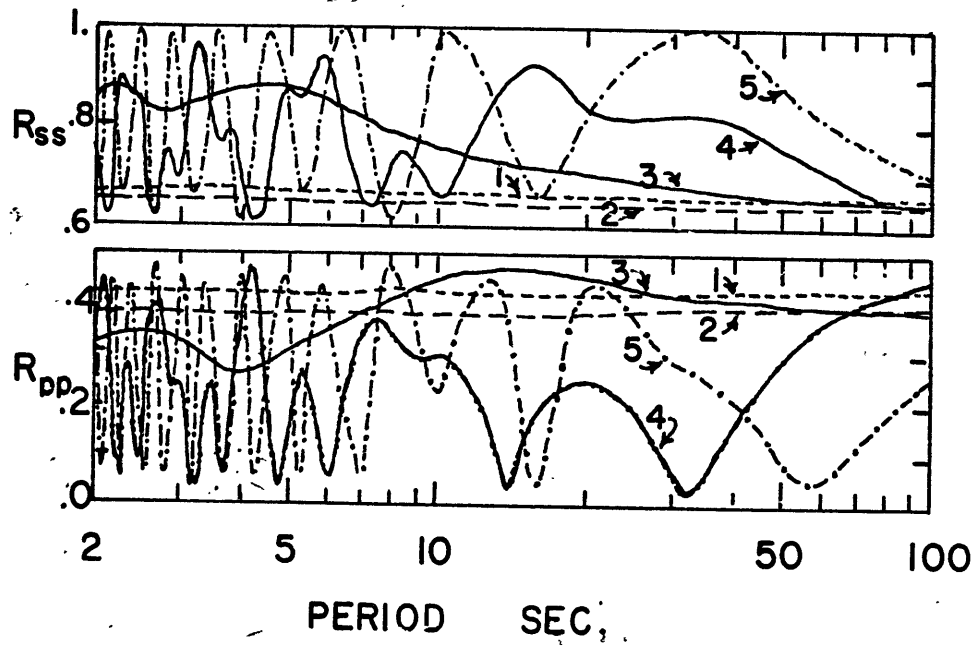


FIGURE 5.9

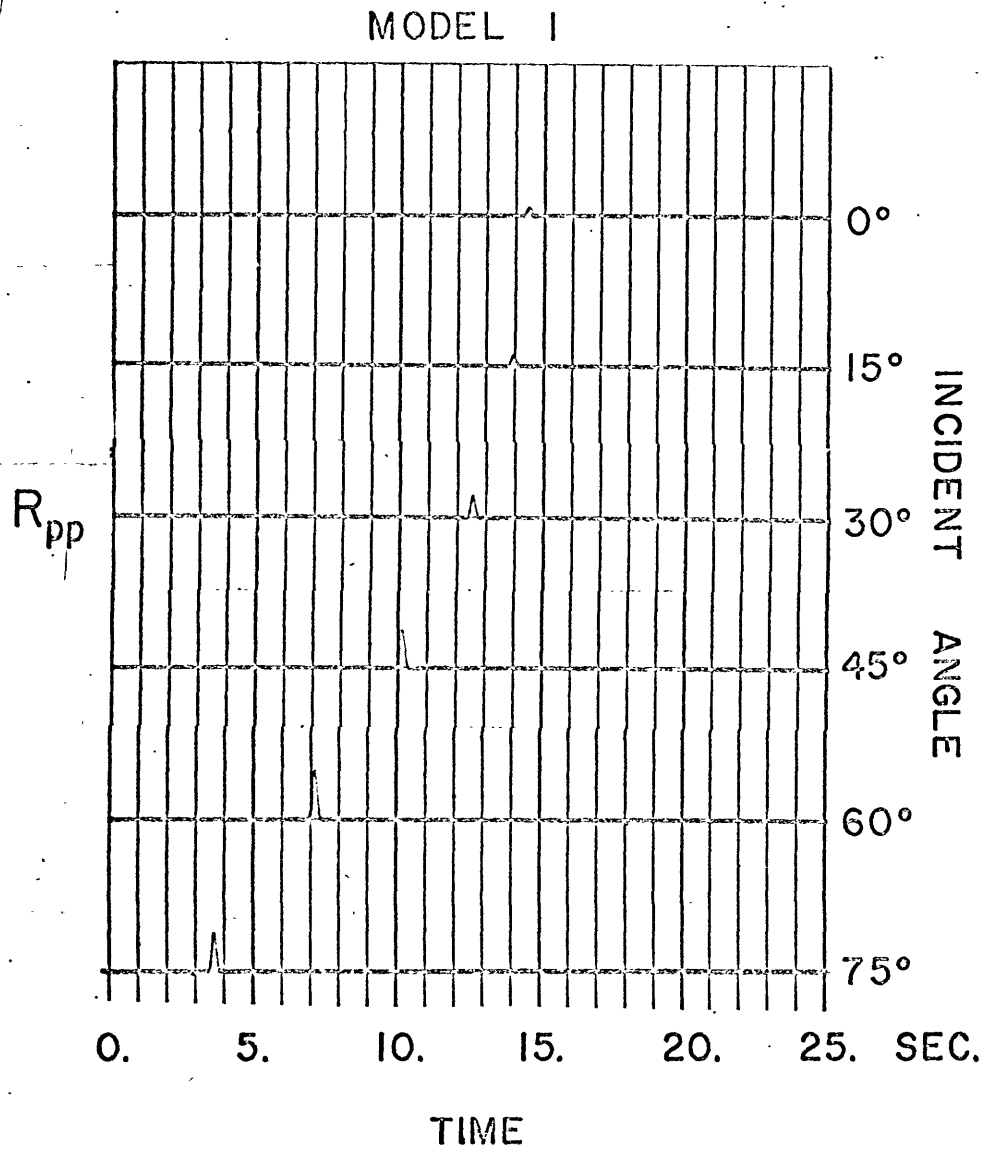


FIGURE 5.10

MODEL 2

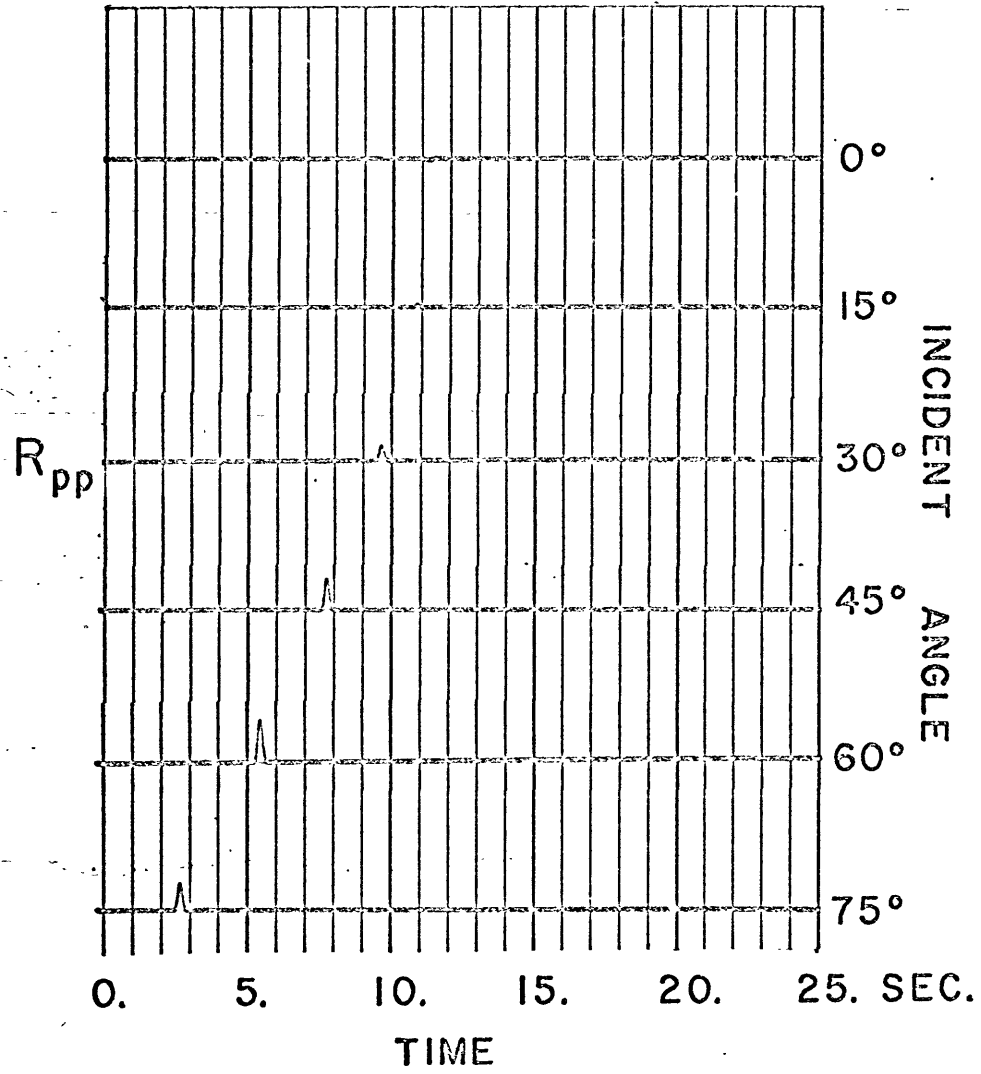


FIGURE 5.11

MODEL 3

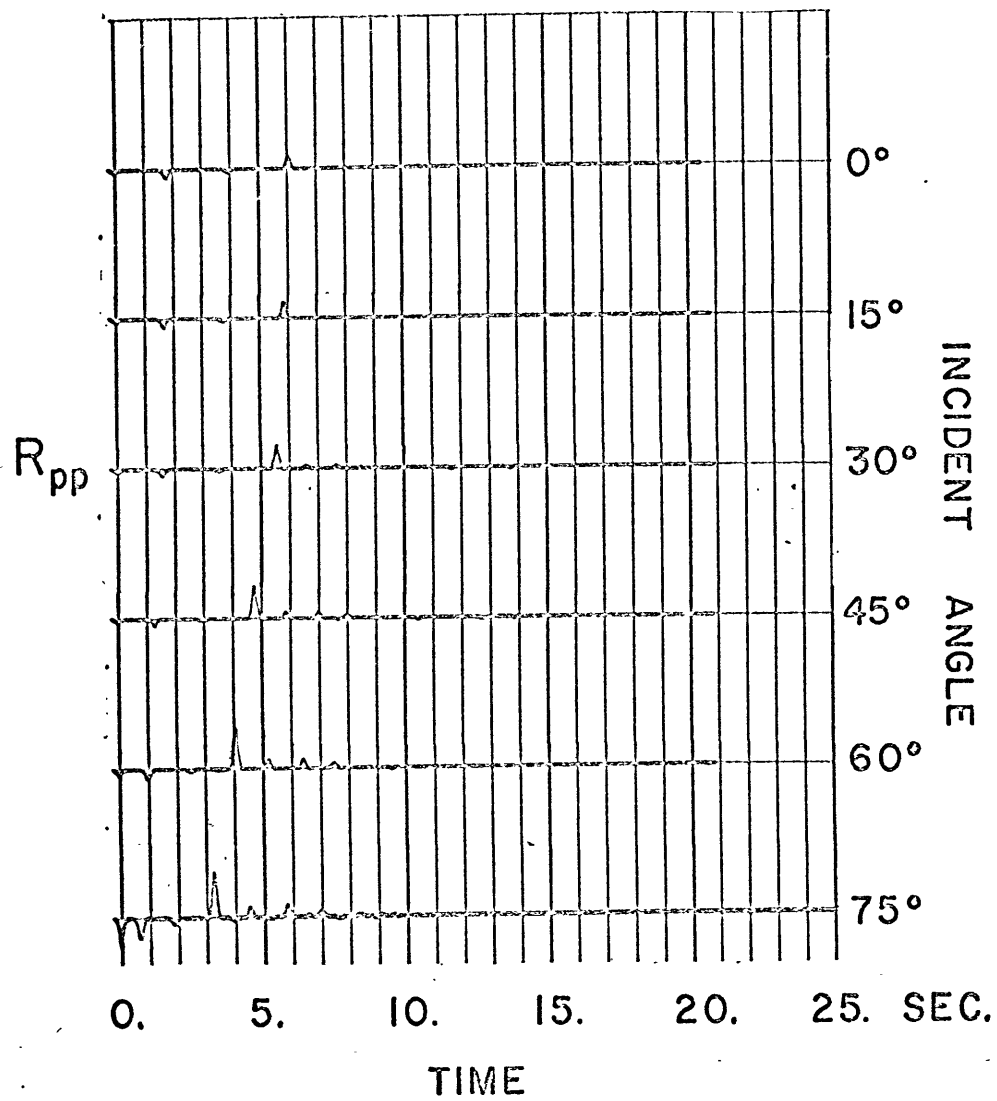


FIGURE 5.12

MODEL 4

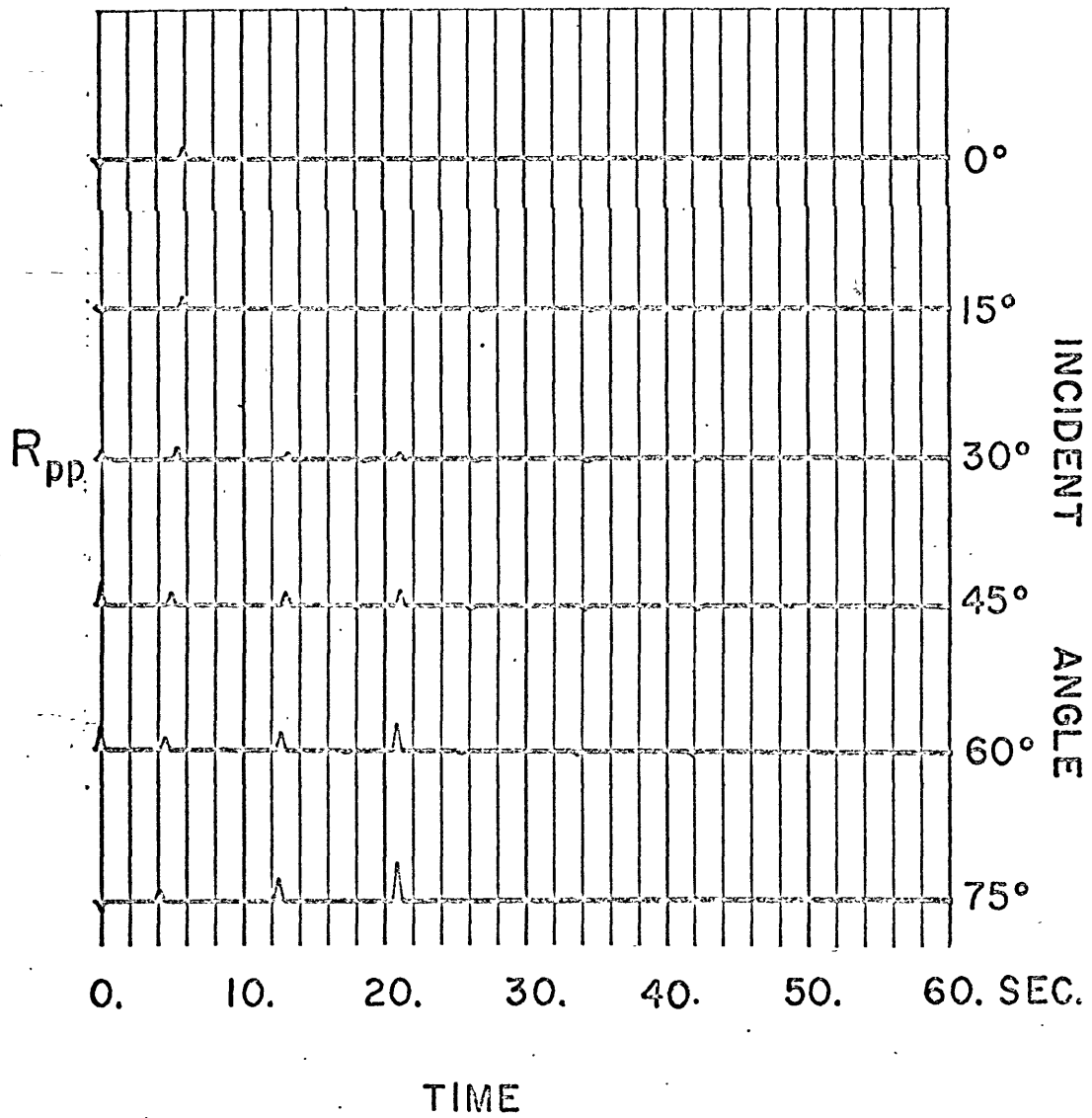


FIGURE 5.13

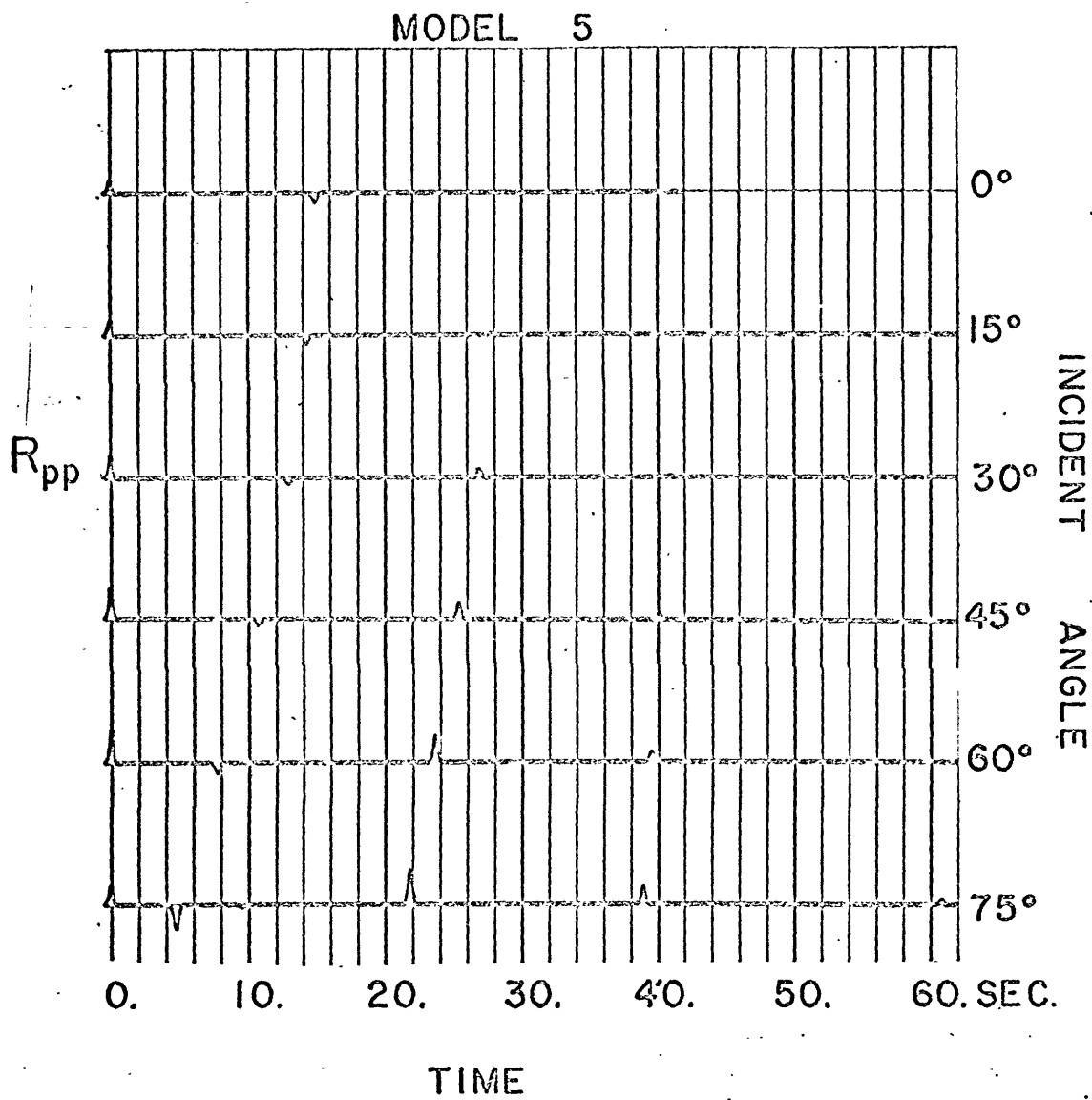


FIGURE 5.14

MODEL I

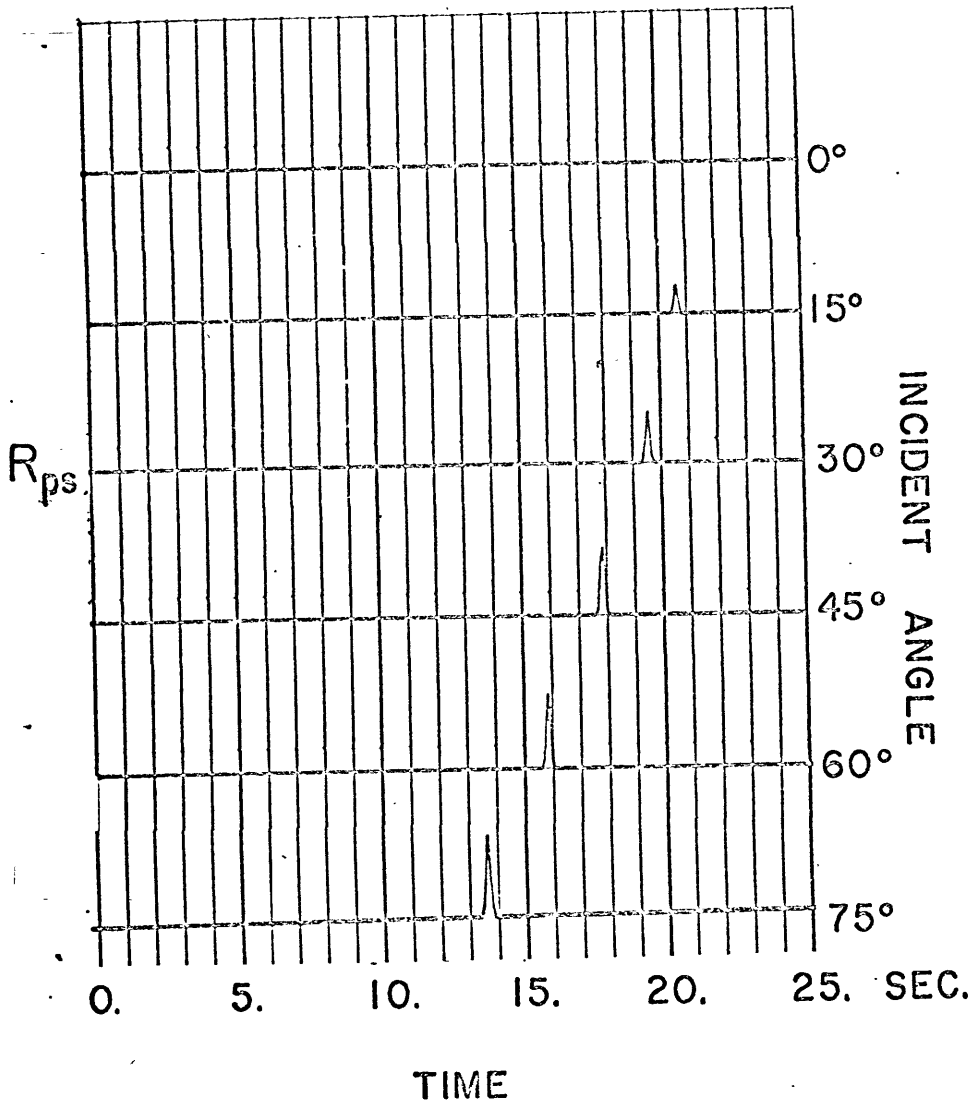


FIGURE 5.15

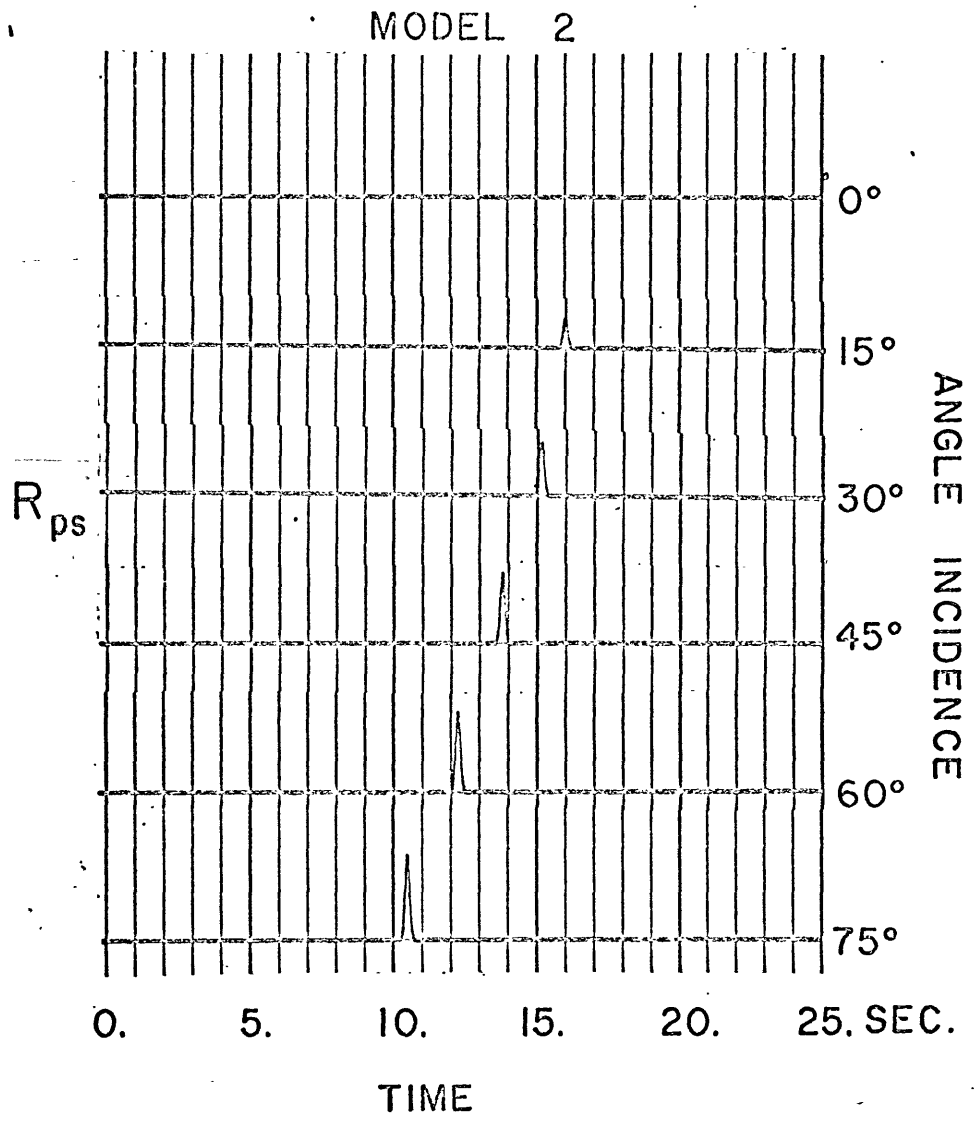


FIGURE 5.16

MODEL 3

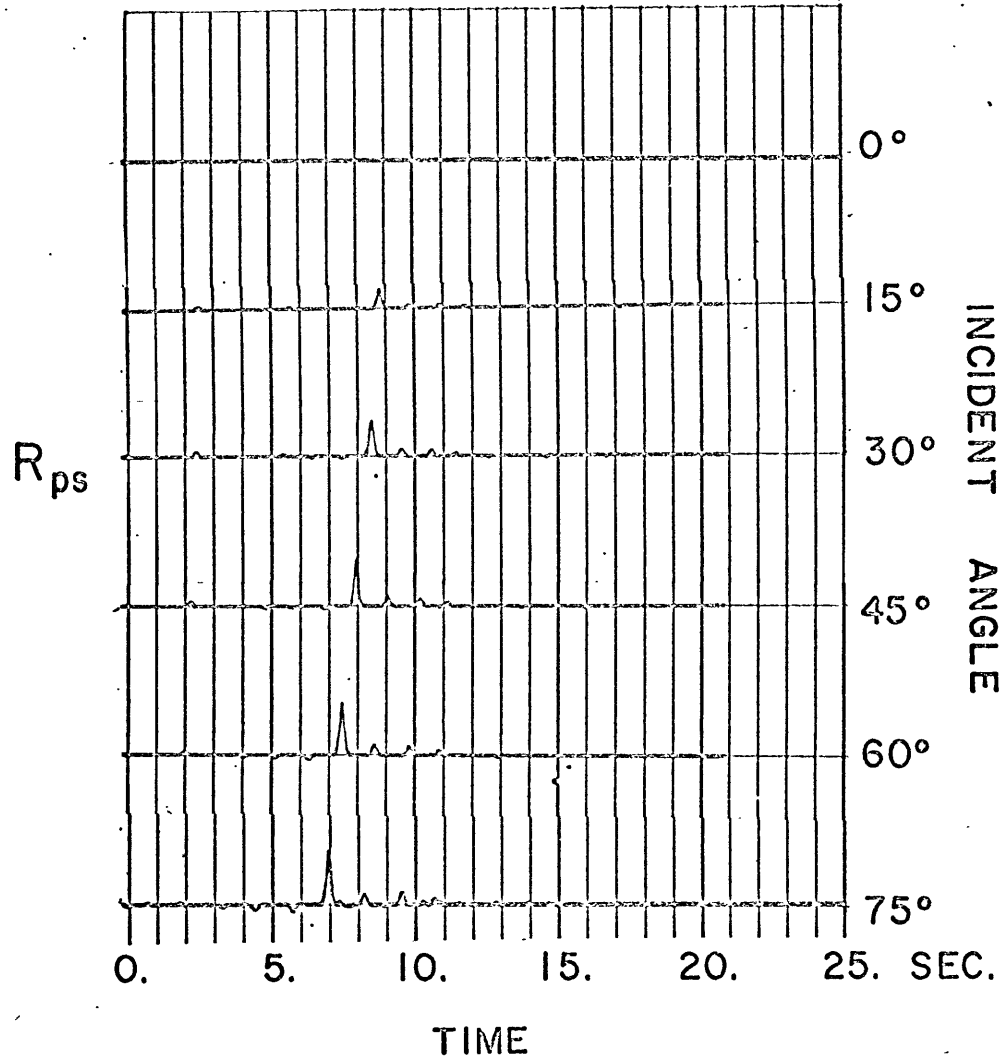


FIGURE 5.17

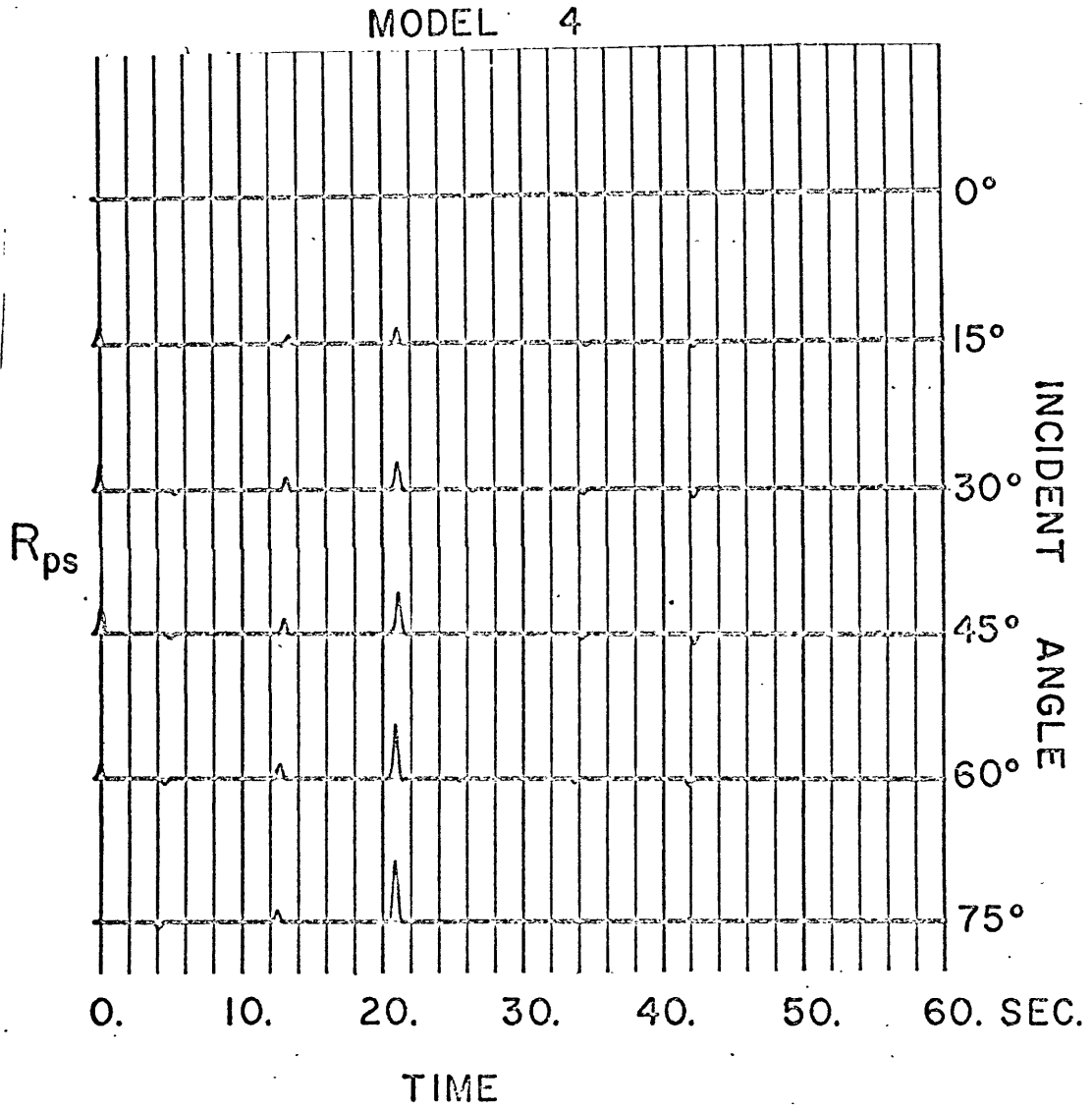


FIGURE 5.18

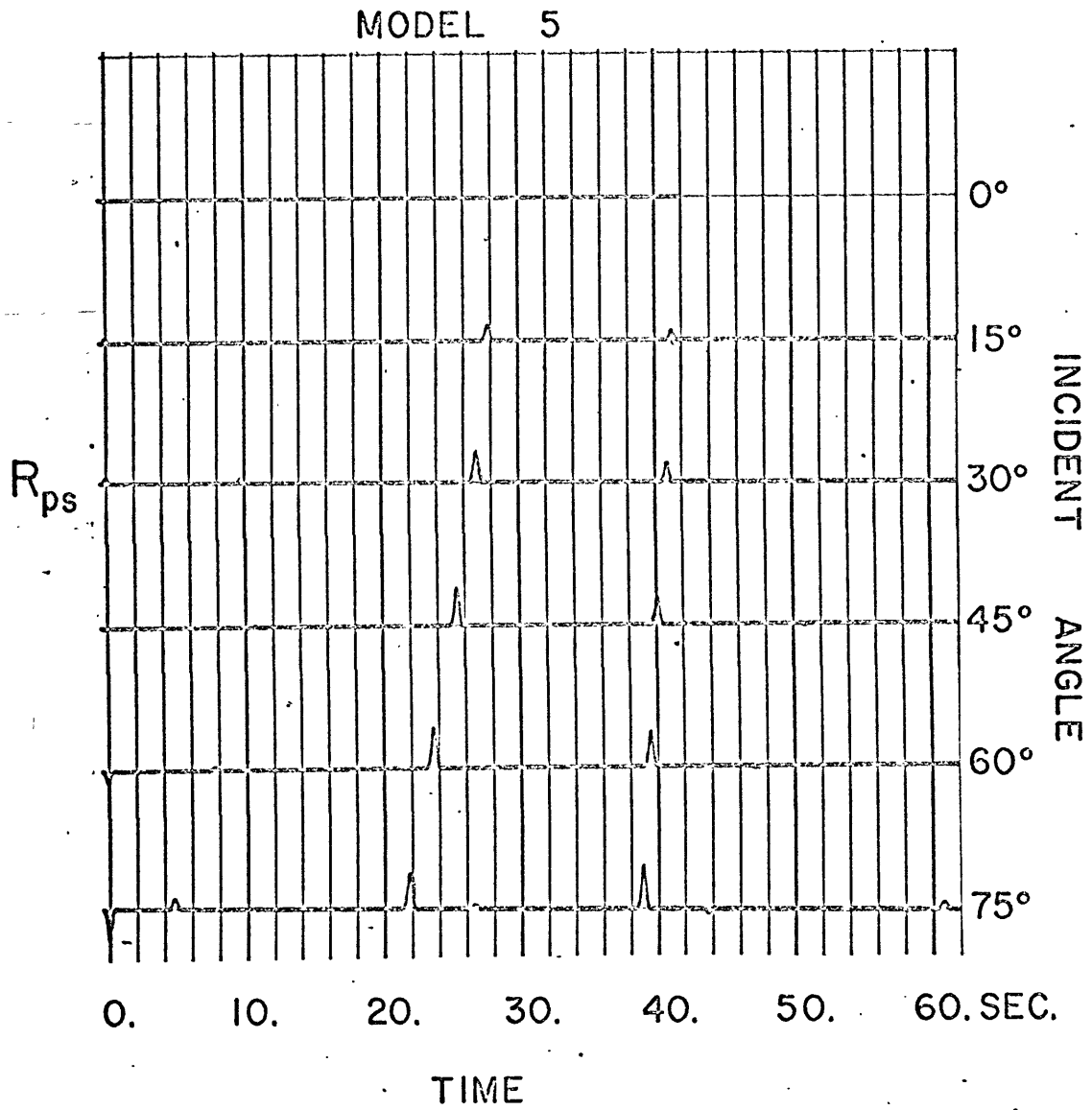


FIGURE 5.19

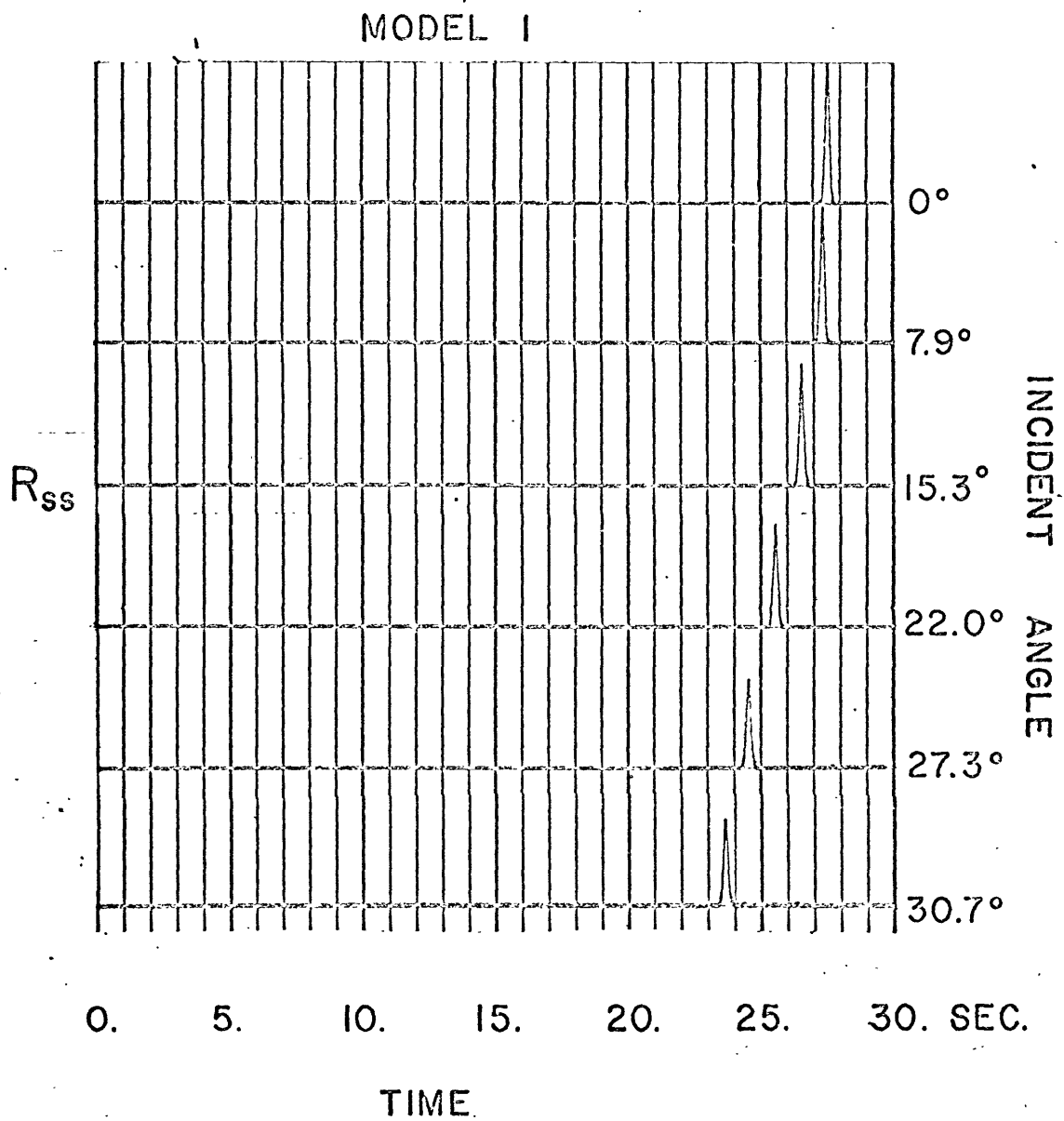


FIGURE 5.20

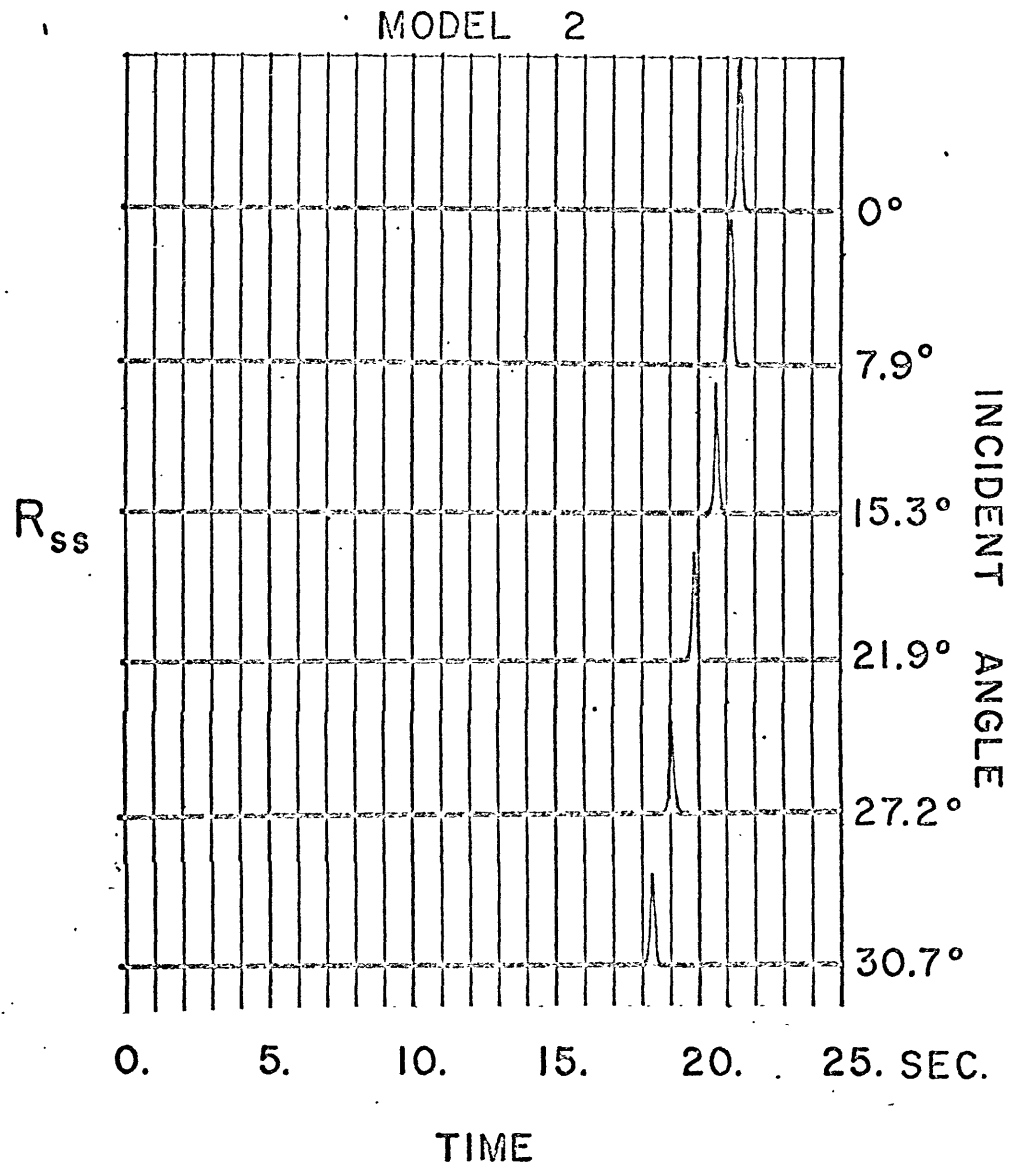


FIGURE 5.21

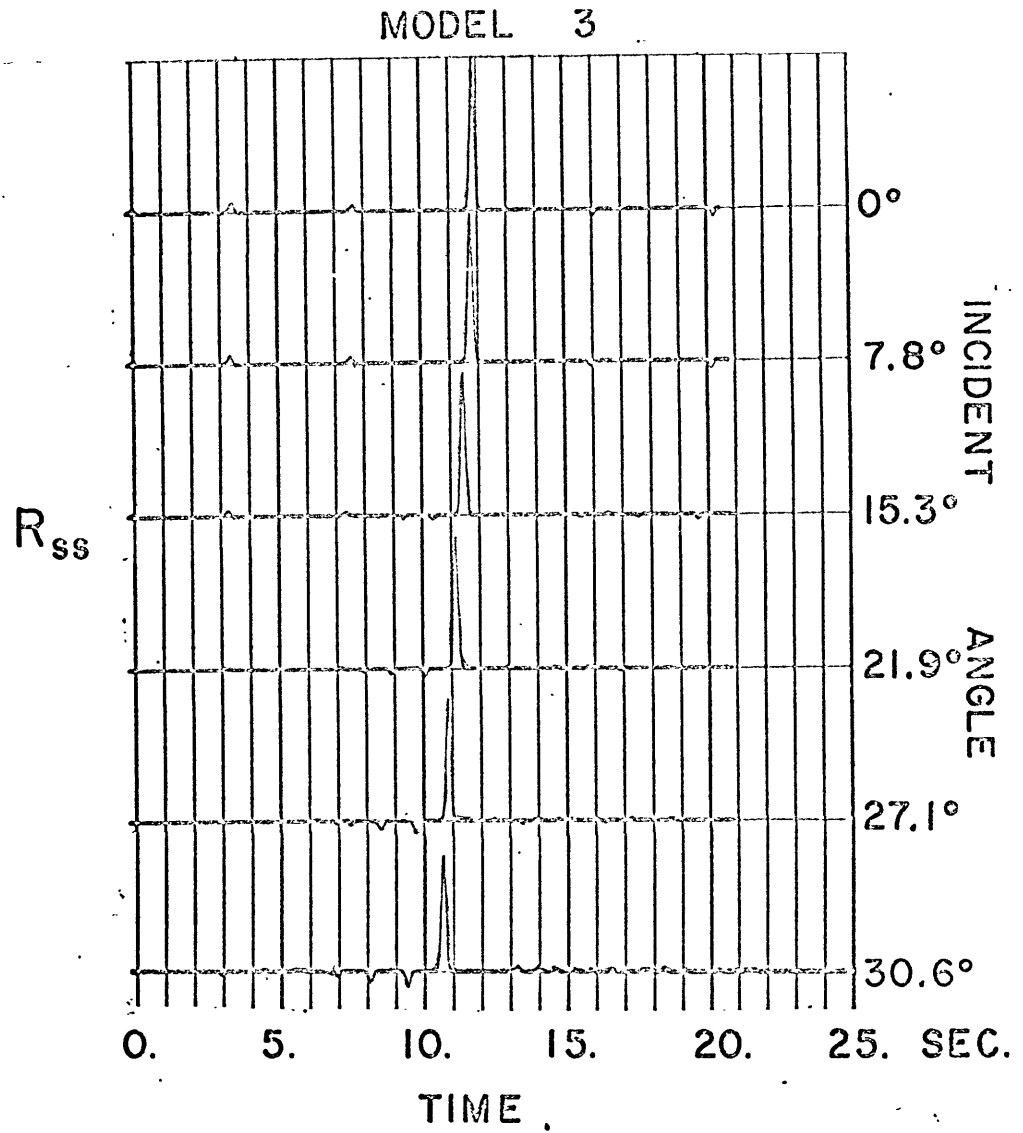


FIGURE 5.22

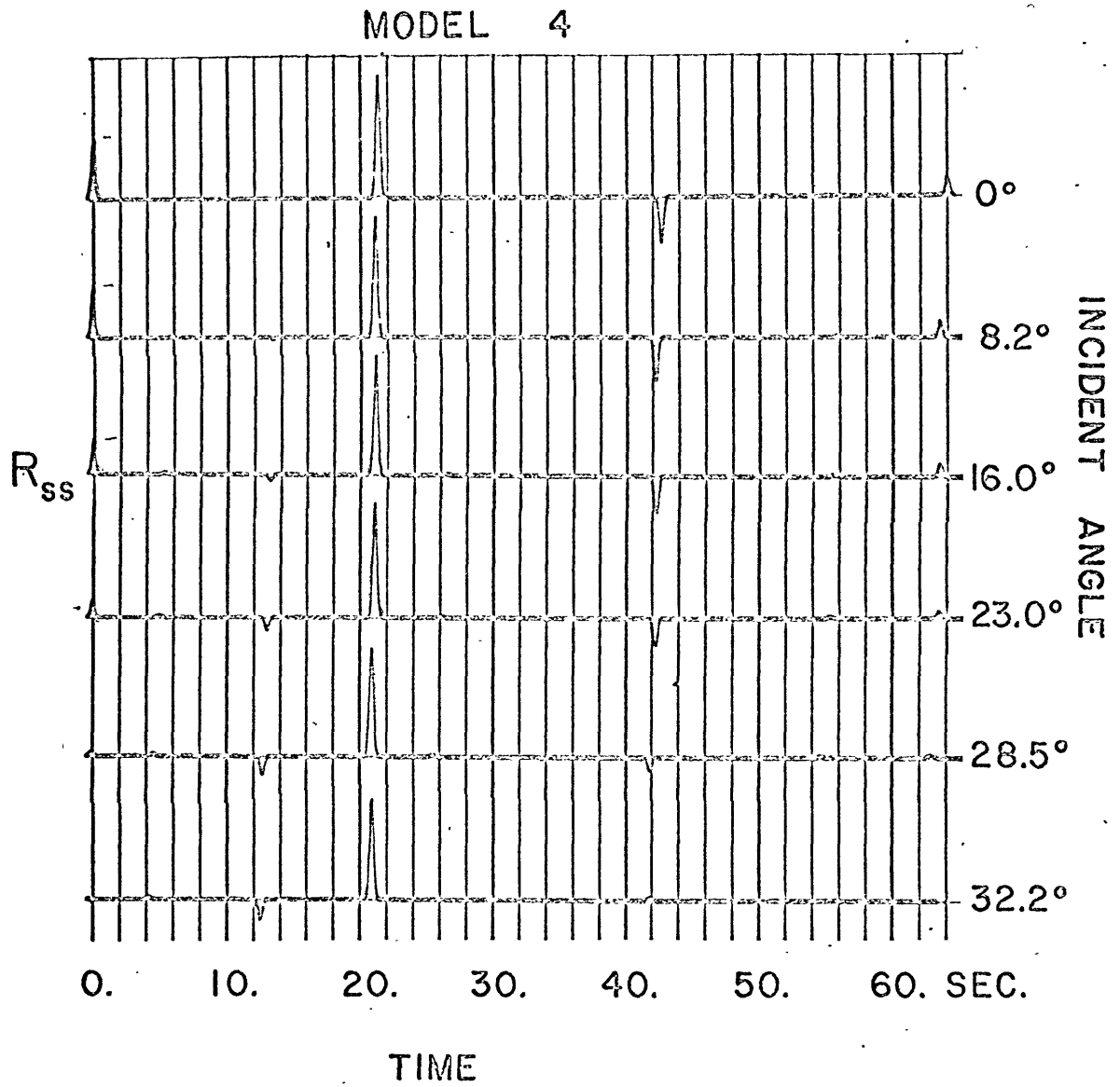


FIGURE 5.23

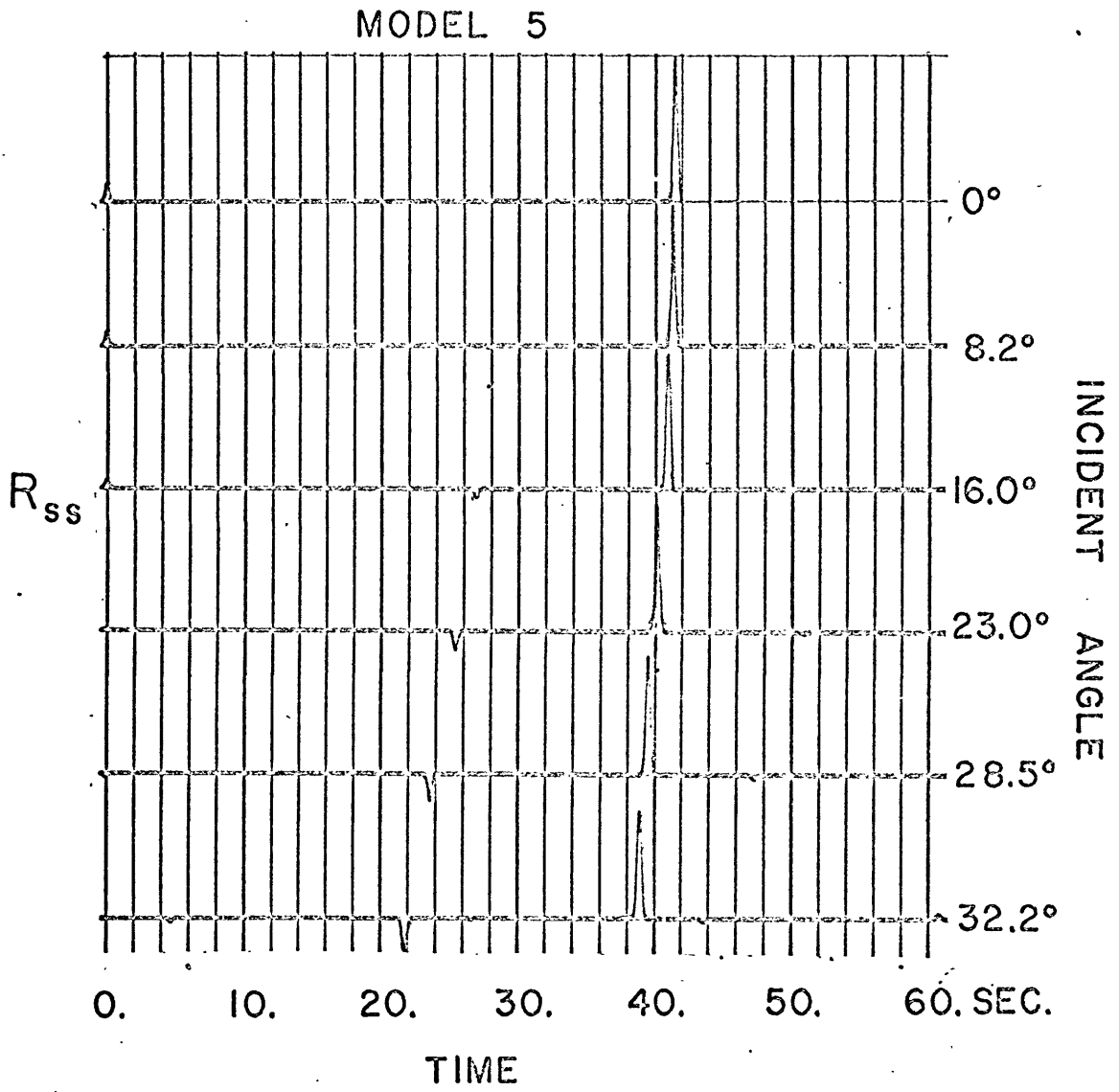


FIGURE 5.24

Chapter VI

Plane Waves in a Medium of Solid and Fluid Layers

6.1 Introduction

In this chapter, the treatment of elastic waves in Chapters II and III is modified so that one may calculate homogeneous plane waves in a medium of solid and fluid layers. Dorman (1962) used Haskell's matrix formulation to obtain the period equation for the normal modes of a layered halfspace for any sequence of solid and fluid layers. Recently, Teng (1967) calculated the frequency response of body waves reflected off and transmitted through various models of the Mantle-Core boundary of the Earth. In an appendix, Teng derived a 4 x 4 fluid layer matrix which can be used with solid layer matrices to compute waves in alternating fluid and solid layers.

As noted by Haskell (1953), the basic difficulty at a solid-fluid interface is that four elastic potentials in the solid cannot be calculated from two velocity potentials in the fluid or from the normal stress τ_{zz} and vertical particle velocity \dot{w} at the interface. In order to solve such an underdetermined system of equations, other boundary conditions for the layered medium have to be imposed. Dorman, for example, used two extra constraints, namely, that the stress components vanish at the free surface, and that no upgoing sources exist in the lower halfspace below his layered model.

We shall consider a problem similar to that solved by Teng. Our layered model consists of a set of horizontal solid and fluid layers sandwiched between two halfspaces. The upper halfspace may be solid, fluid or vacuum, and the lower halfspace may be solid or fluid. The additional constraints are that a known upgoing source be located in the lower halfspace just below the lowest interface, and that no downgoing sources be located in the upper halfspace.

Reflection and transmission responses for the set of layers are calculated, and from these responses, body waves inside each fluid and solid layer can be computed.

6.2 Description of Solid and Fluid Layers

Following Dorman, we assume a horizontally layered medium of homogeneous, isotropic solid and fluid layers. When possible, we combine all adjacent solid layers into single inhomogeneous solid layers, and similarly combine adjacent fluid layers. This results in a model of alternating solid and fluid layers, where each new layer is inhomogeneous if it consists of more than one homogeneous layer. We shall assume in general that the new layers are inhomogeneous.

These layers are numbered 1 to n from top to bottom. We shall assume that the set of layers is bounded from above and below by homogeneous halfspaces. Within the medium, a typical sequence of three such layers is shown in Figure 6.1. Layers k and $k+2$ are solid and layer $k+1$ is fluid. As shown in Appendix A, compressional waves DP and UP in a fluid are obtained by replacing each elastic potential term $f''(\hat{p} \cdot \bar{r} - \alpha t)$ by $\phi'(\hat{p} \cdot \bar{r} - \alpha t)/\alpha$ where ϕ' is the first total derivative of a velocity potential ϕ . In this way, the fluid waves retain the same physical form as in an elastic solid, i.e.,

$$\begin{aligned} UP(\hat{p}_u \cdot \bar{r} - \alpha t) &= \sqrt{\rho \alpha \cos \delta} V_{p_u} \\ DP(\hat{p}_d \cdot \bar{r} - \alpha t) &= \sqrt{\rho \alpha \cos \delta} V_{p_d} \end{aligned} \quad (6-1)$$

where V_{p_u} and V_{p_d} are the total particle velocities associated with the up and downgoing waves respectively. The particle velocity directions are the same as shown in Figure 1 for an elastic solid.

The layer matrix iteration for fluid compressional waves at non-normal or normal incidence has the same form as the uncoupled compressional waves in a solid layer at normal incidence. Since layer $k+1$ consists of adjacent homogeneous fluid layers, we can apply iterations like those of section 3.2 to obtain a matrix relating waves at the top and bottom of the inhomogeneous layer. Let UP_{k+1} and DP_{k+1} be the fluid waves at the top of layer $k+1$, and let UP'_{k+1} and DP'_{k+1} be waves at the bottom of this layer as shown in Figure . Given the thickness, velocity and density of each homogeneous fluid layer within layer $k+1$, we can apply equations (3-5) and (3-7) successively to obtain a relation of the form

$$\begin{bmatrix} DP \\ UP \end{bmatrix}_{k+1} = z^{-p_{k+1}} \begin{bmatrix} f(z) & q(z) \\ z^{2p} q(1/z) & z^{2p} f(1/z) \end{bmatrix} \begin{bmatrix} DP' \\ UP' \end{bmatrix}_{k+1} \quad (6-2)$$

where $p_{k+1} \Delta \tau$ is the one way transit time for compressional plane waves through layer $k+1$. As in (3-8) and (3-10) $f(z)$ and $q(z)$ are polynomials in z . The proof of (6-2) is the same as for (3-8) and will not be repeated here. If layer $k+1$ consists of only one homogeneous fluid layer, then $f(z) = 1$ and $q(z) = 0$.

A similar matrix relation can be derived for layers k and $k+2$ in Figure 6.1. Applying equations (2-26), (2-27), (2-28) and (3-13a), we can relate the waves at the top of each inhomogeneous layer to

those at the bottom. For layer k , one obtains

$$\begin{bmatrix} \dot{d}_k \\ \bar{u}_k \end{bmatrix} = z^{-s_k} \begin{bmatrix} F(z) & G(z) \\ z^{2s} G(1/z) & z^{2s} F(1/z) \end{bmatrix}_k \begin{bmatrix} \dot{d}'_k \\ \bar{u}'_k \end{bmatrix} \quad (6-3)$$

where $F(z)$ and $G(z)$ are 2×2 matrix polynomials in z , and $s_k \Delta \tau$ equals the one-way transit time for plane SV waves through layer k . If layer k consists of a single homogeneous layer, then is the null matrix and

$$F(z) = z^{s_k} \begin{bmatrix} z^{p_k} & 0 \\ 0 & z^{s_k} \end{bmatrix}$$

as shown by (2-25) and (2-26). As in the fluid layer, $p_k \Delta \tau$ equals the P wave transit time through layer k .

The purpose of equations (6-2) and (6-3) is to isolate the solid-fluid interfaces, since no problems arise at solid-solid or fluid-fluid interfaces. In the following section, the problem of calculating the solid waves in layer $k+2$ from those in layer k is solved in detail.

6.3 Recursive Calculation of Reflection Response

In this section, the reflection response matrix $R^{(k+1)}(z)$ is determined for interface $k+1$ in Figure 6.1 such that

$$\bar{d}_{k+2} = R^{(k+1)}(z) \bar{u}_{k+2} \quad (6-4)$$

This reflection response was introduced in Chapter III, equation (3-33)

for a completely solid layered medium. In this case, we shall derive

a recursion formula for finding $R^{(k+1)}(z)$ in terms of $R^{(k)}(z)$.

This recursion can be used to find the reflection response of the complete set of layers. For example, if layer 1 is solid, we have

$$\bar{d}_1 = R_0 \bar{u}_1$$

so that $R^{(0)} = R_0$. Starting with $R^{(0)}$ the reflection response $R^{(n)}(z)$ for all the layers can be calculated if layer $n+1$ is a solid halfspace.

Referring to Figure 6.1, the difficulty is in relating the solid waves in layers k and $k+2$. One cannot directly calculate \bar{d}_{k+2} and \bar{u}_{k+2} from \bar{d}_k and \bar{u}_k because two degrees of freedom are lost in crossing interface k , i.e. four solid waves are linearly combined to give two fluid waves. At interface $k+1$, two fluid waves are not enough to determine the four solid wave components of \bar{d}_{k+2} and \bar{u}_{k+2} .

However, we can calculate a matrix which gives the solid waves \bar{u}'_k and \bar{d}'_{k+2} leaving the fluid layer in terms of the incident waves \bar{u}_{k+2} and \bar{d}'_k . Let $S(z)$ be this 4×4 matrix defined such that

$$\begin{bmatrix} \bar{d}'_{k+2} \\ \bar{u}'_k \end{bmatrix} = \begin{bmatrix} S_{11}(z) & S_{12}(z) \\ S_{21}(z) & S_{22}(z) \end{bmatrix}_{k+1} \begin{bmatrix} \bar{d}'_k \\ \bar{u}_{k+2} \end{bmatrix} \quad (6-5)$$

where $S_{ij}(z)$ are 2×2 partitioned submatrices of $S(z)$. The $S_{ij}(z)$ are derived later on in this section.

Assuming $S(z)$ is known, one can find the recursion formula for calculating $R^{(k+1)}(z)$ from $R^{(k-1)}(z)$. At interface $k-1$, we have

$$\bar{d}'_k = R^{(k-1)}(z) \bar{u}_k \quad (6-6)$$

Substituting this equation into (6-3), we obtain

$$\bar{d}'_k = V^{(k)}(z) \bar{u}'_k \quad (6-7)$$

where

$$V^{(k)}(z) = - \left[F^{(k)}(z) - z^{2S_k} R^{(k-1)}(z) G^{(k)}(1/z) \right]^{-1} \left[G^{(k)}(z) - z^{2S_k} R^{(k-1)}(z) F^{(k)}(1/z) \right] \quad (6-8)$$

We note that $V^{(k)}(z)$ depends only on the physical parameters of the layers above the k -th interface.

The second row of (6-5) gives

$$\bar{u}'_k = S_{21}^{(k+1)}(z) d'_k + S_{22}^{(k+1)}(z) \bar{u}_{k+2} \quad (6-9)$$

Using (6-7) to eliminate d'_k yields

$$\bar{u}'_k = (\bar{I}_2 - S_{21}^{(k+1)}(z) V^{(k)}(z))^{-1} S_{22}^{(k+1)}(z) \bar{u}_{k+2} \quad (6-10)$$

Similarly, putting (6-7) into the first row of (6-5), one gets the relation

$$d_{k+2} = S_{11}^{(k+1)}(z) V^{(k)}(z) \bar{u}'_k + S_{12}^{(k+1)}(z) \bar{u}_{k+2} \quad (6-11)$$

We eliminate \bar{u}'_k in (6-11) by using (6-10). This gives the final result

$$d_{k+2} = \left[S_{11}^{(k+1)}(z) V^{(k)}(z) (\bar{I}_2 - S_{21}^{(k+1)}(z) V^{(k)}(z))^{-1} S_{22}^{(k+1)}(z) + S_{12}^{(k+1)}(z) \right] \bar{u}_{k+2} \quad (6-12)$$

By comparing this equation with (6-4), one sees that

$$R(z) = S_{11}^{(k+1)}(z) V^{(k)}(z) (\bar{I}_2 - S_{21}^{(k+1)}(z) V^{(k)}(z))^{-1} S_{22}^{(k+1)}(z) + S_{12}^{(k+1)}(z) \quad (6-13)$$

This equation is a recursion formula for $R^{(k+1)}(z)$ since $V^{(k)}(z)$ depends on $R^{(k-1)}(z)$. As shown below, the submatrices depend only on the properties of layers $k-1$, k , and $k+1$. Therefore, $R^{(k+1)}(z)$ is a function of layers $k+1$, k , ... 0.

The remainder of this section gives the algebraic details in the calculation of $S(z)$ defined by (6-5). The first step is to write the linear equations relating the solid and fluid waves on each side of interfaces k and $k+1$. These equations are obtained from (2-11) by eliminating those reflection and transmission coefficients which vanish or are undefined at a solid fluid interface. Doing this for interfaces k and $k+1$ gives two sets of equations, i.e.,

$$\left[\begin{array}{cc|cc} t'_{pp} & t'_{sp} & 0 & 0 \\ -r'_{pp} & -r'_{sp} & 1 & 0 \\ \hline -r'_{ps} & -r'_{ss} & 0 & 1 \end{array} \right]_k \begin{bmatrix} DP' \\ DS' \\ \hline UP' \\ US' \end{bmatrix}_k = \begin{bmatrix} 1 & -r_{pp} \\ 0 & t_{pp} \\ \hline 0 & t_{ps} \end{bmatrix}_k \begin{bmatrix} DP \\ \hline UP \end{bmatrix}_{k+1}$$

$$\begin{bmatrix} t_{pp}' & | & 0 \\ \hline t_{ps}' & | & 0 \\ \hline -r_{pp}' & | & 1 \end{bmatrix}_{K+1} \begin{bmatrix} DP' \\ \hline UP' \end{bmatrix}_{K+1} = \begin{bmatrix} 1 & 0 & | & -r_{pp} & -r_{sp} \\ \hline 0 & 1 & | & -r_{ps} & -r_{ss} \\ \hline 0 & 0 & | & t_{pp} & t_{sp} \end{bmatrix}_{K+1} \begin{bmatrix} DP \\ \hline DS \\ \hline UP \\ \hline US \end{bmatrix}_{K+2}$$

(6-15)

For convenience, let us define the following vectors and scalar quantities:

$$\bar{t}_K = \begin{bmatrix} t_{pp} \\ t_{ps} \end{bmatrix}_K = \begin{bmatrix} t_{pp}' \\ t_{sp}' \end{bmatrix}_K$$

$$\bar{t}'_{K+1} = \begin{bmatrix} t_{pp}' \\ t_{ps}' \end{bmatrix}_{K+1} = \begin{bmatrix} t_{pp} \\ t_{sp} \end{bmatrix}_{K+1}$$

$$r_K = [r_{pp}]_K, \quad r'_{K+1} = [r'_{pp}]_{K+1}$$

(6-16)

The equalities between primed and unprimed transmission

coefficients above are proved in Appendix A. They are reciprocity relations, for solid-fluid interfaces similar to the relation $T'=T^*$ for solid-solid interfaces. Substituting these terms and those of (2-12) into (6-14) and (6-15), we obtain

$$\begin{aligned}\bar{\tau}_k^* \cdot d_k' &= DP_{k+1}' - r_k UP_{k+1}' \\ -R_k' d_k' + \bar{u}_k' &= \bar{\tau}_k UP_{k+1}'\end{aligned}\quad (6-17)$$

and

$$\begin{aligned}\bar{\tau}_{k+1}' DP_{k+1}' &= d_{k+2}' - R_{k+1} \bar{u}_{k+2}' \\ -r_{k+1}' DP_{k+1}' + UP_{k+1}' &= \bar{\tau}_{k+1}^* \cdot \bar{u}_{k+2}'\end{aligned}\quad (6-18)$$

The second equation of (6-17) and the first equation of (6-18)

are

$$\begin{aligned}d_{k+2}' &= R_{k+1} \bar{u}_{k+2}' + \bar{\tau}_{k+1}' DP_{k+1}' \\ \bar{u}_k' &= R_k' d_k' + \bar{\tau}_k UP_{k+1}'\end{aligned}\quad (6-19)$$

The fluid waves DP_{k+1}' and UP_{k+1}' can be replaced by expressions in the solid waves. From the first equation of (6-17) and the

and the second equation of (6-18), we

$$\begin{bmatrix} UP' \\ DP \end{bmatrix}_{K+1} - \begin{bmatrix} r'_{K+1} & 0 \\ 0 & r_K \end{bmatrix} \begin{bmatrix} DP' \\ UP \end{bmatrix}_{K+1} = \begin{bmatrix} \bar{\tau}'_{K+1} \cdot \bar{u}_{K+2} \\ \bar{\tau}'_K \cdot \bar{d}'_K \end{bmatrix} \quad (6-20)$$

The inverse matrix relation for (6-2) is

$$\begin{bmatrix} DP' \\ UP' \end{bmatrix}_{K+1} = \frac{1}{z} \begin{bmatrix} z^{2P} f(1/z) & -g(z) \\ -z^{2P} g(1/z) & f(z) \end{bmatrix} \begin{bmatrix} DP \\ UP \end{bmatrix}_{K+1} \quad (6-21)$$

Taking the first row of (6-21) and the second row of (6-2) gives

$$\begin{bmatrix} UP' \\ DP \end{bmatrix}_{K+1} = \frac{1}{f(1/z)} \begin{bmatrix} -z^{2P} g(1/z) & z^P \\ z^P & g(z) \end{bmatrix} \begin{bmatrix} DP' \\ UP \end{bmatrix}_{K+1} \quad (6-22)$$

Substituting this result into (6-20) yields

$$\frac{1}{f(1/z)} \begin{bmatrix} -z^{2P} g(1/z) - r'_{K+1} z^{2P} f(1/z) & z^P \\ z^P & g(z) - r_K z^{2P} f(1/z) \end{bmatrix} \begin{bmatrix} DP' \\ UP \end{bmatrix}_{K+1} = \begin{bmatrix} \bar{\tau}'_{K+1} \cdot \bar{u}_{K+2} \\ \bar{\tau}'_K \cdot \bar{d}'_K \end{bmatrix} \quad (6-23)$$

Inverting the matrix on the left-hand side of this equation, we obtain

$$\begin{bmatrix} DP' \\ UP \end{bmatrix}_{K+1} = \frac{1}{\Delta(z)} \begin{bmatrix} -q(z) + r_K z^{2P} f(1/z) & z^P \\ z^P & z^{2P} q(1/z) + r'_{K+1} z^{2P} f(1/z) \end{bmatrix} \begin{bmatrix} \bar{\tau}'_{K+1} \bar{u}_{K+2} \\ \bar{\tau}'_K \bar{d}'_K \end{bmatrix} \quad (6-24)$$

where

$$\Delta(z) = [f(z) - r_K z^{2P} q(1/z)] + r'_{K+1} [q(z) - r_K z^{2P} f(1/z)] \quad (6-25)$$

using (3-12).

Finally, we substitute (6-24) into (6-19) to obtain the matrix $S(z)$ in (6-5) which relate the solid waves above and below the fluid layer. The resulting submatrices of $S(z)$ are

$$\begin{aligned} S_{11}^{(K+1)}(z) &= \frac{z^P \bar{\tau}'_{K+1} \bar{\tau}'_K}{\Delta(z)} \\ S_{12}^{(K+1)}(z) &= R_{K+1} + \frac{1}{\Delta(z)} (-q(z) + r_K z^{2P} f(1/z)) \bar{\tau}'_{K+1} \bar{\tau}'_{K+1} \\ S_{21}^{(K+1)}(z) &= R'_K + \frac{z^{2P}}{\Delta(z)} (q(1/z) + r'_{K+1} f(1/z)) \bar{\tau}'_K \bar{\tau}'_K \\ S_{22}^{(K+1)}(z) &= \frac{z^P \bar{\tau}'_K \bar{\tau}'_{K+1}}{\Delta(z)} \end{aligned} \quad (6-26)$$

The superscript $k+1$ on each S_{ij} is the layer number of the inhomogeneous fluid layer between solid layers.

To illustrate the use of (6-5), let us consider a single homogeneous fluid layer between two solid halfspaces. Assuming that no downgoing sources exist in the upper halfspace, we set $\bar{d}'_k = 0$.

From (6-5), we then obtain

$$\begin{aligned} \bar{d}'_{k+2} &= S_{12}^{(k+1)}(z) \bar{u}_{k+2} \\ \bar{u}'_k &= S_{22}^{(k+1)}(z) \bar{u}_{k+2} \end{aligned} \quad (6-27)$$

$S_{12}^{(k+1)}(z)$ is the reflection response $R^{(k+1)}(z)$ of the fluid layer, and $S_{22}^{(k+1)}(z)$ is the transmission response. In this case, layer $k+1$ is a homogeneous fluid so that $f(z) = 1$ and $g(z) = 0$. From (6-25) and (6-26), we therefore obtain the reflection response

$$\begin{aligned} S_{12}^{(k+1)}(z) &= R_{k+1} + \frac{r_k z^{2p} \bar{t}'_{k+1} \bar{t}'_{k+1}{}^*}{(1 - r_k r'_{k+1} z^{2p})} \\ &= R_{k+1} + r_k z^{2p} \left[1 + r_k r'_{k+1} z^{2p} + (r_k r'_{k+1} z^{2p})^2 + \dots \right] \bar{t}'_{k+1} \bar{t}'_{k+1}{}^* \end{aligned}$$

The first term, R_{k+1} , is the reflection coefficient matrix for the bottom of the fluid layer. The infinite series in powers of z^{2p} is a sequence of multiply reflected waves inside the fluid layer. An upgoing wave \bar{u}_{k+2} is transmitted across interface $k+1$ by the multiplication

$$\bar{\tau}_{k+1}^{\prime *} \cdot \bar{u}_{k+2} = [t_{pp} \quad t_{sp}]_{k+1} \cdot \bar{u}_{k+2}$$

Each of the multiple reflections generated inside the fluid layer is then transmitted back across interface $k+1$. This is done by multiplying each wave by

$$\bar{\tau}_{k+1}^{\prime} = \begin{bmatrix} t_{pp}^{\prime} \\ t_{ps}^{\prime} \end{bmatrix}_{k+1}$$

The transmission response for the fluid layer is given by (6-26).

Thus,

$$\begin{aligned} S_{22}^{(k+1)}(z) &= \frac{z^p \bar{\tau}_k \bar{\tau}_{k+1}^{\prime *}}{(1 - r_k r_{k+1}^{\prime} z^{2p})} \\ &= z^p \left[1 + r_k r_{k+1}^{\prime} z^{2p} + (r_k r_{k+1}^{\prime} z^{2p})^2 + \dots \right] \bar{\tau}_k \bar{\tau}_{k+1}^{\prime *} \end{aligned}$$

In this case, the multiple reflections inside the fluid layer are transmitted to the upper halfspace. This is indicated by the factor

$$\bar{\tau}_k = \begin{bmatrix} t_{pp} \\ t_{ps} \end{bmatrix}_k$$

in $S_{22}^{(k+1)}(z)$.

6.4 Reflection and Transmission Responses for a Medium of Solid and Fluid Layers.

Using the results of the previous section, we can calculate the reflection and transmission responses of the stack of alternating fluid and solid layers described in Section 6.2. These layers are numbered 1 to n as shown in Figure 6.2. We shall assume that the stack of layers is bounded by two halfspaces. Above interface 0 is a homogeneous halfspace (layer 0) which is solid, fluid, or vacuum. Below interface n is a homogeneous halfspace (layer $n+1$) which is either fluid or solid. A known upgoing source \bar{S}_{n+1} is incident to the stack of layers from below.

As shown in Figure 6.2, there are several cases to consider in calculating the reflection and transmission responses of the layers. For example, layers 1 and n may each be fluid or solid. If the lower halfspace is fluid, then the upgoing source \bar{S}_{n+1} contains only a compressional component UP_{n+1} . Finally, the upper halfspace may be solid, fluid or vacuum. All combinations of these cases will be discussed below.

Let us first calculate the reflection response $R_{(z)}^{(n)}$ for all those cases when the lower halfspace is solid. If layer 1 is solid, we have

$$R_{(z)}^{(0)} = R_0$$

where R_0 is the reflection coefficient matrix for the first interface. R_0 is well defined if the upper halfspace is solid, fluid or vacuum. Then, applying the iteration given by (6-13), we can obtain the reflection response for all layers above the deepest fluid over solid interface. If layer n is fluid, then the iteration yields $R^{(n)}(z)$ which is the reflection response for the complete stack of layers.

If layer 1 is fluid, then we can set $\bar{d}'_1 = 0$ in (6-5) and obtain

$$\bar{d}'_2 = S_{12}^{(1)}(z) \bar{u}_2 \tag{6-28}$$

Thus $R^{(1)}(z) = S_{12}^{(1)}(z)$, and we can iterate from interface 1 down through the layers to obtain $R^{(n)}(z)$ if layer n is fluid.

If layer n is solid, then the iterations above yield $R^{(n-1)}(z)$ where interface $(n-1)$ is the deepest fluid over solid interface. To obtain $R^{(n)}(z)$ from $R^{(n-1)}(z)$ is a straight forward calculation using the method of Section 3.4 since only solid homogeneous layers within layer n and the solid lower halfspace are involved.

We now consider those cases in which the lower halfspace is fluid. The reflection response from below for the complete set of layers is a scalar $r^{(n)}(z)$ which equals the ratio of the downgoing reflected compressional wave to the upgoing incident compressional source.

Again, we consider two cases for layers n . If layer n is solid, then we can calculate $R^{(n-1)}(z)$ exactly as before. Using $R^{(n-1)}(z)$, we

can compute $V^{(n)}(z)$ from (6-8) such that

$$d_n^i = V^{(n)}(z) \bar{u}_n^i \quad (6-29)$$

At the n-th interface, the solid and fluid waves are related by equations (6-17), i.e.,

$$\bar{\tau}_n^* \cdot d_n^i = DP_{n+1} - r_n UP_{n+1} \quad (6-30)$$

$$-R_n^i d_n^i + \bar{u}_n^i = \bar{\tau}_n UP_{n+1} \quad (6-31)$$

Substituting (6-29) into (6-31) and solving for \bar{u}_n^i gives

$$\bar{u}_n^i = (I_2 - R_n^i V^{(n)}(z))^{-1} \bar{\tau}_n UP_{n+1} \quad (6-32)$$

In these equations, UP_{n+1} is the upgoing compressional source in the lower fluid halfspace. Putting (6-32) and (6-29) into (6-30) and solving for the reflected wave DP_{n+1} we obtain

$$DP_{n+1} = \left[r_n + \bar{\tau}_n^* V^{(n)}(z) (I_2 - R_n^i V^{(n)}(z))^{-1} \bar{\tau}_n \right] UP_{n+1} \quad (6-33)$$

Therefore, the reflection response of the complete stack of layers is the scalar coefficient of UP_{n+1} , i.e.,

$$r^{(n)}(z) = r_n + \bar{\tau}_n^* V^{(n)}(z) (\bar{I}_2 - R_n^1 V^{(n)}(z))^{-1} \bar{\tau}_n$$

(6-34)

If layer n is fluid rather than solid, then we select layer $n-1$, which is solid, and repeat the algebra of equations (6-29) to (6-34). In this way, we obtain $r^{(n-1)}(z)$, the reflection response for all layers above interface $n-1$. From $r^{(n-1)}(z)$, one can easily calculate $r^{(n)}(z)$ since layer n consists of homogeneous fluid layers. The form of a product of layer matrices for fluid layers is the same as the matrix in (3-8). This equation can be used to calculate $r^{(n)}(z)$ from $r^{(n-1)}(z)$. The details are omitted here.

From the above discussion, we have shown how to calculate the reflection response $R^{(n)}(z)$ for all cases where the lower halfspace is solid, and the response $r^{(n)}(z)$ if the lower halfspace is fluid. The reflected downgoing waves in each case are

$$d_{n+1} = R^{(n)}(z) \bar{s}_{n+1}$$

and

$$DP_{n+1} = r^{(n)}(z) UP_{n+1}$$

Let us now compute the transmitted body waves generated in the layers by the upgoing source in the lower halfspace. To do this, we derive an iteration which calculates \bar{u}_k from \bar{u}_{k+2} where

layer $k+1$ is an inhomogeneous fluid layer between two solid layers as shown in Figure 6.1. Combining (6-7) and the second equation of (6-5) gives

$$\bar{u}'_k = (\bar{I}_2 - S_{21}^{(k+1)} V^{(k)})^{-1} S_{22}^{(k+1)} \bar{u}_{k+2}$$

$$\bar{d}'_k = V^{(k)} (\bar{I}_2 - S_{21}^{(k+1)} V^{(k)})^{-1} S_{22}^{(k+1)} \bar{u}_{k+2}$$

(6-35)

Finally, we insert these primed waves into (6-3) to obtain the desired iteration for transmitted waves:

$$\bar{u}_k = z^{s_k} \left[G^{(k)} V^{(k)} + F^{(k)} \right] \left[\bar{I}_2 - S_{21}^{(k+1)} V^{(k)} \right]^{-1} S_{22}^{(k+1)} \bar{u}_{k+2}$$

(6-36)

If the lower halfspace is solid and layer n is fluid, we can start this iteration by setting

$$\bar{u}_{n+1} = \bar{s}_{n+1}$$

On the other hand, if the lower halfspace is a fluid and layer n is solid, equation (6-32) can be used to calculate \bar{u}'_n from the compressional course UP_{n-1} . Then from \bar{u}'_n and

$$\bar{d}'_n = V^{(n)} \bar{u}'_n, \quad \text{equations (6-3) yield the imprimed}$$

wave \bar{u}_n at the top of the n -th layer. At this point, the iteration

of equation (6-36) can be used to obtain the transmitted waves in each shallower solid layer.

At the top of the set of layers, layer 1 may be solid or fluid. If layer 1 is solid, the previous iterations finally give \bar{u}_1 , the up-going wave just below the first interface. The wave transmitted into the upper halfspace is

$$\bar{u}'_0 = T_0 \bar{u}_1$$

where T_0 is the transmission coefficient matrix for interface 0. If the upper halfspace is a fluid, the transmitted compressional wave is

$$UP'_0 = [t_{pp} \ t_{sp}] \bar{u}_1$$

T_0 is the null matrix if the upper halfspace is a vacuum. Thus $u'_0 = 0$ if interface 0 is free.

The remaining case to consider is when layer 1 is fluid. The procedure then is to compute \bar{u}_2 from the iteration technique since layer 2 must be solid. From the second equation of (6-5), we obtain the wave

$$\bar{u}'_0 = S_{22}^{(1)} \bar{u}_2$$

directly since no downgoing sources exist in the upper halfspace. The matrix $S_{22}^{(1)}$ is given by (6-26) as

$$\frac{P_1 \bar{\tau}_0 \bar{\tau}_1^*}{\Delta(z)}$$

The vector factor

$$\bar{\tau}_0 = \begin{bmatrix} t_{pp} \\ t_{ps} \end{bmatrix}_0$$

has 0 elements if interface 0 is free and if the upper halfspace is a fluid then $t_{ps} = 0$.

6.5 Figure Captions

6.1 Typical sequence of alternating solid and fluid inhomogeneous layers. Layers k and $k+2$ are each a stack of homogeneous solid layers, and layer $k+1$ is a stack of homogeneous fluid layers.

6.2 Stack of alternating solid and fluid inhomogeneous layers between two homogeneous halfspaces. Source \bar{s}_{n+1} is located in lower halfspace which may be solid or fluid. Upper half space may be solid, fluid or vacuum.

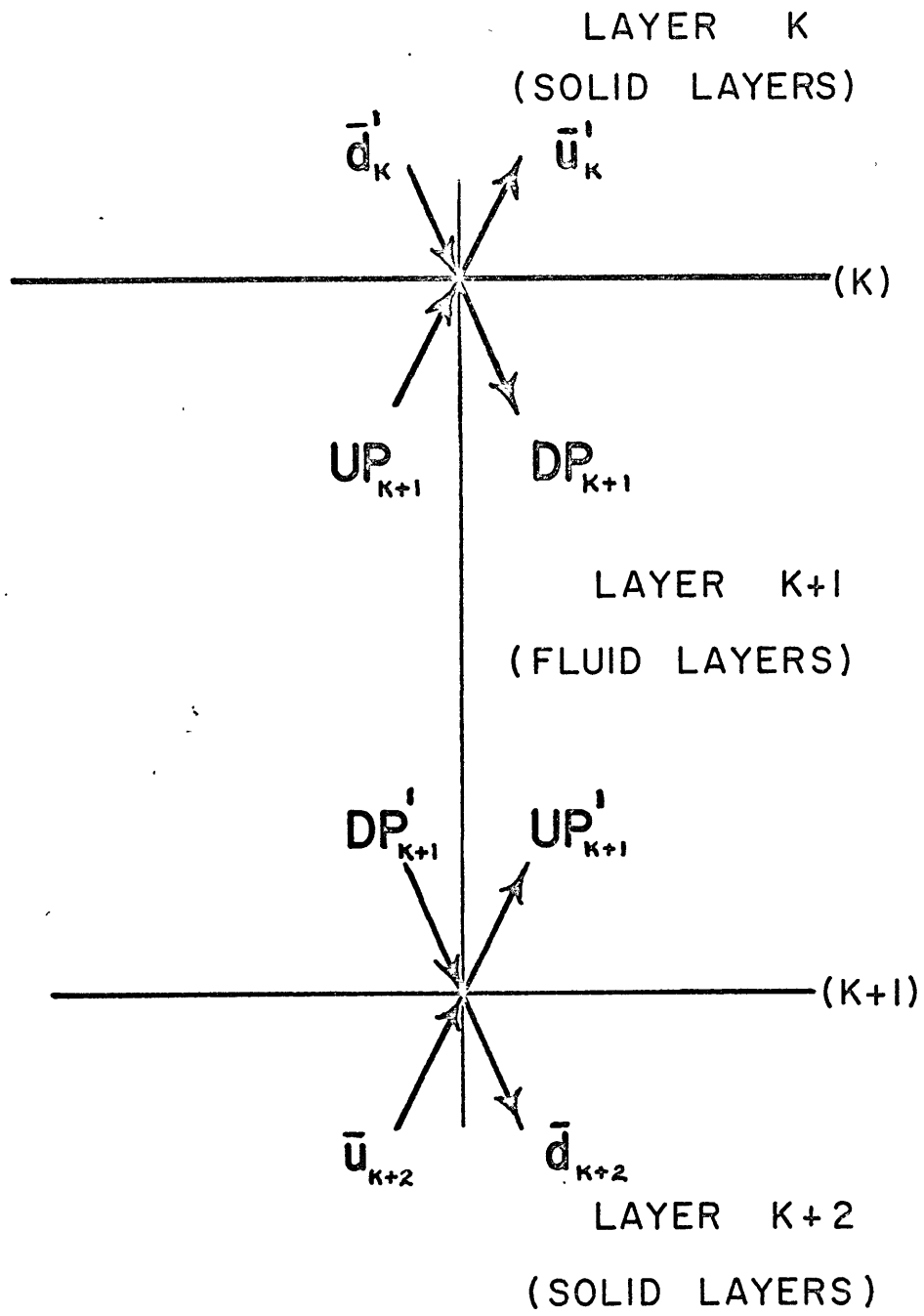


FIGURE 6.1

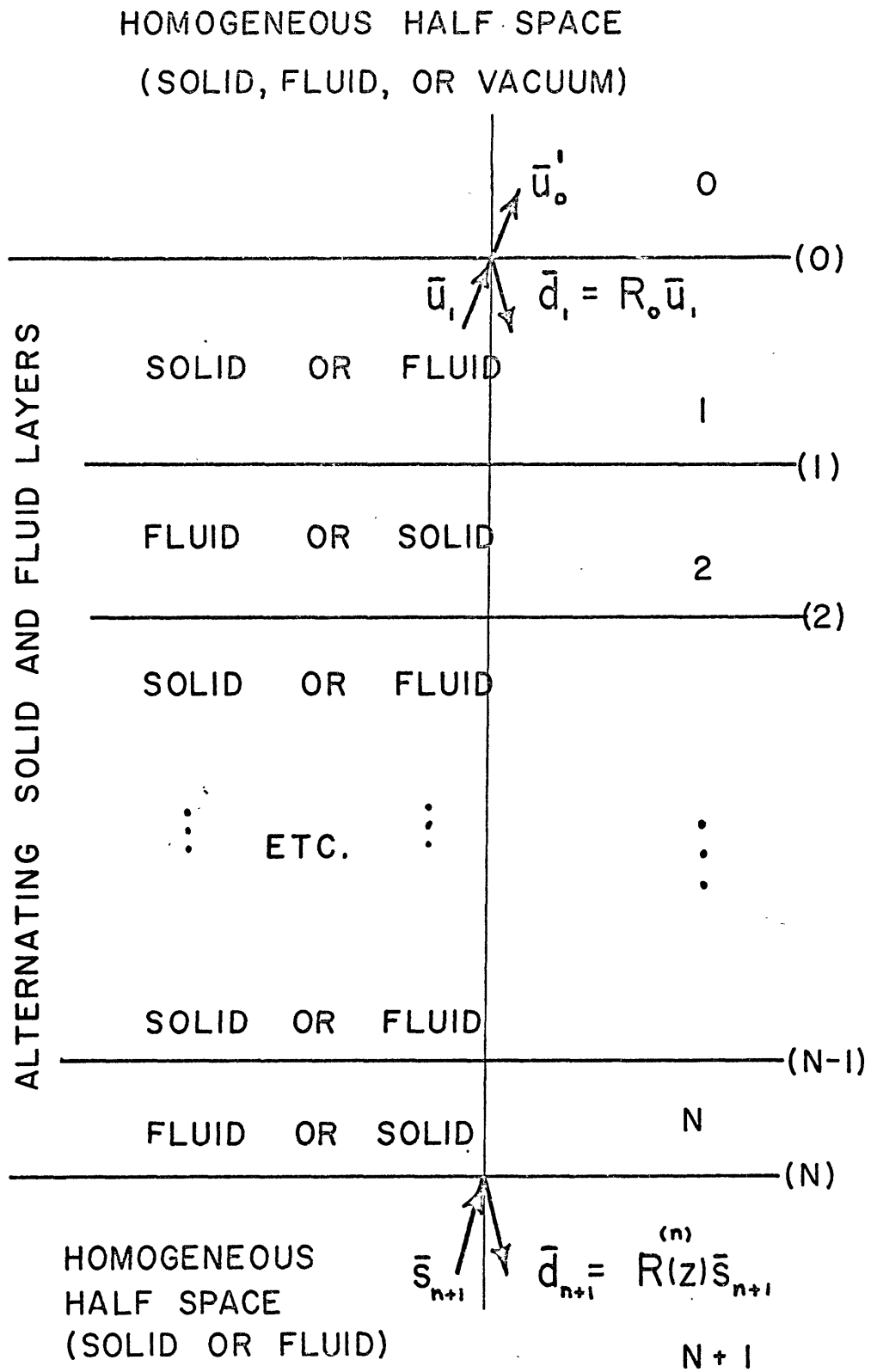


FIGURE 6.2

Chapter VII

Conclusions and Future Work

The theory of the discrete time calculation of homogeneous plane P and SV waves in a plane layered medium has been developed for elastic layers and for interbedded solid and fluid layers. This method has several advantages over the Haskell-Thomson technique for the calculation of body wave responses of layered media. High resolution time domain responses of any window length can be calculated with no spurious precursor introduced by band limiting the spectral response. A layer matrix iteration through the complete set of layers for a given model need be computed only once in the discrete time method. Matrix polynomials containing all the spectral information of the layers are obtained. These polynomials can be rapidly Fourier analyzed to yield the same spectral responses as obtained by Haskell's technique with very little error introduced by the discrete time approximation. On the other hand, Haskell's method requires a new iteration through all the layers for each spectral value which can be time consuming.

Given a crustal structure, the effect of reverberations on teleseismic events recorded on the free surface can be removed by a direct convolution in time, whereas in Haskell's method, spectra must be divided to eliminate the layer effects.

The inversion problem of recovering the layer impedances from

the reflection response of a layered halfspace due to a surface source was previously solved for normal incidence by Kunetz. The extension to non-normal incidence was attempted with some success in that the polynomial matrix $M(z)$ for the layers can be calculated from transmitted waves recorded at the surface. The extraction of the layer impedances from $M(z)$ seems to be difficult at non-normal incidence.

In order to utilize the high resolution of this method, wide band, three component recording of seismic data should be undertaken. This would greatly facilitate comparing theoretical model studies with actual data being recorded in order to determine the fine structure of transition zones of the Earth.

References

- Aki, K., Study of earthquake mechanism by a method of phase equalization applied to Rayleigh and Love waves, J. Geophys. Res., 65, 729-740, 1960.
- Alexander, S.S. and Phinney, R.A., A study of core-mantle boundary using P-waves diffracted by the earth's core, J. Geophys. Res., 71, 5943-5958, 1966.
- Backus, M., J. Burg, D. Baldwin, and E. Bryan, Wide band extraction of mantle P waves from ambient noise, Geophysics, 24, 672-692, 1964.
- Buchbinder, G.G.R., Properties of the core-mantle boundary and observations of PcP, J. Geophys. Res., 75, 5901-5923, 1968.
- Claerbout, J.F., Synthesis of a layered medium from its acoustic transmission response, Geophysics, 33, 264-269, 1968.
- Dorman, J., Period equation for waves of Rayleigh type on a layered, liquid-solid halfspace, Bull. Seism. Soc. Am., 52, 389-397, 1962.
- Dorman, J., Ewing, J., and Alsop, L.E., Oscillations of the earth: a new core-mantle boundary model based on low order free vibrations, Proc. Nat. Acad. Sci., 54, 364-368, 1965.
- Fernandez, L., The determination of crustal thickness from the spectrum of P waves, Scientific Report No. 13, St. Louis Univ., Contract AF19(604) -7399.
- Glover, P., and Alexander, S.S., Lateral variations in crustal structure beneath the Montana LASA, J. Geophys. Res., 74, 505-531, 1969.
- Goupillaud, P.L., An approach to inverse filtering of near-surface layer effects from seismic records, Geophysics, 26, 754-760, 1961.
- Hannon, W.J., An application of the Haskell-Thomson matrix method to the synthesis of the surface motion due to dilatational waves, Bull. Seism. Soc. Am., 54, 2007-2083, 1964.
- Harkrider, D.G., Theoretical and observed acoustic gravity waves from explosive sources in the atmosphere, J. Geophys. Res., 69, 5295-5321, 1964.
- Haskell, N.A., The dispersion of surface waves on multilayered media, Bull. Seism. Soc. Am., 43, 17-34, 1953.
- Haskell, N.A., Crustal reflection of plane SH waves, J. Geophys. Res., 65, 4147-4150, 1960.
- Haskell, N.A., Crustal reflection of plane P and SV waves, J. Geophys. Res., 67, 4751-4767, 1962.
- Kanamori, H., Spectrum of P and PcP in relation to the mantle-core boundary and attenuation in the mantle, J. Geophys. Res., 72, 559-571, 1967.

- Knott, C.G., Reflexion and refraction of elastic waves with seismological applications, Phil. Mag., 5th ser., 48, 64-97, 1899.
- Kunetz, G. and D'Erceville, Sur certaines proprietes d'une onde acoustique plane de compression dans un milieu stratifie, Annales de Geophys., 18, 351-359, 1962.
- Landisman, M., Sato, Y., and Nafe, J., Free vibration of the earth and the properties of its deep interior regions, Part 1: density, Geophys. J., 9, 469, 1965.
- Leblanc, Gabriel, Truncated crustal transfer functions and fine crustal structure determination, Bull. Seism. Am., 57, 719-733, 1967.
- Macelwane, J.B., Reflection and refraction of seismic waves, Introduction to Theoretical Seismology, 147-179, 1936.
- Morse, P.M., and Feshbach, H., Methods of Theoretical Physics Part I, McGraw-Hill Book Co., 1953.
- Phinney, R.A., Structure of the Earth's crust from spectral behavior of long-period body waves, J. Geophys. Res., 69, 2997-3017, 1964.
- Schneider, W.A., K.L. Larner, J.P. Burg, and M.M. Backus, A new data processing technique for the elimination of ghost arrivals on reflection seismograms, Geophysics, 29, 783-805, 1964.
- Sherwood, J.W.C., and Trorey, A.W., Minimum-phase and related properties of a horizontally stratified absorptive earth to plane acoustic waves, Geophysics, 20, 191-197, 1965.
- Teng, T.L., Reflection and transmission from a plane layered core mantle boundary, Bull. Seism. Soc. Am., 57, 477-499, 1967.
- Thomson, W.T., Transmission of elastic waves through a stratified, solid medium, J. App. Phys., 21, 89-93, 1950.
- Treitel, S., and Robinson, E.A., Seismic wave propagation in layered media in terms of communication theory, Geophysics, 31, 17-32, 1966.
- Wiggins, R., and Robinson, E.A., Recursive solution to the multi-channel filtering problem, J. Geophys. Res., 70, 1885-1891, 1965.
- Wuenshel, P.C., Seismogram synthesis including multiples and transmission coefficients, Geophysics, 25, 106-129, 1960.

Appendix ACalculation of Reflection
and Transmission CoefficientsA.1 Solid over Solid Interface

Reflection and transmission coefficients for plane waves incident to an interface between elastic media were first calculated by Knott (1899). His coefficients gave ratios of reflected and transmitted potentials to incident potentials. Zoeppritz (1917) computed coefficients which were ratios of particle displacements. From these fundamental equations, many authors have computed the effect of various layers in the Earth on seismic waves. Two excellent and readable reviews of significant papers with corrections of errors are given by Macelwane (1936) and Richter (1958).

In this Appendix, we calculate the reflection and transmission matrices, R and T , defined by equations (2-12) in the text. The elements of these matrices are reflection and transmission coefficients which are ratios of waves such as defined in (2-7) and (2-8). Let us consider incident waves from above interface 1 as shown in Figure A-1. We use subscripts i , r , and t to denote incident, reflected and transmitted potentials ϕ and F in each layer. Using (2-4) (2-7) and (2-8) we define the following waves at interface 1:

$$\begin{aligned}
 DP_1' &= -\sqrt{\rho_1 \alpha_1 \cos \delta_1} \alpha_1 f_i'' \\
 DS_1' &= -\sqrt{\rho_1 \beta_1 \cos \delta_1} \beta_1 F_i'' \\
 UP_1' &= -\sqrt{\rho_1 \alpha_1 \cos \delta_1} \alpha_1 f_r'' \\
 US_1' &= +\sqrt{\rho_1 \beta_1 \cos \delta_1} \beta_1 F_r'' \\
 DP_2 &= -\sqrt{\rho_2 \alpha_2 \cos \delta_2} \alpha_2 f_t'' \\
 DS_2 &= -\sqrt{\rho_2 \beta_2 \cos \delta_2} \beta_2 F_t''
 \end{aligned}$$

(A-1)

These waves are vector quantities measured in the directions shown by arrows in Figure A-1. To obtain the desired reflection and transmission coefficients, we divide the reflected and transmitted waves defined above by one incident wave, the other incident wave being 0. Doing this for each incident wave at the same phase velocity c , we obtain the reflection and transmission matrices

$$\begin{aligned}
 R' &= \begin{bmatrix} r_{pp} & r_{sp} \\ r_{ps} & r_{ss} \end{bmatrix} = \begin{bmatrix} \frac{f_r''}{f_i''} & \sqrt{\frac{\rho_{\alpha 1}}{\rho_{\beta 1}}} \frac{\alpha_1^2 f_r''}{\beta_1^2 F_i''} \\ -\sqrt{\frac{\rho_{\beta 1}}{\rho_{\alpha 1}}} \frac{\beta_1^2 F_r''}{\alpha_1^2 f_i''} & -\frac{F_r''}{F_i''} \end{bmatrix} \\
 T' &= \begin{bmatrix} t_{pp} & t_{sp} \\ t_{ps} & t_{ss} \end{bmatrix} = \begin{bmatrix} \sqrt{\frac{\rho_2 \rho_{\alpha 2}}{\rho_1 \rho_{\alpha 1}}} \frac{\alpha_2^2 f_t''}{\alpha_1^2 f_i''} & \sqrt{\frac{\rho_2 \rho_{\alpha 2}}{\rho_1 \rho_{\beta 1}}} \frac{\alpha_2^2 f_t''}{\beta_1^2 F_i''} \\ \sqrt{\frac{\rho_2 \rho_{\beta 2}}{\rho_1 \rho_{\alpha 1}}} \frac{\beta_2^2 F_t''}{\alpha_1^2 f_i''} & \sqrt{\frac{\rho_2 \rho_{\beta 2}}{\rho_1 \rho_{\beta 1}}} \frac{\beta_2^2 F_t''}{\beta_1^2 F_i''} \end{bmatrix}
 \end{aligned}$$

(A-2)

where

$$P_{\alpha n} = \sqrt{\left(\frac{c}{\alpha_n}\right)^2 - 1}$$

$$P_{\beta n} = \sqrt{\left(\frac{c}{\beta_n}\right)^2 - 1}$$

(A-3)

In this section of the Appendix, we state the usual 4 x 4 matrix equations in the potentials by matching particle velocities and stresses across the interface. These equations are scaled and partitioned so that R' and T' can be computed by inverting only 2 x 2 matrices. From this solution, three useful theorems are proved, i.e.

$$(i) \quad T^* = T' \quad (A-4a)$$

$$(ii) \quad R'^* = R', \quad R^* = R \quad (A-4b)$$

$$(iii) \quad R' = -TRT^{-1} \quad (A-4c)$$

We recall that primed matrices are calculated for incident waves from above an interface, whereas unprimed matrices are for incident waves from below. The asterisk (*) indicates the transpose of a matrix.

Theorems (i) and (ii) are statements of the principle of reciprocity between a plane wave source and a receiver, both near a flat interface between two half spaces. These two theorems are also true for an interface between any combination of solid and fluid half spaces as shown in later sections of this Appendix. Theorem (iii) in conjunction with (i),

and (ii) show that the primed matrices, R' and T' , can be computed from R and T .

It should be emphasized that theorems (i) to (iii) are essential for obtaining the simple form of the layer matrix in Chapter 2. Other choices for up and down going waves than those of (A-1) do not seem to give as simple a layer matrix.

In medium 1 the incident and reflected compressional potentials are

$$\begin{aligned} f_i &= f_i(x \sin \delta_1 + z \cos \delta_1 - \alpha_1 t) \\ f_r &= f_r(x \sin \delta_1 - z \cos \delta_1 - \alpha_1 t) \end{aligned} \quad (\text{A-5})$$

whereas the incident and reflected shear potentials are

$$\begin{aligned} F_i &= F_i(x \sin \gamma_1 + z \cos \gamma_1 - \beta_1 t) \\ F_r &= F_r(x \sin \gamma_1 - z \cos \gamma_1 - \beta_1 t) \end{aligned} \quad (\text{A-6})$$

The transmitted compressional and shear potentials are

$$\begin{aligned} f_t &= f_t(x \sin \delta_2 + z \cos \delta_2 - \alpha_2 t) \\ F_t &= F_t(x \sin \gamma_2 + z \cos \gamma_2 - \beta_2 t) \end{aligned} \quad (\text{A-7})$$

The particle velocity components are given by

$$\begin{aligned}\dot{u} &= \frac{\partial}{\partial t} \left(\frac{\partial f}{\partial x} + \frac{\partial F}{\partial z} \right) \\ \dot{w} &= \frac{\partial}{\partial t} \left(\frac{\partial f}{\partial z} - \frac{\partial F}{\partial x} \right)\end{aligned}\tag{A-8}$$

and the stress components are

$$\begin{aligned}\tau_{zz} &= \lambda \nabla^2 f + 2\mu \frac{\partial w}{\partial z} \\ \tau_{zx} &= \mu \left(\frac{\partial u}{\partial z} + \frac{\partial w}{\partial x} \right)\end{aligned}\tag{A-9}$$

To evaluate these velocities and stresses in each medium, we set

$$\begin{aligned}f_1 &= f_i + f_r \\ F_1 &= F_i + F_r\end{aligned}$$

in medium 1, and in medium 2 we let

$$\begin{aligned}f_2 &= f_t \\ F_2 &= F_t\end{aligned}$$

The necessary boundary conditions at the interface are continuity of particle velocity and stress components. The resulting equations are essentially those of Knott (1899) and have been rederived by many

authors. Keeping both incident waves in the formulation, we obtain the following equations:

$$\begin{array}{l} \frac{\dot{u}}{c} : \\ \tau_{zz} : \\ \frac{\dot{w}}{c} : \\ \tau_{zx} : \end{array} \begin{bmatrix} 1 & -P_{\beta 1} & -1 & P_{\beta 2} \\ P_1 \gamma_1 & 2P_1 \left(\frac{\beta_1}{c}\right)^2 P_{\beta 1} & -P_2 \gamma_2 & 2P_2 \left(\frac{\beta_2}{c}\right)^2 P_{\beta 2} \\ -P_{\alpha 1} & 1 & P_{\alpha 2} & -1 \\ -2P_1 \left(\frac{\beta_1}{c}\right)^2 P_{\alpha 1} & P_1 \gamma_1 & -2P_2 \left(\frac{\beta_2}{c}\right)^2 P_{\alpha 2} & -P_2 \gamma_2 \end{bmatrix} \begin{bmatrix} \alpha_1^2 f_r'' \\ \beta_1^2 F_r'' \\ \alpha_2^2 f_t'' \\ \beta_2^2 F_t'' \end{bmatrix}$$

$$= \begin{bmatrix} -1 & -P_{\beta 1} \\ -P_1 \gamma_1 & 2P_1 \left(\frac{\beta_1}{c}\right)^2 P_{\beta 1} \\ P_{\alpha 1} & -1 \\ -2P_1 \left(\frac{\beta_1}{c}\right)^2 P_{\alpha 1} & -P_1 \gamma_1 \end{bmatrix} \begin{bmatrix} \alpha_1^2 f_i'' \\ \beta_1^2 F_i'' \end{bmatrix}$$

(A-10)

where

$$\gamma_i = 1 - 2 \left(\frac{\beta_i}{c}\right)^2 \quad (\text{A-10a})$$

We now consider each incident wave separately. Setting $F_i'' = 0$ in (A-10) and dividing by $\alpha_i^2 f_i''$ gives us a matrix equation in the coefficients of the first column of R' and T' in (A-2). Similarly setting $f_i'' = 0$ and dividing by $\beta_i^2 F_i''$ yields equations for the second column of coefficients in R' and T'. Combining these matrix equations gives

$$\left[\begin{array}{cc|cc} -1 & -P_{\beta 1} & -1 & P_{\beta 2} \\ -P_1 \gamma_1 & 2\rho_1 \left(\frac{\beta_1}{c}\right)^2 P_{\beta 1} & -P_2 \gamma_2 & 2\rho_2 \left(\frac{\beta_2}{c}\right)^2 P_{\beta 2} \\ \hline -P_{\alpha 1} & 1 & P_{\alpha 2} & -1 \\ +2\rho_1 \left(\frac{\beta_1}{c}\right)^2 P_{\alpha 1} & P_1 \gamma_1 & -2\rho_2 \left(\frac{\beta_2}{c}\right)^2 P_{\alpha 2} & -P_2 \gamma_2 \end{array} \right] \left[\begin{array}{cc} -r_{pp}' & -r_{sp}' \sqrt{\frac{P_{\beta 1}}{P_{\alpha 1}}} \\ -r_{ps}' \sqrt{\frac{P_{\alpha 1}}{P_{\beta 1}}} & -r_{ss}' \\ \hline t_{pp}' \sqrt{\frac{P_1 P_{\alpha 1}}{P_2 P_{\alpha 2}}} & t_{sp}' \sqrt{\frac{P_1 P_{\beta 1}}{P_2 P_{\alpha 2}}} \\ t_{ps}' \sqrt{\frac{P_1 P_{\alpha 1}}{P_2 P_{\beta 2}}} & t_{ss}' \sqrt{\frac{P_1 P_{\beta 1}}{P_2 P_{\beta 2}}} \end{array} \right]$$

$$= \left[\begin{array}{cc|cc} -1 & -P_{\beta 1} & & \\ -P_1 \gamma_1 & 2\rho_1 \left(\frac{\beta_1}{c}\right)^2 P_{\beta 1} & & \\ \hline P_{\alpha 1} & -1 & & \\ -2\rho_1 \left(\frac{\beta_1}{c}\right)^2 P_{\alpha 1} & -P_1 \gamma_1 & & \end{array} \right]$$

This equation can be solved by partitioning it into 2 x 2 matrices.

We define the following matrices:

$$A_i = \begin{bmatrix} -P_{\alpha i} & 1 \\ 2P_i \left(\frac{\beta_i}{\epsilon}\right)^2 P_{\alpha i} & P_i \gamma_i \end{bmatrix}$$

$$B_i = \begin{bmatrix} -1 & -P_{\beta i} \\ -P_i \gamma_i & 2P_i \left(\frac{\beta_i}{\epsilon}\right)^2 P_{\beta i} \end{bmatrix}$$

$$R = \begin{bmatrix} r'_{pp} & r'_{sp} \sqrt{\frac{P_{\beta 1}}{P_{\alpha 1}}} \\ r'_{ps} \sqrt{\frac{P_{\alpha 1}}{P_{\beta 1}}} & r'_{ss} \end{bmatrix}$$

$$\tau = \begin{bmatrix} t'_{pp} \sqrt{\frac{P_1 P_{\alpha 1}}{P_2 P_{\alpha 2}}} & t'_{sp} \sqrt{\frac{P_1 P_{\beta 1}}{P_2 P_{\beta 2}}} \\ t'_{ps} \sqrt{\frac{P_1 P_{\alpha 1}}{P_2 P_{\beta 2}}} & t'_{ss} \sqrt{\frac{P_1 P_{\beta 1}}{P_2 P_{\beta 2}}} \end{bmatrix}$$

$$L_i = \begin{bmatrix} \sqrt{P_i P_{\alpha i}} & 0 \\ 0 & \sqrt{P_i P_{\beta i}} \end{bmatrix}$$

We wish to solve for R' and T' defined by (A-2). From the above equations, we can show that \mathcal{R} and \mathcal{T} conveniently factor as

$$\mathcal{R} = L_1^{-1} R' L_1$$

$$\mathcal{T} = L_2^{-1} T' L_1$$

(A-13)

Therefore, (A-11) can be written in the partitioned form

$$\begin{bmatrix} B_1 & B_2 \\ A_1 & -A_2 \end{bmatrix} \begin{bmatrix} -L_1^{-1} R' L_1 \\ L_2^{-1} T' L_1 \end{bmatrix} = \begin{bmatrix} B_1 \\ -A_1 \end{bmatrix}$$

(A-14)

Solving for R' and T' we get equations

$$R' - L_1^{-1} B_1 B_2^{-1} L_2^{-1} T' = -I$$

$$R' + L_1^{-1} A_1^{-1} A_2 L_2^{-1} T' = I$$

(A-15)

Hence

$$\begin{aligned} T' &= 2 L_2 (B_1^{-1} B_2 + A_1^{-1} A_2)^{-1} L_1^{-1} \\ R' &= \frac{1}{2} L_1 (B_1^{-1} B_2 - A_1^{-1} A_2)^{-1} L_2^{-1} T' \end{aligned} \quad (\text{A-16})$$

To obtain the unprimed reflection and transmission coefficients, which are for incident waves from below the interface, we interchange indices 1 and 2 in (A-16). This gives

$$\begin{aligned} T &= 2 L_1 (B_2^{-1} B_1 + A_2^{-1} A_1)^{-1} L_2^{-1} \\ R &= \frac{1}{2} L_2 (B_2^{-1} B_1 - A_2^{-1} A_1)^{-1} L_1^{-1} T \end{aligned} \quad (\text{A-17})$$

Using these solutions, we now prove the three theorems given by (A-4). From (A-16) and (A-17), we obtain

$$\begin{aligned} T'^{-1} &= 2 L_1 (B_1^{-1} B_2 + A_1^{-1} A_2)^{-1} L_2^{-1} \\ T'^{* -1} &= 2 L_1^{-1} (B_2^{-1} B_1 + A_2^{-1} A_1)^{*} L_2 \end{aligned} \quad (\text{A-18})$$

To prove (A-4a), we show that the right hand sides of (A-18) are equal.

It is sufficient to show that

$$L_1^2 (B_1^{-1} B_2 + A_1^{-1} A_2) = \left[L_2^2 (B_2^{-1} B_1 + A_2^{-1} A_1) \right]^* \quad (A-19)$$

From (A-12) we obtain

$$\begin{aligned} L_1^2 B_1^{-1} B_2 &= - \begin{bmatrix} P_1 P_{\alpha 1} & 0 \\ 0 & P_1 P_{\beta 1} \end{bmatrix} \begin{bmatrix} P_1 P_{\beta 1} (1 - \gamma_1) & P_{\beta 1} \\ P_1 \gamma_1 & -1 \end{bmatrix} \begin{bmatrix} -1 & -P_{\beta 2} \\ -P_2 \gamma_2 & P_2 P_{\beta 2} (1 - \gamma_2) \end{bmatrix} \Big/ P_1 P_{\beta 1} \\ &= \begin{bmatrix} P_{\alpha 1} (P_2 \gamma_2 - P_1 [\gamma_1 - 1]) & P_{\alpha 1} P_{\beta 2} (P_2 [\gamma_2 - 1] - P_1 [\gamma_1 - 1]) \\ -(P_2 \gamma_2 - P_1 \gamma_1) & -P_{\beta 2} (P_2 [\gamma_2 - 1] - P_1 \gamma_1) \end{bmatrix} \end{aligned} \quad (A-20)$$

and

$$L_1^2 A_1^{-1} A_2 = \begin{bmatrix} P_{\alpha 2} (P_1 \gamma_1 - P_2 [\gamma_2 - 1]) & -(P_1 \gamma_1 - P_2 \gamma_2) \\ P_{\alpha 2} P_{\beta 1} (P_1 [\gamma_1 - 1] - P_2 [\gamma_2 - 1]) & -P_{\beta 1} (P_1 [\gamma_1 - 1] - P_2 \gamma_2) \end{bmatrix} \quad (A-21)$$

If we interchange indices 1 and 2 in (A-21) and transpose the result, we obtain (A-20). Thus we have shown that

$$L_1 B_1^{-1} B_2 = (L_2 A_2^{-1} A_1)^* \quad (\text{A-22})$$

and

$$L_2 A_1^{-1} A_2 = (L_1 B_1^{-1} B_2)^* \quad (\text{A-23})$$

This proves (A-19) and therefore the first theorem, which is

$$T^* = T^{-1} \quad (\text{A-24})$$

The second theorem, equation (A-4b), is easily proved from results used in the first theorem. From (A-16), we deduce that

$$\begin{aligned} R^{-1} &= L_1 (B_1^{-1} B_2 - A_1^{-1} A_2) (B_1^{-1} B_2 + A_1^{-1} A_2)^{-1} L_1^{-1} \\ &= I - 2L_1 (B_1^{-1} B_2 A_2^{-1} A_1 + I)^{-1} L_1^{-1} \\ &= I - 2(I + L_1 B_1^{-1} B_2 A_2^{-1} A_1 L_1^{-1})^{-1} \end{aligned} \quad (\text{A-25})$$

In order to show that $R'^* = R'$, we need only show that $M = M^*$, where

$$M = L_1 B_1^{-1} B_2 A_2^{-1} A_1 L_1^{-1} \quad (A-26)$$

From (A-22), we have

$$L_1 B_1^{-1} B_2 L_2^{-1} = \left[L_2 A_2^{-1} A_1 L_1^{-1} \right]^* \quad (A-27)$$

Therefore,

$$M = \left[L_2 A_2^{-1} A_1 L_1^{-1} \right]^* L_2 A_2^{-1} A_1 L_1^{-1} = M^* \quad (A-28)$$

This proves theorem (ii), i.e. $R'^* = R'$. If we interchange subscripts 1 and 2, the result is $R^* = R$.

Finally, we prove theorem (iii), equation (A-4c). Using (A-16) and (A-17), we can write

$$TR = \frac{1}{2} T \left[L_2 (B_2^{-1} B_1 - A_2^{-1} A_1) L_1^{-1} \right] T \quad (A-29)$$

$$-(T'R')^* = \frac{1}{2} T'^* \left[L_2^{-1} (A_1^{-1} A_2 - B_1^{-1} B_2) L_1 \right] T'^* \quad (A-30)$$

The bracketed terms in each equation are equal because of (A-22) and (A-23). Also $T'^* = T$ by theorem (i). Therefore,

$$TR = -(TR')^* \quad (A-31)$$

Using theorems (i) and (ii), this equation becomes

$$R' = -TRT^{-1} \quad (A-32)$$

which proves theorem (iii).

We now consider the solution of (A-11) as c goes to infinity. From (A-3) and (A-10), we have

$$P_{\alpha n}/c \rightarrow 1/\alpha_n \quad (A-33)$$

$$P_{\beta n}/c \rightarrow 1/\beta_n \quad (A-34)$$

$$\gamma_n \rightarrow 1 \quad (A-35)$$

as c goes to infinity. Dividing the first and third row of (A-11) by c and then letting c go to infinity results in the matrix equation

$$\left[\begin{array}{cc|cc} 0 & -1/\beta_1 & 0 & -1/\beta_2 \\ -\rho_1 & 0 & -\rho_2 & 0 \\ \hline -1/\alpha_1 & 0 & 1/\alpha_2 & 0 \\ 0 & \rho_1 & 0 & -\rho_2 \end{array} \right] \begin{bmatrix} -r'_{pp} & -r'_{sp}\sqrt{\frac{\alpha_1}{\beta_1}} \\ -r'_{ps}\sqrt{\frac{\beta_1}{\alpha_1}} & -r'_{ss} \\ t'_{pp}\sqrt{\frac{\rho_1\alpha_2}{\rho_2\alpha_1}} & t'_{sp}\sqrt{\frac{\rho_1\alpha_2}{\rho_2\beta_1}} \\ t'_{ps}\sqrt{\frac{\rho_1\beta_2}{\rho_2\alpha_1}} & t'_{ss}\sqrt{\frac{\rho_1\beta_2}{\rho_2\beta_1}} \end{bmatrix}$$

$$= \left[\begin{array}{cc|cc} 0 & -1/\beta_1 & & \\ -\rho_1 & 0 & & \\ \hline 1/\alpha_1 & 0 & & \\ 0 & -\rho_1 & & \end{array} \right]$$

(A-37)

This equation separates into two 2 x 2 matrix equations, which

are

$$\begin{bmatrix} \rho_1 & -\rho_2 \\ 1/\alpha_1 & 1/\alpha_2 \end{bmatrix} \begin{bmatrix} r'_{pp} & r'_{sp}\sqrt{\frac{\alpha_1}{\beta_1}} \\ t'_{pp}\sqrt{\frac{\rho_1\alpha_2}{\rho_2\alpha_1}} & t'_{sp}\sqrt{\frac{\rho_1\alpha_2}{\rho_2\beta_1}} \end{bmatrix} = \begin{bmatrix} -\rho_1 & 0 \\ 1/\alpha_1 & 0 \end{bmatrix}$$

(A-38a)

$$\begin{bmatrix} \rho_1 & -\rho_2 \\ 1/\beta_1 & 1/\beta_2 \end{bmatrix} \begin{bmatrix} -r'_{ss} & -r'_{ps}\sqrt{\frac{\beta_1}{\alpha_1}} \\ t'_{ss}\sqrt{\frac{\rho_1\beta_2}{\rho_2\beta_1}} & t'_{ps}\sqrt{\frac{\rho_1\beta_2}{\rho_2\alpha_1}} \end{bmatrix} = \begin{bmatrix} -\rho_1 & 0 \\ 1/\beta_1 & 0 \end{bmatrix}$$

(A-38b)

The second column on the right hand side of each of these two equations is zero. Thus, the equations are homogeneous in the unknown coefficients $r'_{sp}, t'_{sp}, r'_{ps}, t'_{ps}$. Since the left hand most matrix in each equation has a non-zero determinant, these mode conversion coefficients must vanish, as expected for normal incidence.

Solving for the remaining reflection and transmission coefficients gives

$$r'_{pp} = \frac{\rho_2\alpha_2 - \rho_1\alpha_1}{\rho_2\alpha_2 + \rho_1\alpha_1}$$

$$t'_{pp} = \frac{2\sqrt{\rho_1\alpha_1\rho_2\alpha_2}}{\rho_2\alpha_2 + \rho_1\alpha_1}$$

$$r'_{ss} = -\frac{\rho_2\beta_2 - \rho_1\beta_1}{\rho_2\beta_2 + \rho_1\beta_1}$$

$$t'_{ss} = \frac{2\sqrt{\rho_1\beta_1\rho_2\beta_2}}{\rho_2\beta_2 + \rho_1\beta_1}$$

(A-39)

The unprimed reflection and transmission coefficients are obtained from the above equations by interchanging subscripts 1 and 2. One can then verify the three theorems in (A-4) by inspection since each R and T matrix is diagonal.

A.2 Solid over Fluid Interface

Previous equations can be modified to treat the case where medium 1 or 2 is a fluid. The necessary changes are the following:

(i) Continuity of \dot{u} is not necessary at a solid-fluid interface so that the first rows of (A-10) and (A-11) should be eliminated.

(ii) The tangential stress τ_{zx} must vanish at the interface. This occurs if either μ_1 , or μ_2 vanishes in the second equation of (A-9). Hence, for any liquid-solid interface, τ_{zx} goes to zero automatically if β_1 , or β_2 go to zero.

(iii) In the fluid medium, no shear potentials exist, and each compressional potential f must be replaced by an equivalent term in a velocity potential ϕ . To see the relationship between f and ϕ we define the velocity potential to be the plane wave.

$$\phi = \phi(\hat{p} \cdot \bar{r} - \alpha t)$$

from which we obtain the particle velocity component \dot{w} and negative pressure τ_{zz} as

$$\dot{w} = - \frac{\partial \phi}{\partial z} = - \cos \delta \phi'$$

$$\tau_{zz} = -\rho \frac{\partial \phi}{\partial t} = \rho \alpha \phi'$$

(A-40)

For a solid medium, the corresponding terms due to a displacement

potential f are computed from (A-8) and (A-9) to be

$$\dot{\omega} = -\alpha \cos \delta f''$$

$$\tau_{zz} = \rho \alpha^2 (1 - 2\mu \sin^2 \delta) f''$$

(A-41)

As the rigidity μ goes to zero, this last pressure term goes to

$$\tau_{zz} = \rho \alpha^2 f''$$

From these equations, we see that replacing f'' by ϕ'/α , letting $\mu \rightarrow 0$, and dropping shear potential terms in \mathbf{F} converts either medium to a fluid.

The first case we consider is a solid over fluid interface. Applying changes (i), (ii) and (iii) described above to equations (A-10) and (A-11) we obtain the following matrix equation:

$$\begin{bmatrix} -\rho_1 \gamma_1 & 2\rho_1 \left(\frac{\beta_1}{c}\right)^2 P_{\beta 1} & -P_2 \\ -P_{\alpha 1} & 1 & P_{\alpha 2} \\ 2\rho_1 \left(\frac{\beta_1}{c}\right)^2 P_{\alpha 1} & \rho_1 \gamma_1 & 0 \end{bmatrix} \begin{bmatrix} -r_{pp}' & -r_{sp}' \sqrt{\frac{P_{\beta 1}}{P_{\alpha 1}}} \\ -r_{ps}' \sqrt{\frac{P_{\alpha 1}}{P_{\beta 1}}} & -r_{ss}' \\ t_{pp}' \sqrt{\frac{P_1 P_{\alpha 1}}{P_2 P_{\alpha 2}}} & t_{sp}' \sqrt{\frac{P_1 P_{\beta 1}}{P_2 P_{\alpha 2}}} \end{bmatrix} = \begin{bmatrix} -\rho_1 \gamma_1 & 2\rho_1 \left(\frac{\beta_1}{c}\right)^2 P_{\beta 1} \\ P_{\alpha 1} & -1 \\ -2\rho_1 \left(\frac{\beta_1}{c}\right)^2 P_{\alpha 1} & -\rho_1 \gamma_1 \end{bmatrix}$$

(A-42)

Since the lower medium is a fluid, we note that the transmission coefficients are obtained from (A-2) by replacing f_t'' by ϕ_t'/α_2 , i.e.

$$t'_{pp} = \sqrt{\frac{\rho_2 \rho_{\alpha 2}}{\rho_1 \rho_{\alpha 1}}} \cdot \frac{\alpha_2 \phi_t'}{\alpha_1^2 f_i''}, \quad t'_{sp} = \sqrt{\frac{\rho_2 \rho_{\alpha 2}}{\rho_1 \rho_{\beta 1}}} \cdot \frac{\alpha_2 \phi_t'}{\beta_1^2 F_i''}.$$

Let us define the following vectors:

$$\begin{aligned} \bar{b}_1^* &= -\rho_1 [\gamma_1, -2\left(\frac{\beta_1}{\alpha_1}\right)^2 \rho_{\beta 1}] = -\rho_1 [\gamma_1, (\gamma_1 - 1) \rho_{\beta 1}] \\ \bar{a}_2^* &= - [\rho_{\alpha 2}, 0] \\ \bar{\tau}^* &= [t'_{pp}, t'_{sp}] \end{aligned} \tag{A-43}$$

The asterisk (*) indicates the transpose of a vector.

Matrix equation (A-42) can be written in partitioned form as

$$\left[\begin{array}{c|c} \bar{b}_1^* & -\rho_2 \\ \hline A_1 & -\bar{a}_2 \end{array} \right] \left[\begin{array}{c} -L_1^* R L_1 \\ \hline \frac{1}{\sqrt{\rho_2 \rho_{\alpha 2}}} \bar{\tau}^* L_1 \end{array} \right] = \left[\begin{array}{c} \bar{b}_1^* \\ \hline -A_1 \end{array} \right] \tag{A-44}$$

where A_1 , R and L_1 are defined in (A-12). This equation is a degenerate form^{of} (A-14). Writing out these equations enables us to solve

for R' and $\bar{\tau}'$. Thus

$$-\bar{b}_1^* L_1^{-1} R' L_1 - \frac{\rho_2 \bar{\tau}'^* L_1}{\sqrt{\rho_2 \rho_{\alpha 2}}} = \bar{b}_1^*$$

$$-A_1 L_1^{-1} R' L_1 - \frac{\bar{a}_2 \bar{\tau}'^* L_1}{\sqrt{\rho_2 \rho_{\alpha 2}}} = -A_1$$

and finally

$$\bar{\tau}'^* = \frac{2\sqrt{\rho_2 \rho_{\alpha 2}} \bar{b}_1^* L_1^{-1}}{(\bar{b}_1^* A_1^{-1} \bar{a}_2 - \rho_2)} \quad (\text{A-45a})$$

$$R' = I - \frac{2L_1 A_1^{-1} \bar{a}_2 \bar{b}_1^* L_1^{-1}}{(\bar{b}_1^* A_1^{-1} \bar{a}_2 - \rho_2)} \quad (\text{A-45b})$$

As in the solid over solid interface case, we can prove that

$$R' = R'^*$$

To do this, we calculate the following two vectors using (A-12)

and (A-43):

$$L_1 A_1^{-1} \bar{a}_2 = \rho_{\alpha 2} \sqrt{\rho_1} \begin{bmatrix} \gamma_1 / \sqrt{\rho_{\alpha 1}} \\ (\gamma_1 - 1) \sqrt{\rho_{\beta 1}} \end{bmatrix} \quad (\text{A-46})$$

and

$$\bar{b}_1^* L_1^{-1} = -\sqrt{P_1} \left[\gamma_1 / \sqrt{P_{\alpha 1}}, (\gamma_1 - 1) \sqrt{P_{\beta 1}} \right] \quad (A-47)$$

The denominator in (A-45a and b) is a scalar determined by dotting these two vectors, i.e.

$$\left(\bar{b}_1^* L_1^{-1} \right) \left(L_1 A_1^{-1} \bar{a}_2 \right) - P_2 = -P_1 P_{\alpha 2} \left(\gamma_1^2 / P_{\alpha 1} + [\gamma_1 - 1]^2 P_{\beta 1} \right) - P_2$$

From (A-46) and (A-47), we see that

$$L_1 A_1^{-1} \bar{a}_2 = -P_{\alpha 2} \left(\bar{b}_1^* L_1^{-1} \right)^* \quad (A-48)$$

Hence, the second term of R' in (A-45b) contains the matrix product

$$\left(L_1 A_1^{-1} \bar{a}_2 \right) \left(\bar{b}_1^* L_1^{-1} \right) = -P_{\alpha 2} \left(\bar{b}_1^* L_1^{-1} \right)^* \left(\bar{b}_1^* L_1^{-1} \right)$$

which is symmetric. This shows that R' is symmetric. Substituting (A-46) and (A-47) into (A-45a) and (A-45b), yields explicit expressions for the elements of \bar{r}' and R' , i.e.

$$\bar{r}'^* = \frac{2\sqrt{P_1 P_2 P_{\alpha 2}}}{\Delta} \left[\gamma_1 / \sqrt{P_{\alpha 1}}, (\gamma_1 - 1) \sqrt{P_{\beta 1}} \right]$$

$$R' = I - \frac{2P_1 P_{\alpha 2}}{\Delta} \begin{bmatrix} \gamma_1^2 / P_{\alpha 1} & \gamma_1 (\gamma_1 - 1) \sqrt{\frac{P_{\beta 1}}{P_{\alpha 1}}} \\ \gamma_1 (\gamma_1 - 1) \sqrt{\frac{P_{\beta 1}}{P_{\alpha 1}}} & (\gamma_1 - 1)^2 P_{\beta 1} \end{bmatrix} \quad (\text{A-49})$$

where

$$\Delta = P_1 P_{\alpha 2} \left[\gamma_1^2 / P_{\alpha 1} + (\gamma_1 - 1)^2 P_{\beta 1} \right] + P_2 \quad (\text{A-50})$$

At normal incidence, the equations for reflection and transmission coefficients are most easily obtained from (A-42). Dividing the second row of this matrix equation by c and letting c go to infinity yields the equation

$$\begin{bmatrix} -P_1 & 0 & -P_2 \\ -1/\alpha_1 & 0 & 1/\alpha_2 \\ 0 & P_1 & 0 \end{bmatrix} \begin{bmatrix} -r'_{pp} & -r'_{sp} \sqrt{\frac{\alpha_1}{\beta_1}} \\ -r'_{ps} \sqrt{\frac{\beta_1}{\alpha_1}} & -r'_{ss} \\ t'_{pp} \sqrt{\frac{P_1 \alpha_2}{P_2 \alpha_1}} & t'_{sp} \sqrt{\frac{P_1 \alpha_2}{P_2 \beta_1}} \end{bmatrix} = \begin{bmatrix} -P_1 & 0 \\ 1/\alpha_1 & 0 \\ 0 & -P_1 \end{bmatrix} \quad (\text{A-50a})$$

From this equation, we easily obtain the solutions

$$r'_{PP} = \frac{\rho_2 \alpha_2 - \rho_1 \alpha_1}{\rho_2 \alpha_2 + \rho_1 \alpha_1}$$

$$t'_{PP} = \frac{2\sqrt{\rho_1 \alpha_1 \rho_2 \alpha_2}}{\rho_2 \alpha_2 + \rho_1 \alpha_1}$$

$$r'_{SS} = 1$$

$$t'_{SS} = 0$$

(A-50b)

The other coefficients, which convert energy from one mode to another, all vanish. The solutions given above can be obtained from the solutions for a solid over solid interface, equations (A-39), by setting $\beta_2 = 0$.

We now consider an incident **P** wave in the lower fluid medium. The matrix equations are obtained from (A-11) by interchanging subscripts 1 and 2 everywhere, unpriming the reflection and transmission coefficients, deleting the first row and second column of the 4 x 4 matrix and deleting the second column of reflection and transmission coefficients, and finally letting β_2 go to zero.

The result of all these changes is the equation

$$\begin{bmatrix} -P_2 & -P_1\gamma_1 & 2P_1\left(\frac{\beta_1}{c}\right)^2 P_{\beta 1} \\ -P_{\alpha 2} & P_{\alpha 1} & -1 \\ 0 & -2P_1\left(\frac{\beta_1}{c}\right)^2 P_{\alpha 1} & -P_1\gamma_1 \end{bmatrix} \begin{bmatrix} -r_{PP} \\ t_{PP} \sqrt{\frac{P_2 P_{\alpha 2}}{P_1 P_{\alpha 1}}} \\ t_{PS} \sqrt{\frac{P_2 P_{\alpha 2}}{P_1 P_{\beta 1}}} \end{bmatrix} = \begin{bmatrix} -P_2 \\ P_{\alpha 2} \\ 0 \end{bmatrix}$$

(A-51)

which can be expressed in terms of partitioned matrices as

$$P_2 r_{PP} + \sqrt{P_2 P_{\alpha 2}} \bar{b}_1^* L_1^{-1} \bar{\tau} = -P_2 \quad (\text{A-51a})$$

$$\bar{a}_2 r_{PP} + \sqrt{P_2 P_{\alpha 2}} A_1 L_1^{-1} \bar{\tau} = \bar{a}_2 \quad (\text{A-51b})$$

where

$$\bar{\tau} = \begin{bmatrix} t_{PP} \\ t_{PS} \end{bmatrix}$$

From (A-51b) we obtain

$$\bar{\tau} = \frac{1}{\sqrt{P_2 P_{\alpha 2}}} L_1 A_1^{-1} \bar{a}_2 (1 - r_{PP})$$

Substituting this into (A-51a) gives the reflection coefficient

$$r_{pp} = \frac{(\bar{b}_1^* A_1^{-1} \bar{a}_2 + \rho_2)}{(\bar{b}_1^* A_1^{-1} \bar{a}_2 - \rho_2)} \quad (\text{A-52})$$

Putting this relation into (A-51b) yields

$$\bar{\tau} = \frac{-2\rho_2 L_1 A_1^{-1} \bar{a}_2}{\sqrt{\rho_2 \rho_{\alpha 2}} (\bar{b}_1^* A_1^{-1} \bar{a}_2 - \rho_2)} \quad (\text{A-53})$$

At this point, we can easily prove that $\bar{\tau}^* = \bar{\tau}'^*$. Transposing (A-53) and using (A-48) we obtain

$$\bar{\tau}^* = \frac{2\sqrt{\rho_2 \rho_{\alpha 2}} \bar{b}_1^* L_1^{-1}}{(\bar{b}_1^* A_1^{-1} \bar{a}_2 - \rho_2)}$$

which equals $\bar{\tau}'^*$ by comparison with (A-45a). We can also write this as

$$\begin{bmatrix} t'_{pp} & t'_{sp} \\ 0 & 0 \end{bmatrix} = \begin{bmatrix} t_{pp} & 0 \\ t_{ps} & 0 \end{bmatrix}^*$$

which is a degenerate case of theorem (i), equation (A-4a) for a solid over solid interface, i.e.

$$T' = T^*$$

Expanding the expressions (A-52) and (A-53) gives

$$\bar{\tau} = -\frac{2\sqrt{\rho_1\rho_2\rho\alpha_2}}{\Delta} \begin{bmatrix} \delta_1/\sqrt{\rho\alpha_1} \\ (\delta_1-1)\sqrt{\rho\beta_1} \end{bmatrix} \quad (\text{A-54})$$

$$r_{pp} = \frac{-\Delta + 2\rho_2}{-\Delta} \quad (\text{A-55})$$

where Δ is given by (A-50).

For the normal incidence case we divide the second row of (A-51) by c and let c go to infinity. This gives the matrix equation

$$\begin{bmatrix} -\rho_2 & -\rho_1 & 0 \\ -1/\alpha_2 & 1/\alpha_1 & 0 \\ 0 & 0 & -\rho_1 \end{bmatrix} \begin{bmatrix} -r_{pp} \\ t_{pp}\sqrt{\frac{\rho_2\alpha_1}{\rho_1\alpha_2}} \\ t_{ps}\sqrt{\frac{\rho_2\beta_1}{\rho_1\alpha_2}} \end{bmatrix} = \begin{bmatrix} -\rho_2 \\ 1/\alpha_2 \\ 0 \end{bmatrix} \quad (\text{A-56})$$

which has the solution

$$r_{pp} = \frac{p_1 \alpha_1 - p_2 \alpha_2}{p_1 \alpha_1 + p_2 \alpha_2}$$

$$t_{pp} = \frac{2\sqrt{p_1 \alpha_1 p_2 \alpha_2}}{p_1 \alpha_1 + p_2 \alpha_2}$$

$$t_{ps} = 0$$

(A-57)

A.3 Fluid over Fluid Interface

We treat now an interface between two fluid media using equation (A-51). Since no shear waves exist in a fluid medium, we eliminate the third column of the 3×3 matrix in this equation and set $\beta_1 = 0$.

This gives the result

$$\begin{bmatrix} P_2 & -P_1 \\ P_{\alpha 2} & P_{\alpha 1} \end{bmatrix} \begin{bmatrix} r_{PP} \\ t_{PP} \sqrt{\frac{P_2 P_{\alpha 2}}{P_1 P_{\alpha 1}}} \end{bmatrix} = \begin{bmatrix} -P_2 \\ P_{\alpha 2} \end{bmatrix}$$

which has the solution

$$r_{PP} = \frac{P_1 P_{\alpha 2} - P_2 P_{\alpha 1}}{P_1 P_{\alpha 2} + P_2 P_{\alpha 1}}$$

$$t_{PP} = \frac{2 \sqrt{P_1 P_{\alpha 1} P_2 P_{\alpha 2}}}{P_1 P_{\alpha 2} + P_2 P_{\alpha 1}}$$

(A-58)

As c becomes very large

$$P_{\alpha n}/c \rightarrow 1/\alpha_n$$

Therefore, at normal incidence equations (A-58) reduce to

$$r_{PP} = \frac{\rho_1 \alpha_1 - \rho_2 \alpha_2}{\rho_1 \alpha_1 + \rho_2 \alpha_2}$$

$$t_{PP} = \frac{2\sqrt{\rho_1 \alpha_1 \rho_2 \alpha_2}}{\rho_1 \alpha_1 + \rho_2 \alpha_2}$$

(A-59)

which are the same solutions given by (A-57).

A.4 Free Surface

If we set $p_2 = 0$, then the interface between the two media is free, and no transmitted waves exist in medium 2. The boundary conditions reduce to two, i.e. the vanishing of τ_{zz} and τ_{zx} at the interface.

The matrix equation for the reflection and transmission coefficients is obtained by deleting the first and third rows and last two columns of the 4×4 matrix in (A-11). This gives the 2×2 equation

$$\begin{bmatrix} \gamma_1 & -2\left(\frac{\beta_1}{c}\right)^2 P_{\beta 1} \\ -2\left(\frac{\beta_1}{c}\right)^2 P_{\alpha 1} & -\gamma_1 \end{bmatrix} \begin{bmatrix} r'_{pp} & r'_{sp} \sqrt{\frac{P_{\beta 1}}{P_{\alpha 1}}} \\ r'_{ps} \sqrt{\frac{P_{\alpha 1}}{P_{\beta 1}}} & r'_{ss} \end{bmatrix} = \begin{bmatrix} -\gamma_1 & 2\left(\frac{\beta_1}{c}\right)^2 P_{\beta 1} \\ -2\left(\frac{\beta_1}{c}\right)^2 P_{\alpha 1} & -\gamma_1 \end{bmatrix} \quad (\text{A-60})$$

which is valid for a free surface over a solid medium.

Inverting the left most matrix we obtain

$$\begin{bmatrix} r'_{pp} & r'_{sp} \sqrt{\frac{P_{\beta 1}}{P_{\alpha 1}}} \\ r'_{ps} \sqrt{\frac{P_{\alpha 1}}{P_{\beta 1}}} & r'_{ss} \end{bmatrix} = \frac{1}{\det} \begin{bmatrix} -\gamma_1 & 2\left(\frac{\beta_1}{c}\right)^2 P_{\alpha 1} \\ 2\left(\frac{\beta_1}{c}\right)^2 P_{\alpha 1} & \gamma_1 \end{bmatrix} \begin{bmatrix} -\gamma_1 & 2\left(\frac{\beta_1}{c}\right)^2 P_{\beta 1} \\ -2\left(\frac{\beta_1}{c}\right)^2 P_{\alpha 1} & -\gamma_1 \end{bmatrix}$$

where

$$\det = -(\gamma_1^2 + 4\left(\frac{\beta_1}{c}\right)^4 P_{\alpha 1} P_{\beta 1})$$

Thus

$$r'_{pp} = -r'_{ss} = \frac{-\gamma_1^2 + 4\left(\frac{\beta_1}{c}\right)^4 P_{\alpha 1} P_{\beta 1}}{\gamma_1^2 + 4\left(\frac{\beta_1}{c}\right)^4 P_{\alpha 1} P_{\beta 1}}$$

$$r'_{ps} = r'_{sp} = \frac{4\left(\frac{\beta_1}{c}\right)^2 \sqrt{P_{\alpha 1} P_{\beta 1}} \gamma_1}{\gamma_1^2 + 4\left(\frac{\beta_1}{c}\right)^4 P_{\alpha 1} P_{\beta 1}}$$

(A-61)

If we define the reflection coefficient matrix

$$R' = \begin{bmatrix} r'_{pp} & r'_{sp} \\ r'_{ps} & r'_{ss} \end{bmatrix}$$

then we can prove directly from (A-61) that

$$R'^* R' = I$$

which is a special case of the conservation of energy theorem given by (a-18a) when no transmission coefficients exist.

At normal incidence (A-60) reduces to

$$r'_{pp} = -r'_{ss} = -1$$

$$r'_{ps} = r'_{sp} = 0$$

Finally, we consider the reflection coefficient r'_{pp} at the free

surface of a fluid. Since no shear waves exist in a fluid, the only non-vanishing equation in (A-60) is

$$\gamma_i r'_{pp} = -\gamma_i$$

Thus

$$r'_{pp} = -1$$

for all phase velocities c .

A.5 Figure Captions

A-1 Incident, reflected and transmitted waves at an interface between two isotropic, homogeneous halfspaces.

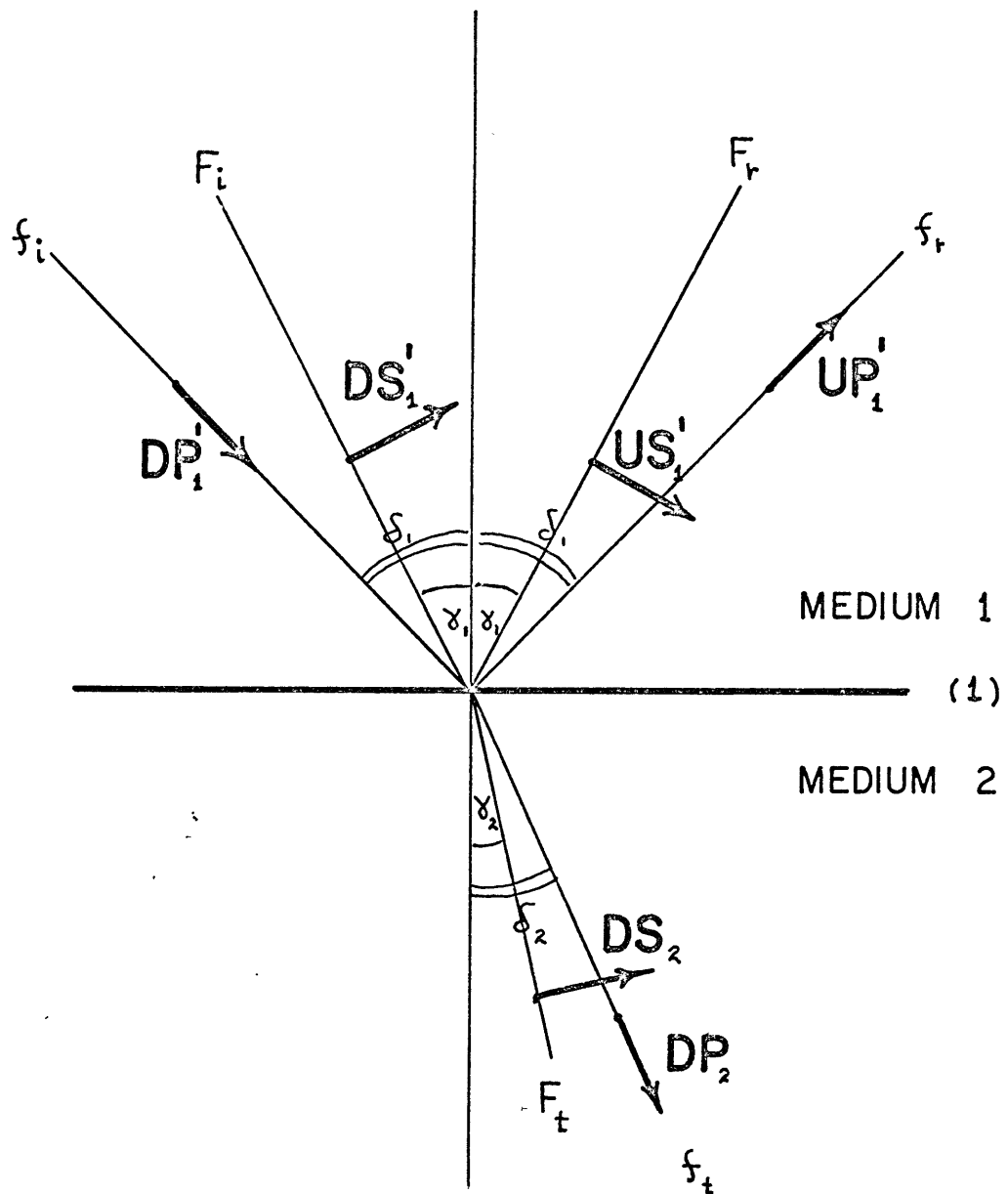


FIGURE A-1

Appendix BOrthogonality Relation for P and SV Waves

In this appendix, we calculate the energy density flows for plane P and SV waves incident to a horizontal interface. It is shown that when both P and SV waves have the same horizontal phase velocity then the energy density for both waves together equals the sum of the individual energy density flows. Thus, no cross terms in the P and SV waves occur.

Let $f(\hat{p} \cdot \vec{r} - \alpha t)$ and $F(\hat{s} \cdot \vec{r} - \beta t)$ be elastic displacement potentials for P and SV waves respectively as described in Section 2.2. Following Morse and Feshbach (1953), Vol. 1, section 2.2, we define the intensity vector

$$\vec{S} = - \frac{\partial \vec{u}}{\partial t} \cdot \vec{\bar{L}} \quad (\text{B-1})$$

where \vec{u} equals the particle displacement vector due to both P and SV incident waves, and $\vec{\bar{L}}$ is the stress dyadic associated with the particle displacement. The instantaneous power carried by the P and SV waves across a unit area with normal vector \hat{n} equals

(B-2)

We first calculate the intensity vector \bar{S} . From (2-3a,b) we obtain the total displacement vector

$$\begin{aligned}\bar{u} &= f' \hat{p} + F' \hat{q} \times \hat{s} \\ &= (p_x f' + s_z F') \hat{x} + (p_z f' - s_x F') \hat{z}\end{aligned}\quad (\text{B-3})$$

where \hat{x} and \hat{z} are unit vectors in the x and z directions. Unit vectors \hat{p} and \hat{s} have (x, z) components given by

$$\begin{aligned}\hat{p} &= (p_x, p_z) \\ \hat{s} &= (s_x, s_z)\end{aligned}\quad (\text{B-4})$$

Taking the time derivative $\frac{\partial \bar{u}}{\partial t}$ yields

$$-\frac{\partial \bar{u}}{\partial t} = (\alpha p_x f'' + \beta s_z F'') \hat{x} + (\alpha p_z f'' - \beta s_x F'') \hat{z}\quad (\text{B-4})$$

The stress dyadic \bar{L} is calculated from

$$\bar{L} = \lambda \bar{I} (\bar{\nabla} \cdot \bar{u}) + \mu [\bar{\nabla} \bar{u} + (\bar{\nabla} \bar{u})^T]\quad (\text{B-5})$$

where λ and μ are the Lamé constants for a homogeneous isotropic medium. The divergence of \bar{u} contains terms in f

only since F causes no dilation in the medium. Thus, from

(B-3)

$$\bar{\nabla} \cdot \bar{u} = (p_x^2 + p_z^2) f'' = f''$$

(B-6)

and

$$\bar{I} (\bar{\nabla} \cdot \bar{u}) = \hat{x}\hat{x} f'' + \hat{z}\hat{z} f''$$

(B-6)

The dyadic $\bar{\nabla} \bar{u}$ is given by

$$\bar{\nabla} \bar{u} = \hat{x} \frac{\partial \bar{u}}{\partial x} + \hat{z} \frac{\partial \bar{u}}{\partial z}$$

Therefore

$$\begin{aligned} \bar{\nabla} \bar{u} &= \hat{x}\hat{x} (p_x^2 f'' + s_x s_z F'') + \hat{x}\hat{z} (p_x p_z f'' - s_x^2 F'') \\ &+ \hat{z}\hat{x} (p_x p_z f'' + s_z^2 F'') + \hat{z}\hat{z} (p_z^2 f'' - s_x s_z F'') \end{aligned}$$

(B-7)

Adding $\bar{\nabla} \bar{u}$ to its transpose yields the symmetric dyadic

$$\begin{aligned} \bar{\nabla} \bar{u} + (\bar{\nabla} \bar{u})^T &= \hat{x}\hat{x} 2(p_x^2 f'' + s_x s_z F'') + \hat{x}\hat{z} (2p_x p_z f'' + [s_z^2 - s_x^2] F'') \\ &+ \hat{z}\hat{x} (2p_x p_z f'' + [s_z^2 - s_x^2] F'') + \hat{z}\hat{z} 2(p_z^2 f'' - s_x s_z F'') \end{aligned}$$

(B-8)

Substituting equations (B-8) and (B-6) into (B-5), we obtain the symmetric stress dyadic,

$$\begin{aligned} \bar{\mathbf{L}} = & \hat{x}\hat{x} [(\lambda + 2\mu p_x^2) \mathcal{F}'' + 2\mu s_x s_z F''] + \hat{x}\hat{z} \mu [2p_x p_z \mathcal{F}'' + (s_z^2 - s_x^2) F''] \\ & + \hat{z}\hat{x} \mu [2p_x p_z \mathcal{F}'' + (s_z^2 - s_x^2) F''] + \hat{z}\hat{z} [(\lambda + 2\mu p_z^2) \mathcal{F}'' - 2\mu s_x s_z F''] \end{aligned} \quad (\text{B-9})$$

Putting (B-9) and (B-4) into (B-1), we obtain an expression for the intensity vector $\bar{\mathbf{S}}$:

$$\begin{aligned} \bar{\mathbf{S}} = & \hat{x} \left\{ [\alpha p_x \mathcal{F}'' + \beta s_z F''] [(\lambda + 2\mu p_x^2) \mathcal{F}'' + 2\mu s_x s_z F''] + \right. \\ & \left. + [\alpha p_z \mathcal{F}'' - \beta s_x F''] [2\mu p_x p_z \mathcal{F}'' + \mu (s_z^2 - s_x^2) F''] \right\} \\ & + \hat{z} \left\{ [\alpha p_x \mathcal{F}'' + \beta s_z F''] [2\mu p_x p_z \mathcal{F}'' + \mu (s_z^2 - s_x^2) F''] + \right. \\ & \left. + [\alpha p_z \mathcal{F}'' - \beta s_x F''] [(\lambda + 2\mu p_z^2) \mathcal{F}'' - 2\mu s_z s_x F''] \right\} \end{aligned} \quad (\text{B-10})$$

The power transmitted through a unit area of horizontal interface with normal vector $\hat{\mathbf{z}}$ is therefore

$$\begin{aligned} \bar{\mathbf{S}} \cdot \hat{\mathbf{z}} = & [\alpha p_x \mathcal{F}'' + \beta s_z F''] [2\mu p_x p_z \mathcal{F}'' + \mu (s_z^2 - s_x^2) F''] \\ & + [\alpha p_z \mathcal{F}'' - \beta s_x F''] [(\lambda + 2\mu p_z^2) \mathcal{F}'' - 2\mu s_z s_x F''] \end{aligned} \quad (\text{B-11})$$

...Substituting the identities

$$\begin{aligned} \mu &= \rho\beta^2, \quad \lambda = \rho(\alpha^2 - 2\beta^2) \\ p_z^2 &= 1 - p_x^2, \quad s_z^2 = 1 - s_x^2 \end{aligned}$$

into (B-11), we obtain after some algebra

$$\begin{aligned} \bar{S} \cdot \hat{z} &= \rho\alpha^3 p_z f''^2 + \rho\beta^3 s_z F''^2 + \\ &+ \rho f'' F'' [\beta p_x - \alpha s_x] [2\beta^2 (p_z s_z + p_x s_x) + \alpha\beta] \end{aligned} \quad (B-12)$$

The cross terms in $f'' F''$ do not vanish for arbitrary directions \hat{p} and \hat{s} , so that in general the energy flow across a unit horizontal area contains these terms. However, if f and F have the same horizontal phase velocity c , then \hat{p} and \hat{s} are related by Snell's law, i.e.

$$\begin{aligned} p_x &= \sin \delta = \alpha/c \\ s_x &= \sin \gamma = \beta/c \end{aligned} \quad (B-13)$$

Substituting these components into the first brackets of (B-12) causes the coefficients of $f'' F''$ to vanish. Therefore,

$$\bar{S} \cdot \hat{z} = \rho\alpha^3 p_z f''^2 + \rho\beta^3 s_z F''^2 \quad (B-14)$$

Comparing this equation to the waves defined in (2-4), we see that the upgoing energy flow across a unit horizontal area equals

$$UP^2 + US^2$$

and the downgoing energy flow is

$$DP^2 + DS^2$$

This is the motivation for the particular choice of P and SV waves defined in (2-4). As a result, several useful conservation of energy theorems are proved in Chapters 2, 3, and 4 for layered media.